AD____________________

Award Number: DAMD17-99-1-9022

TITLE: Periscopic Spine Surgery

PRINCIPAL INVESTIGATOR: Kevin Cleary, Ph.D.

CONTRACTING ORGANIZATION: Georgetown University
Washington, DC 20057

REPORT DATE: February 2000

TYPE OF REPORT: Annual

PREPARED FOR: U.S. Army Medical Research and Materiel Command
Fort Detrick, Maryland 21702-5012

DISTRIBUTION STATEMENT: Approved for public release;
distribution unlimited

The views, opinions and/or findings contained in this report are those of the author(s) and should not be construed as an official Department of the Army position, policy or decision unless so designated by other documentation.

20000324 062

DTIC QUALITY INSPECTED 3

REPORT DOCUMENTATION PAGE

Form Approved OMB No. 074-0188

Public reporting burden for this collection of information is estimated to average 1 hour per response, including the time for reviewing instructions, searching existing data sources, gathering and maintaining the data needed, and completing and reviewing this collection of information. Send comments regarding this burden estimate or any other aspect of this collection of information, including suggestions for reducing this burden to Washington Headquarters Services, Directorate for Information Operations and Reports, 1215 Jefferson Davis Highway, Suite 1204, Arlington, VA 22202-4302, and to the Office of Management and Budget, Paperwork Reduction Project (0704-0188), Washington, DC 20503

1. AGENCY USE ONLY (Leave blank)	2. REPORT DATE	3. REPORT TYPE AND DATES COVERED
	February 2000	Annual (15 Jan 99 - 14 Jan 00)

4. TITLE AND SUBTITLE
Periscopic Spine Surgery

5. FUNDING NUMBERS
DAMD17-99-1-9022

6. AUTHOR(S)
Kevin Cleary, Ph.D.

7. PERFORMING ORGANIZATION NAME(S) AND ADDRESS(ES)
Georgetown University
Washington, DC 20057

E-MAIL:
cleary@isis.imac.georgetown.edu

8. PERFORMING ORGANIZATION REPORT NUMBER

9. SPONSORING / MONITORING AGENCY NAME(S) AND ADDRESS(ES)

U.S. Army Medical Research and Materiel Command
Fort Detrick, Maryland 21702-5012

10. SPONSORING / MONITORING AGENCY REPORT NUMBER

11. SUPPLEMENTARY NOTES

12a. DISTRIBUTION / AVAILABILITY STATEMENT
Approved for public release; distribution unlimited

12b. DISTRIBUTION CODE

13. ABSTRACT *(Maximum 200 Words)*
This project is aimed at improving the state of the art of image-guided and minimally invasive spine procedures by developing a new generation of clinical techniques along with the computer-based hardware and software needed for their implementation. The statement of work was modified in August 1999 to reflect a new focus on robotically assisted spine procedures, but the overall direction of the project remains the same.

Key research accomplishments for the first year are:

- Demonstrated the value of intraoperative CT for visualization and verification of the anatomy in complex spine surgeries in the neurosurgery operating room
- Demonstrated the value of intraoperative CT for visualizing needle trajectories and bone cement placement in percutaneous vertebroplasty in interventional radiology
- Demonstrated the feasibility of incorporating mobile CT for intraprocedure use in the hospital environment, including radiation medicine and the intensive care unit
- Developed an improved algorithm for three-dimensional visualization of isosurfaces and demonstrated this algorithm on percutaneous vertebroplasty data sets
- Defined an architecture for an advanced interventional suite incorporating mobile CT, robotics, optical tracking, and a user interface for control
- Developed an initial set of requirements for applying a robotic device to percutaneous spine needle placement

14. SUBJECT TERMS
image-guided, minimally invasive, spine procedures, technology development, mobile CT, medical robotics, visualization

15. NUMBER OF PAGES
94

16. PRICE CODE

17. SECURITY CLASSIFICATION OF REPORT	18. SECURITY CLASSIFICATION OF THIS PAGE	19. SECURITY CLASSIFICATION OF ABSTRACT	20. LIMITATION OF ABSTRACT
Unclassified	Unclassified	Unclassified	Unlimited

FOREWORD

Opinions, interpretations, conclusions and recommendations are those of the author and are not necessarily endorsed by the U.S. Army.

___ Where copyrighted material is quoted, permission has been obtained to use such material.

___ Where material from documents designated for limited distribution is quoted, permission has been obtained to use the material.

JLC Citations of commercial organizations and trade names in this report do not constitute an official Department of Army endorsement or approval of the products or services of these organizations.

N/A In conducting research using animals, the investigator(s) adhered to the "Guide for the Care and Use of Laboratory Animals," prepared by the Committee on Care and use of Laboratory Animals of the Institute of Laboratory Resources, national Research Council (NIH Publication No. 86-23, Revised 1985).

X For the protection of human subjects, the investigator(s) adhered to policies of applicable Federal Law 45 CFR 46.

N/A In conducting research utilizing recombinant DNA technology, the investigator(s) adhered to current guidelines promulgated by the National Institutes of Health.

N/A In the conduct of research utilizing recombinant DNA, the investigator(s) adhered to the NIH Guidelines for Research Involving Recombinant DNA Molecules.

N/A In the conduct of research involving hazardous organisms, the investigator(s) adhered to the CDC-NIH Guide for Biosafety in Microbiological and Biomedical Laboratories.

/Lorin Cleary 2/9/00

PI - Signature Date

4 Table of Contents

5 Introduction

This project is aimed at improving the state of the art of image-guided and minimally invasive spine procedures by developing a new generation of clinical techniques along with the computer-based hardware and software needed for their implementation. The statement of work was modified in August 1999 to reflect a new focus on robotically assisted spine procedures, but the overall direction of the project remains the same. This project is a partnership joining the scientific and engineering expertise of the Imaging Science and Information Systems (ISIS) Center at Georgetown University Medical Center, and clinical participants at Georgetown and Walter Reed Army Medical Center

6 Report Body

As specified in the reporting instructions from the U.S. Army Medical Research and Materiel Command (USAMRMC), this section describes the research accomplishments associated with each task in the approved statement of work. Since this is the annual report for the first year, the year 1 tasks will be covered in this report.

6.1 Task 1: Program Planning and Management

The major accomplishment in program planning and management was modifying the statement of work in August 1999 to reflect our new focus on robotically assisted spine procedures. The Urology Robotics Laboratory of the Johns Hopkins Medical Institutions is now a subcontractor to Georgetown University as part of this research effort. Johns Hopkins will modify their "needle driver" robot so that it can be applied to percutaneous spine procedures at Georgetown.

Other management tasks have included the submission of quarterly reports to the Telemedicine and Advanced Technology Research Center (TATRC) at Fort Detrick.

6.2 Task 2: Integrate Mobile CT Scanner Into Clinical Procedures

At Georgetown, the mobile CT scanner (Figures 1 and 2) has been used in the interventional radiology suite, the operating room, radiation medicine, the neurosurgery intensive care unit (ICU), and the pediatrics ICU [Cleary 1999a]. The major procedures impacted are spine tumor resections and complex cranio-cervical surgeries in the neurosurgical operating room, and percutaneous vertebroplasty in the interventional radiology suite and. The CT scanner is an FDA approved device. Since both the gantry and the table can move during scanning, the gantry can be used with the CT table (as done in the operating room) or with another table such as a fluoroscopy table (as done in the interventional suite).

Our initial experience with neurosurgical spine cases shows that the use of intraoperative CT scanning changed the course of the surgery in 6 out of the 17 cases [Hum 1999a]. CT was beneficial in facilitating adequate ventral clival and craniocervical decompressions, assisting in more complete tumor resections, and verifying correct graft and instrument

placement before surgical closing. The equipment layout in the operating room is shown in Figure 3, and the intraoperative use of CT during spine surgery is shown in Figure 4.

In interventional radiology, the mobile CT scanner is used in percutaneous spine procedures such as vertebroplasty. Percutaneous vertebroplasty is a relatively new interventional technique in which polymethlymethacrylate (PMMA) bone cement is injected into the vertebral body to strengthen the vertebra and stabilize the spine. A photograph of a typical case in the interventional suite is shown in Figure 5. The procedure itself is done under bi-plane fluoroscopy (Siemens Neurostar TOP). The injection of PMMA is shown in Figure 6. The mobile CT gantry is positioned at the back of the room and the fluoroscopy table can be rotated 90 degrees as needed so that it can be slid into the CT gantry for scanning on an as-needed basis (Figure 7). The mobile CT is used for several purposes: 1) prior to vertebroplasty to define defects in cortical bone and plan the needle trajectory; 2) during the procedure to evaluate indeterminant PMMA extravasation and to check the needle placement; and 3) post-procedure for immediate evaluation of possible complications such as PMMA extravasation and to verify the amount of filling within the vertebral body. The equipment placement and room layout is shown in Figure 8.

6.3 Task 3: Develop 3D Visualization for Vertebroplasty

As described in Task 2, percutaneous vertebroplasty is a relatively new interventional technique in which PMMA is injected into the vertebral body. As a feasibility study, 3D visualization software was developed to examine the spread of bone cement after vertebroplasty procedures [Choi 1999a, Cleary 1999d]. This visualization software is part of a larger software package called the ISIS Center Spine Procedures Imaging and Navigation Engine (I-SPINE).

The images were acquired by the mobile CT scanner. Offline, the images were then transferred to a Windows NT personal computer using the digital image communications in medicine (DICOM) standard. The I-SPINE software was then used to segment the bone cement and vertebral body based on histogram windowing (Figure 9). The resulting images are rendered in 3D for viewing by the interventional radiologist (Figure 10). At the moment, only preliminary work has been done, but the interventional radiologist has stated that the images are useful for visualizing the spread of bone cement. As part of this task, work has also been done on developing improved visualization algorithms [Choi 1999b].

6.4 Task 4: Develop System Architecture and Requirements

A system architecture for integrating advanced imaging, instrumentation, and visualization has been investigated through developing an advanced software package. This software packing is called the ISIS Center Spine Procedures Imaging and Navigation Engine (I-SPINE) and runs on a Windows NT personal computer [Choi 1999a, Cleary 1999d]. The software package includes the following capabilities:

- DICOM receiver to accept images from mobile CT, fluoroscopy, and DSA units

- 2D viewing capability (single slices or multiple slices up to 8 by 8)
- Segmentation function based on histogram thresholding
- 3D visualization
- Registration of DSA images by manual pixel shifting

The opening screen of the user interface for I-SPINE is shown in Figure 11. This screen presents the user with a list of patient names (only abbreviations are shown here for patient confidentiality) and study dates. From this screen, a user can select studies for 2-D viewing, segmentation by histogram thresholding, or 3-D visualization.

Recently, we have also begun developing the architecture for a robotic biopsy testbed incorporating a mobile CT scanner, a small "needle driver" robot, an optical tracking system, and a user interface. A system diagram is shown in Figure 12.

This robotic biopsy testbed is part of our collaboration with the Urology Robotics Laboratory of the Johns Hopkins Medical Institutions, under the direction of Dan Stoianovici, Ph.D. We are also coordinating with Russell Taylor, Ph.D., Director of the Computer Integrated Surgical Systems and Technology Center at Johns Hopkins University, and one of the original developers of the urology robot.

The testbed components are described in the following paragraphs.

Mobile CT scanner and operator's workstation. The mobile CT scanner provides a series of axial images of the patient. Each images is 512 by 512 pixels, and a typical data set consists of from 10 to 100 images. The operator's workstation provides a graphical user interface to operate the scanner. The only interface to the outside world is a DICOM interface, where the images can be sent over a network to another DICOM capable system. In this testbed, after the scans are acquired, they are sent to a Windows NT workstation running our I-SPINE software.

Robot. The robot will hold the biopsy needle. The robot will be based on the existing needle driver robot developed at Johns Hopkins. The needle will be automatically oriented and driven by the robot. The robot is controlled by the NT workstation via a hardware and software interface. A C++ language API has been developed at Johns Hopkins, which includes commands to move the robot, determine its current position, etc.

Optical tracker. The optical tracker is capable of determining the location of objects in space with respect to a pre-defined coordinate frame. For each object to be tracked, special reflective sensors are positioned on the object. These sensors can be detected by the optical tracker and used to determine the location of the object. The optical tracker interfaces to the NT Workstation through the serial port. ASCII commands are sent through the serial port to invoke tracker functions, and the results are returned in a similar manner.

I-SPINE software. In the initial version of this testbed currently under development, the I-SPINE software described above is being modified to incorporate the robot and optical tracker. The scenario envisioned for robotic spine biopsy is as follows:

1. The patient is positioned on the table and a series of axial scans are obtained
2. The scans are sent from the operator's workstation to the I-SPINE software
3. The user interface of the I-SPINE software allows the physician to select the axial scan of interest and the region to be biopsied
4. The entry location for the biopsy is marked on the patient's skin
5. The robot is manually positioned at the skin entry point
6. The robot automatically orients the needle and inserts it
7. A CT scan is obtained to verify the needle position
8. The biopsy sample is taken

The testbed will be verified on phantoms and cadavers before any clinical trials are planned. The initial goal is to evaluate the accuracy obtainable using robotically assisted biopsy as compared to "standard" biopsy where no robotic assist is provided.

6.5 Task 5: Develop Requirements for Robotic Device

As mentioned earlier, the research focus of the project was revised in August 1999 to focus on robotically assisted spine procedures. In addition to the robotic biopsy testbed described in Task 4, we are pursuing clinical spine applications. Our partner in this effort is the Urology Robotics Laboratory at Johns Hopkins Medical Institutions. A subcontract has been issued to the Urology Robotics Group to adapt their kidney puncture robot for spine applications. To date, there have been four meetings at Georgetown with Johns Hopkins personnel, and plans for clinical application of the robot have been formulated.

The purpose of this research study is to evaluate a robotic device to help with percutaneous spine procedures including biopsy, facet and nerve blocks, vertebroplasty, discography, and radiofrequency and laser ablations. The robotic device consists of a mechanical instrument holder and driver and a computer-based control system. We are evaluating whether this device can assist the physician in placing and advancing instruments, such as needles, in the spine. We believe this device may increase the accuracy and efficiency by which these instruments are placed and manipulated, which may lead to better patient outcomes.

6.6 Task 6: Investigate Tracking Component

As part of the robotic biopsy testbed described in Task 4, we are investigating optical tracking technology. A Polaris optical tracker has been procured (this is the tracking component shown in Figure 12) and we have begun developing the software to track objects. We are working with a consultant, Neil Glossop, PhD, of Traxtal Technologies (http://www.traxtal.com) to develop tracking technologies, with particular emphasis to tracking of the spine.

6.7 Tasks 7/8: Reports

The last tasks for Year 1 in the Statement of Work are reporting requirements, which are covered by the quarterly reports submitted to TATRC and this annual report.

6.8 Year 2 Tasks

The focus for year 2 and beyond will be on robotically assisted spine procedures. We intend to further develop the robotic biopsy testbed as described in Task 4 and the clinical spine applications of the robot as described in Task 5. After these systems have been developed, they will be evaluated and suggestions for the next generation of equipment will be made.

6.9 Walter Reed Collaboration

As part of this project, we are collaborating with Walter Reed Army Medical Center to investigate new clinical techniques and technological developments for spine procedures. The primary collaboration is with the Department of Radiology, under the direction of Col. Michael Brazaitis, MD, Chairman, and Irwin Feuerstein, MD, EBCT Radiologist. We have also been working with LTC David Polly, MD, of the Orthopaedic Surgery Service.

In the Department of Radiology, the primary focus is on the use of Electron Beam CT (EBCT) in osteoporosis screening. We have procured a quantitative CT (QCT) bone densitometry software package, and begun developing the relevant protocols. A demonstration screen capture from this software package is shown in Figure 13. Once the protocol is approved, we plan to start by screening the lumbar and thoracic spine in military personnel from the Army War College. The major aims are to compare bone mineral density (BMD) in the active-duty military population with that in the general population and attempt to determine the risk factors related to osteoporosis.

In the Orthopaedic Surgery Service, the FluoroNav™ fluoroscopy-based image-guided surgery system from Sofamor Danek has been purchased to provide image guidance in complex spinal cases. A photograph of this system is shown in Figure 14. Walter Reed is also a test site for this equipment and plans to record process measure data on the use of FluoroNav compared to conventional fluoroscopy.

As part of these developments, discussions concerning additional future potential collaborations have been ongoing, and the interchange so far has been beneficial to both Georgetown and Walter Reed.

7 Key Research Outcomes

As directed in the reporting instructions, this section provides a bulleted list of key research accomplishments as follows:

- Demonstrated the value of intraoperative CT for visualization and verification of the anatomy in complex spine surgeries in the neurosurgery operating room

- Demonstrated the value of intraoperative CT for visualizing needle trajectories and the placement of bone cement in percutaneous vertebroplasty in the interventional radiology suite
- Demonstrated the feasibility of incorporating mobile CT for intraprocedure use in the hospital environment, including radiation medicine and the intensive care unit
- Developed an improved algorithm for three-dimensional visualization of isosurfaces and demonstrated this algorithm on percutaneous vertebroplasty data sets
- Defined an architecture for an advanced interventional suite incorporating mobile CT, robotics, optical tracking, and a user interface for control
- Developed an initial set of requirements for applying a robotic device to percutaneous spine needle placement

8 Reportable Outcomes

As directed in the reporting instructions, this section provides a list of reportable outcomes. The major product of the first year is the list of manuscripts given in Section 10, References. Six conference papers were published or submitted, five poster presentations were made, and one journal article was submitted. Copies of these documents are provided in the appendix.

In addition, two grant applications to the National Institutes of Health were submitted based on this work.

9 Conclusions

The first year of work on the Periscopic Spine Surgery project has laid the foundation for a focus on robotically assisted spine procedures in the second year. The integration of the mobile CT scanner at Georgetown has demonstrated the value of intraoperative imaging in the operating room and the interventional suite. A research team, including clinicians from the Neurosurgery and Radiology departments and scientists from the ISIS Center, is now in place, which should facilitate the clinical utilization of the technology developed. We intend to continue to focus on technology development for image-guided and minimally invasive spine techniques in the near term, but also plan to look for other clinical applications and synergistic efforts.

10 References

[Choi 1999a] Choi J, Cleary K, Zeng J, Gary K, Freedman M, Watson V, Lindisch D, Mun S, "I-SPINE: a software package for advances in image-guided and minimally invasive spine proceedings," presented at and to be published in the proceedings, SPIE Applied Imagery Pattern Recognition workshop, Oct 13-15, 1999, Washington, DC.

[Choi 1999b] Choi J, Lee Y, Shin Y, Cleary K, Mun S, "Interactive multi-level isosurface rendering," submitted to Eurographics 2000, August 20-25, 2000, Interlaken, Switzerland.

[Cleary 1999a] Cleary K, Henderson F, Rodgers J, Watson V, Freedman M, "Integrating a mobile computed tomographic scanner in hospital operations, " poster presentation and abstract published in proceedings, *Computer Assisted Radiology and Surgery (CARS)*, Elsevier Press, 1999, page 1053.

[Cleary 1999b] Cleary K, Freedman M, Zeng J, Mun SK, Watson V, Henderson F, "Developing a program in image-guided, minimally invasive spine procedures," *Computer Assisted Radiology and Surgery (CARS)*, Elsevier Press, 1999, 736-740.

[Cleary 1999c] Cleary K, Carignan C, Traynor L, "Realistic force feedback for a spine biopsy simulator," *International Workshop on Haptic Devices in Medical Applications*, Dillmann R, Salb T, Eds. 1999, 66-75.

[Cleary 1999d] Cleary K, Choi J, Gary K, Freedman M, Levy E, Watson V, Lindisch D, Zeng J, "I-SPINE: a software package for advances in image-guided and minimally invasive spine procedures," poster presentation, Medical Imaging Computing and Computer Aided Interventions, Sept 19-22, 1999, Cambridge, England.

[Cleary 1999e] Cleary K, editor, "Workshop report: technical requirements for image-guided spine procedures," workshop held April 17-20, 1999, Ellicott City, Maryland, report printed by Westend Press, Washington, DC. (Report is 119 pages and is not included here. Report is on the web: go to http://www.isis.georgetown.edu/ and follow the links to conferences and the spine workshop).

[Hum 1999a] Hum B, Feigenbaum F, Cleary K, Henderson F, "Intraoperative computed tomography for complex cranio-cervical surgeries and spine tumor resections," submitted to *Neurosurgery*, Dec. 1999.

[Hum 1999b] Hum B, Cleary K, Watson V, Feigenbaum F, Henderson F, "Intraoperative computed tomography for spinal procedures," poster presentation, Image-Guided Surgery Conference, St. Thomas, Dec 9-11, 1999.

[Traynor 2000] Traynor L, Levy E, Choi J, Cleary K, Zeng J, and Lindisch D, "Software development for registration of digital subtraction angiography (DSA) images in uterine fibroid embolization," accepted for presentation and publication in the proceedings, 8th Annual Medicine Meets Virtual Reality Conference, Jan 27-30, 2000, Newport Beach, California.

[Watson 1999] Watson VE, Cleary KR, Lindisch D, "Mobile CT assessment of needle placement and distribution of polymethlymethacrylate (PMMA) during percutaneous vertebroplasty," Scientific Exhibit, RSNA 1999, Chicago, Certificate of Merit award.

[Zeng 1999] Zeng J, Gary K, Levy E, Yi J, Ra J, Traynor L, Cleary K, Kim J, Kim K, Mun S, "A three-dimensional training system for spine needle biopsy," Scientific Exhibit, RSNA 1999, Chicago.

11 Appendices

11.1 Figures

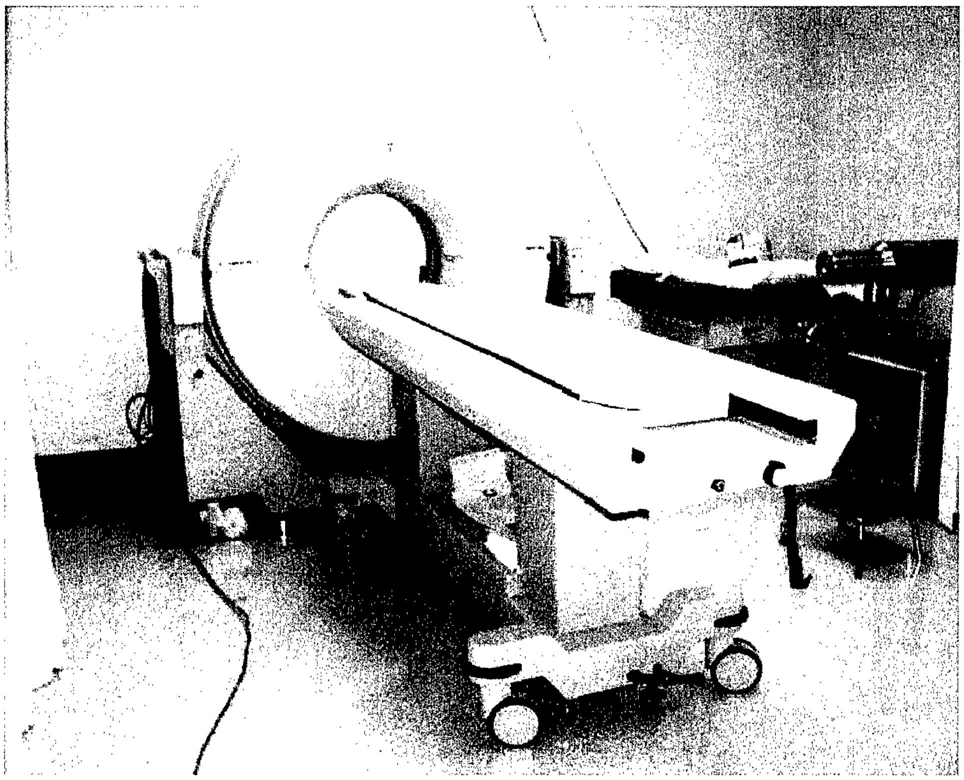

Figure 1: Mobile CT gantry and table

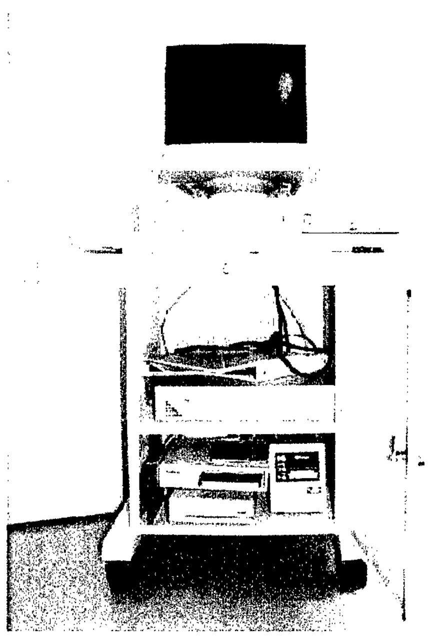

Figure 2: Operator's workstation

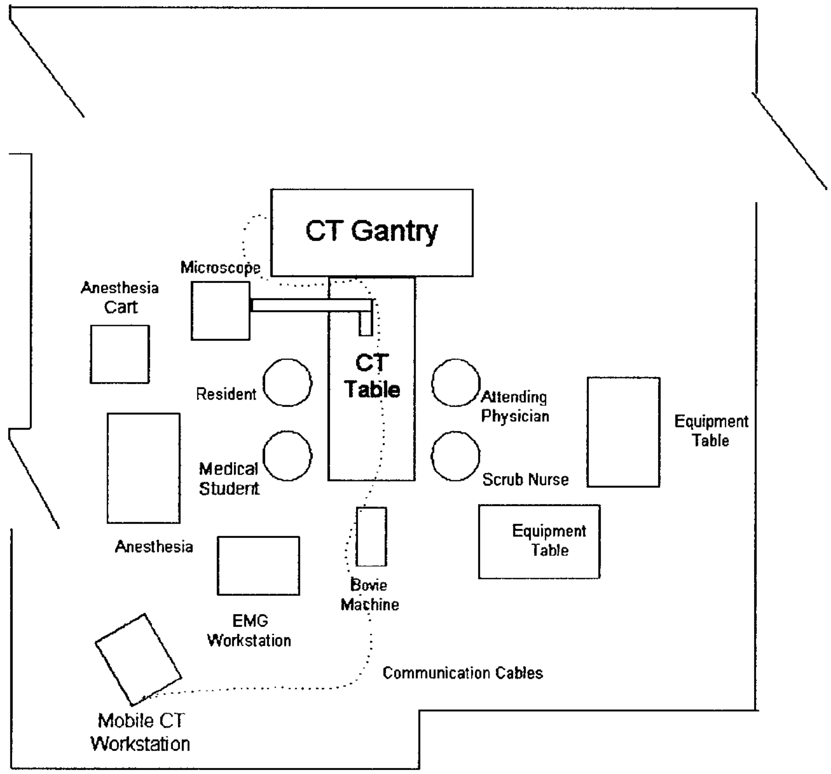

Figure 3: Equipment layout of operating room

Figure 4: Intraoperative use of CT during spine surgery

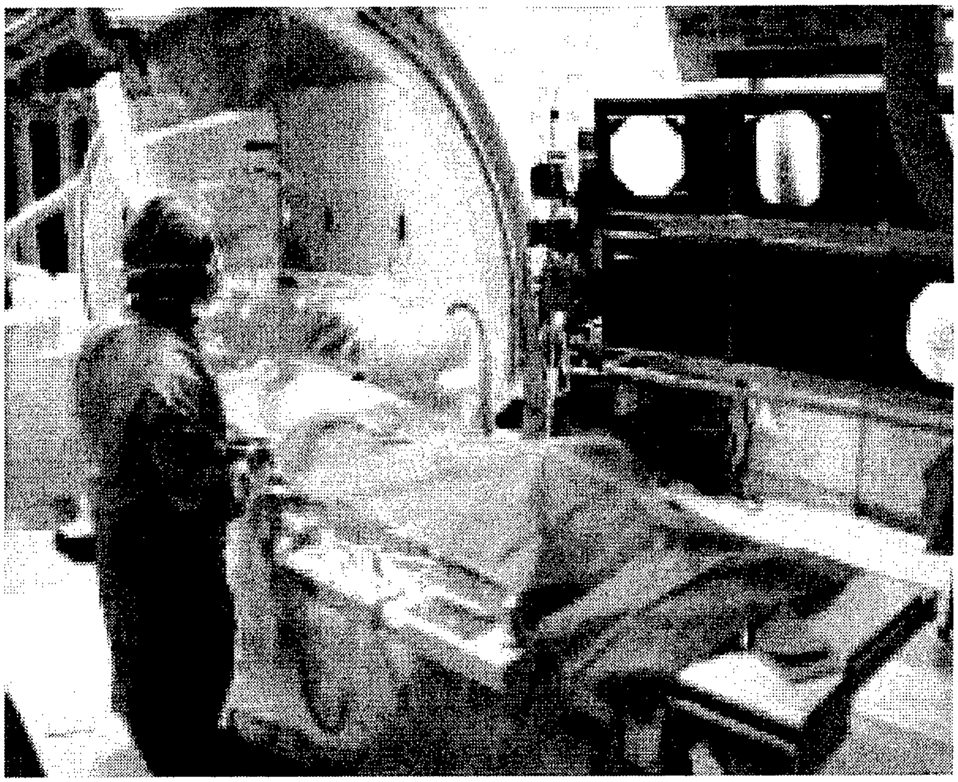

Figure 5: Bi-plane fluoroscopy in the interventional suite

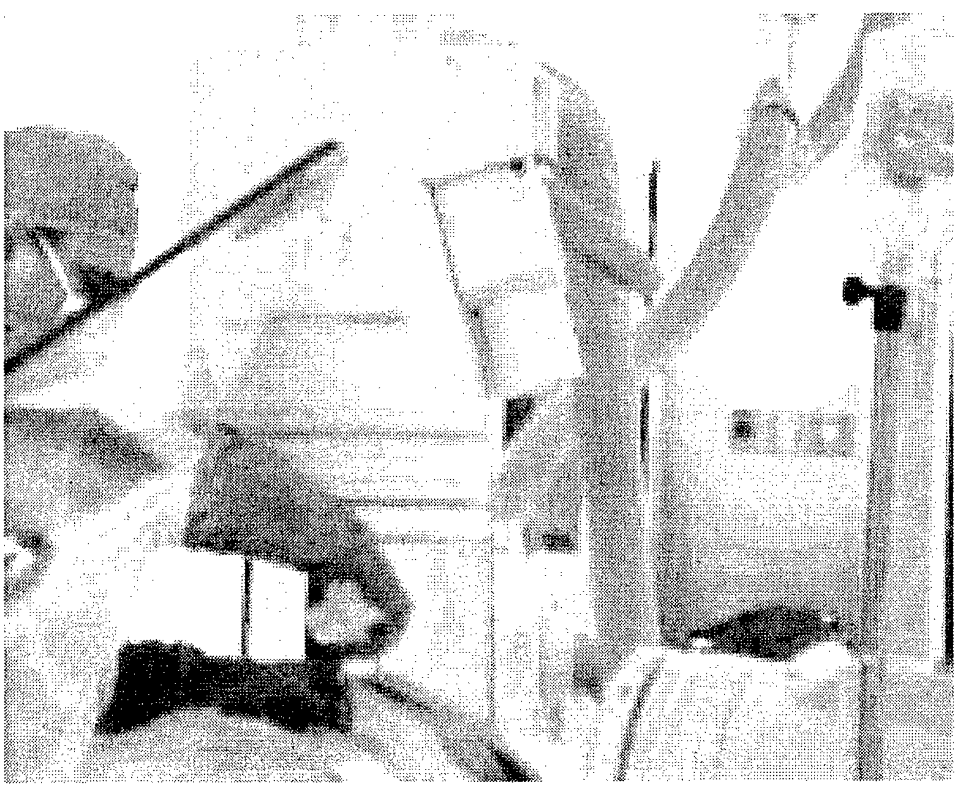

Figure 6: Injection of PMMA during percutaneous vertebroplasty

Figure 7: Preparing for mobile CT scanning in the interventional suite

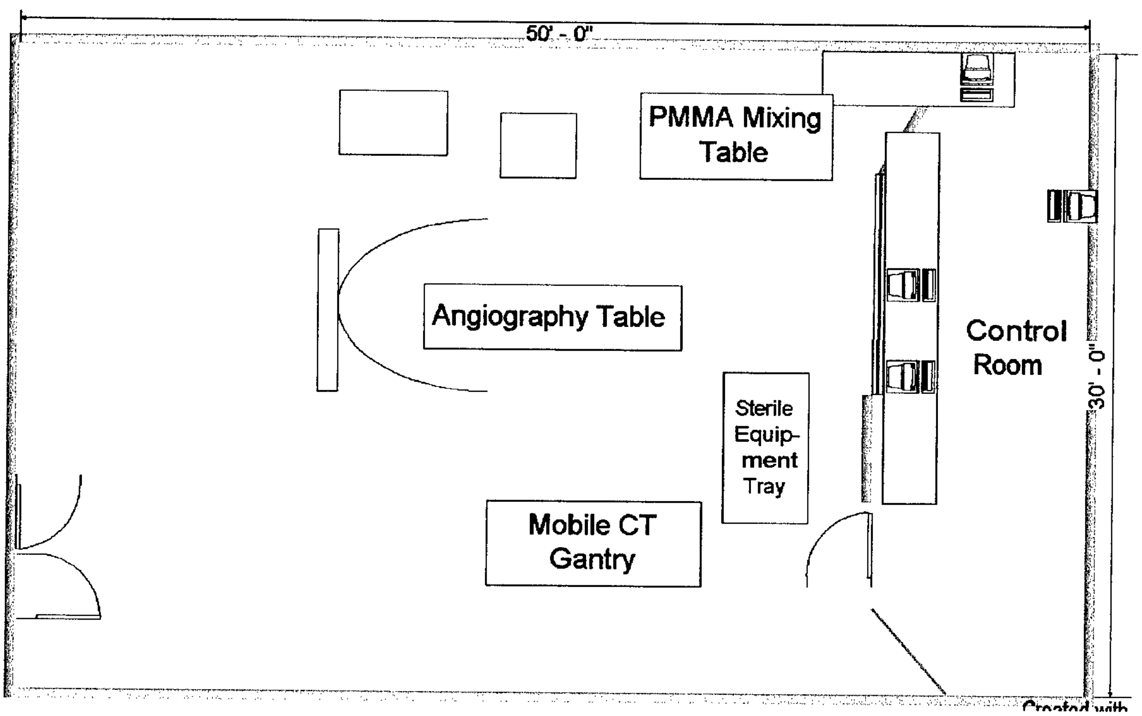

Figure 8: Interventional suite equipment layout

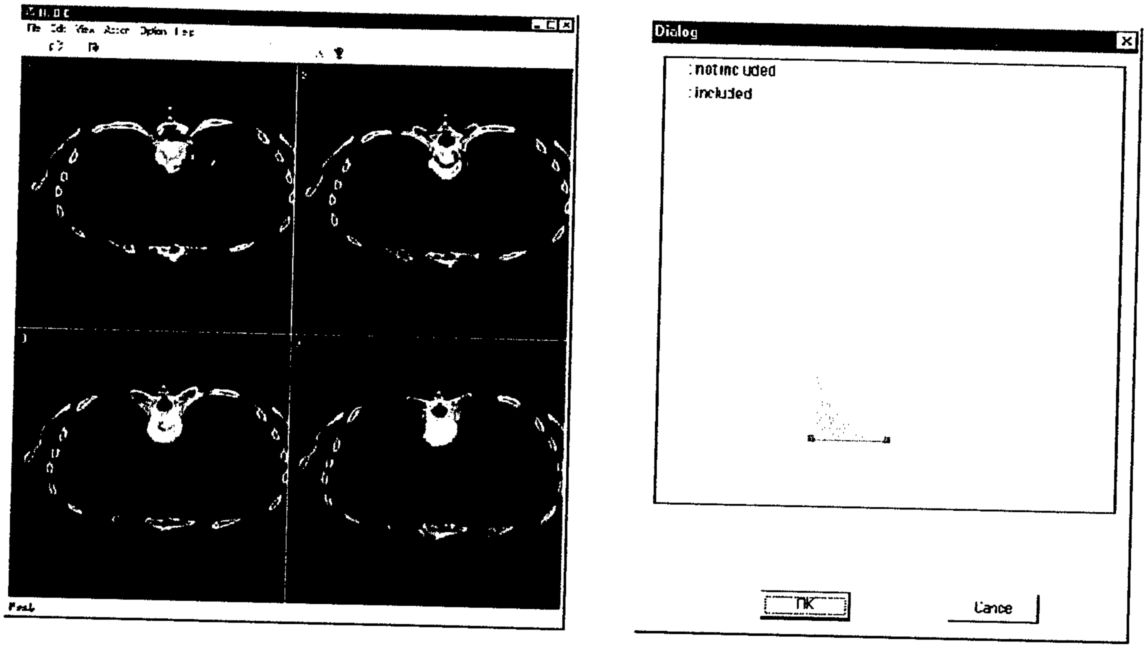

Figure 9: Thresholding of vertebroplasty images
(Left: thresholded images. Right: volume histogram.)

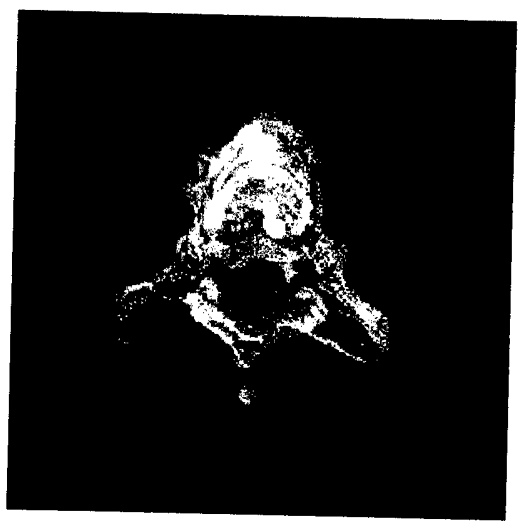

Figure 10: 3D visualization of bone cement

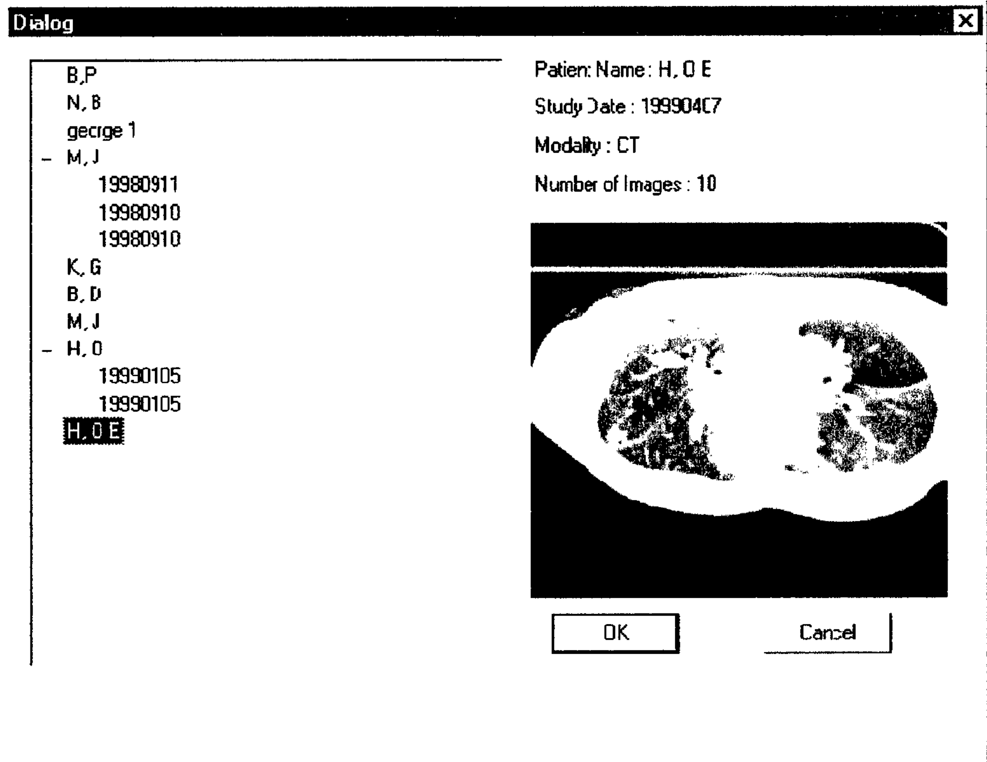

Figure 11: I-SPINE user interface

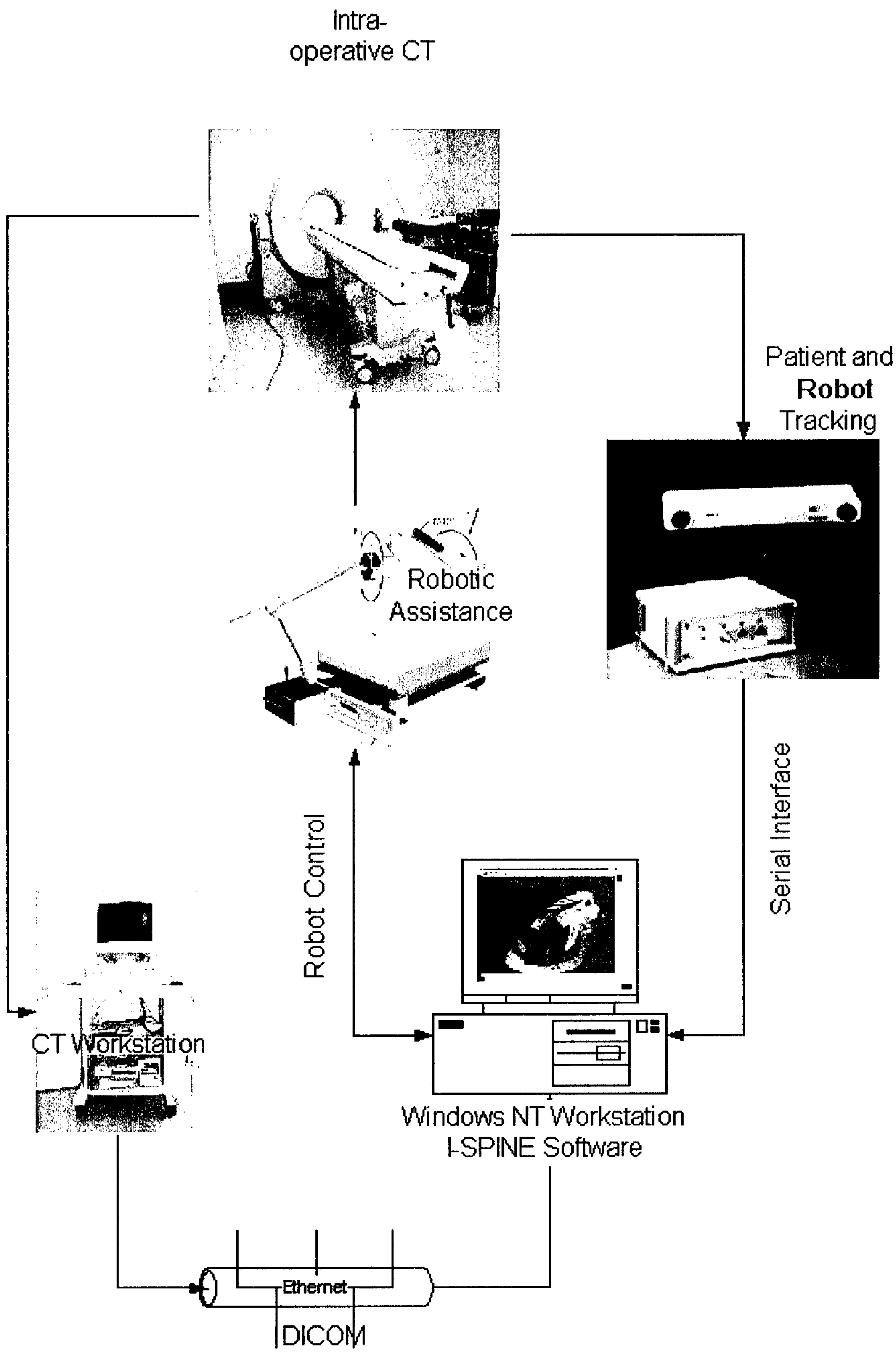

Figure 12: Robotic biopsy testbed concept architecture

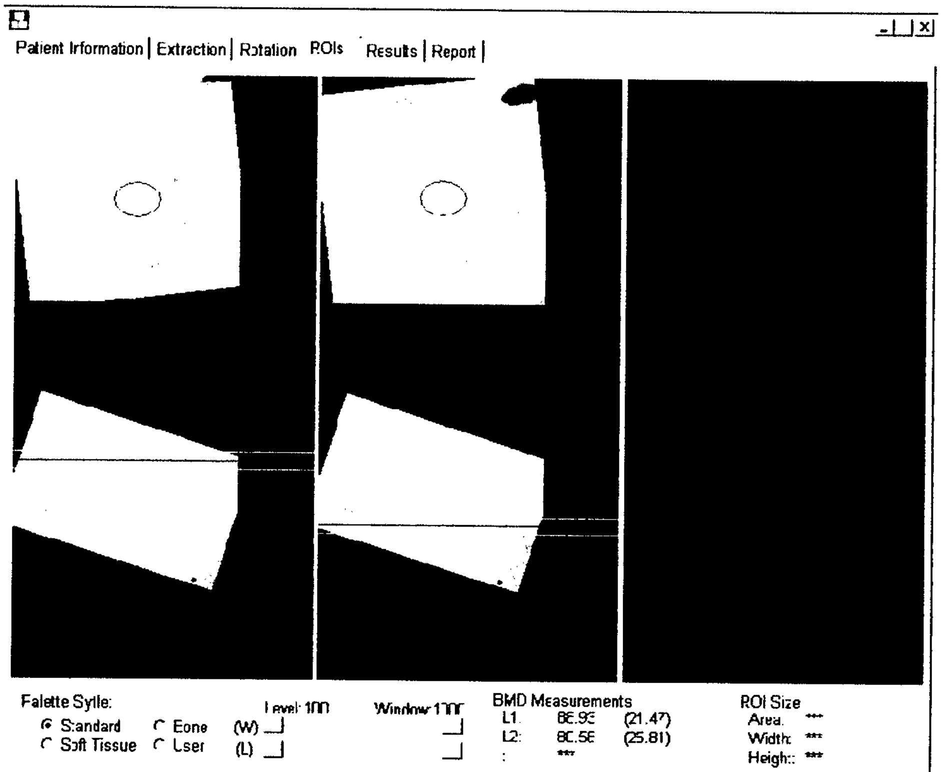

Figure 13. Quantitative CT (QCT) software demonstration interface

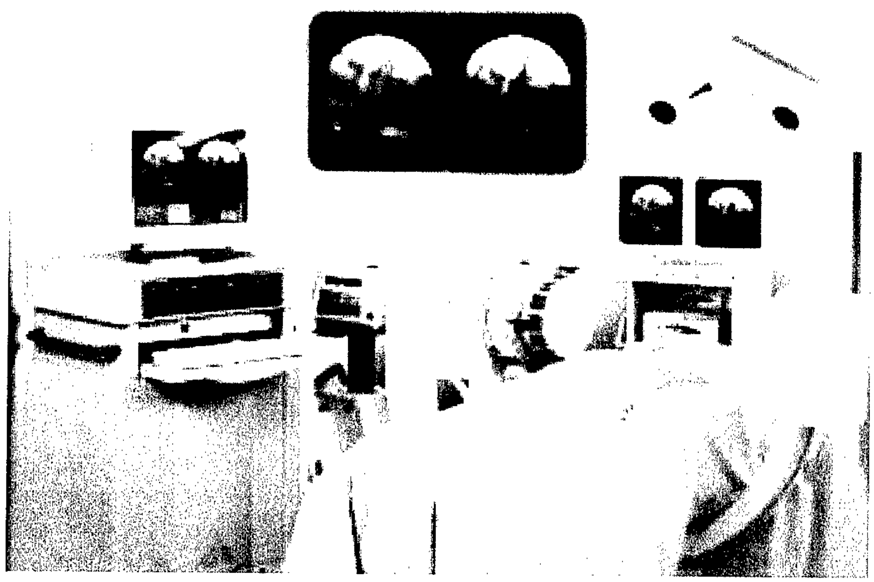

Figure 14. FluoroNav™ Fluoroscopy-Based Image-Guided Surgery System (Courtesy of Medtronic—Surgical Navigation Technologies)

11.2 Papers

Copies of the six conference papers published or submitted and the one journal paper submitted are reproduced in this section.

11.2.1 Choi 1999a: I-SPINE: a software package …

Reprint begins on the next page and is 6 pages long.

Presented at and to be published in the proceedings of the 1999 Applied Imagery Pattern Recognition workshop, SPIE, Oct 13-15, 1999, Washington, DC.

I-SPINE: A Software Package for Advances in Image-guided and Minimally Invasive Spine Procedures

Jae Jeong Choi[a], MS, Kevin Cleary[a*], PhD, Jianchao Zeng[a], PhD, Kevin Gary[b], PhD, Matthew Freedman[a], MD, Vance Watson[a], MD, David Lindisch[a], RT, Seong K. Mun, PhD[a]

[a]Imaging Science and Information Systems (ISIS) Center, 2115 Wisconsin Avenue, Suite 603, Radiology Department, Georgetown University Medical Center, Washington, DC, 20007
[b]Computer Science Department, The Catholic University of America, Washington, DC

Keyword List: visualization, image-guided, minimally invasive, spine, software, volume rendering

1.0 Introduction

While image guidance is now routinely used in the brain in the form of frameless stereotaxy, it is beginning to be more widely used in other clinical areas such as the spine. At Georgetown University Medical Center, we are developing a program to provide advanced visualization and image guidance for minimally invasive spine procedures. This is a collaboration between an engineering-based research group and physicians from the radiology, neurosurgery, and orthopaedics departments. A major component of this work is the ISIS Center Spine Procedures Imaging and Navigation Engine (I-SPINE), which is a software package under development as the base platform for technical advances.

This paper begins with a short overview of our program in Section 2, followed by an introduction to the I-SPINE software in Section 3. The vertebroplasty application is then presented in Section 4. In Section 5, a brief review of 3-D visualization and a modified algorithm for faster rendering are given, along with some example rendered images. The paper concludes with a summary in Section 6.

2.0 Program Overview

The long-range goal of this program is to improve the state of the art of minimally invasive spine surgery by developing a new generation of image-guided clinical techniques along with the necessary technology and equipment for their implementation. We plan to achieve this goal through a combination of technology developments and clinical feasibility studies. Specifically, we want to increase the accuracy with which instruments can be placed and manipulated, which we believe should improve diagnosis and treatment. The technology developments of interest here include:

- Intraoperative computed tomography (CT)
- 3-D visualization
- Instrument tracking
- Magnetic resonance imaging (MRI) and CT registration
- Mechanical guidance

The overall concept along with some of the equipment and technology is shown in Figure 1. While this figure shows an integrated system, it is more likely that only some of the components depicted will be used at one time. The intraoperative CT is currently in use for both operating room and interventional cases. A 3-D visualization module has been completed and will be described in this paper. Instrument tracking, in the form of an optical localizer, will be added in the next phase of the research along with mechanical guidance using a robotic device. The registration of intraoperative CT and pre-operative MRI has been demonstrated on test images, but is not currently feasible for clinical use.

3.0 I-SPINE Software

To analyze and manipulate the images used in this project, we have developed our own software package, called I-SPINE. This software is built on the Analyze™ toolkit from Mayo Clinic and runs on a Windows NT platform. This software provides basic functionality as well as a platform for specialized applications. The first specialized application was 3-D visualization of bone cement for vertebroplasty, which will be presented here.

* Author for correspondence. Email: cleary@isis.imac.georgetown.edu

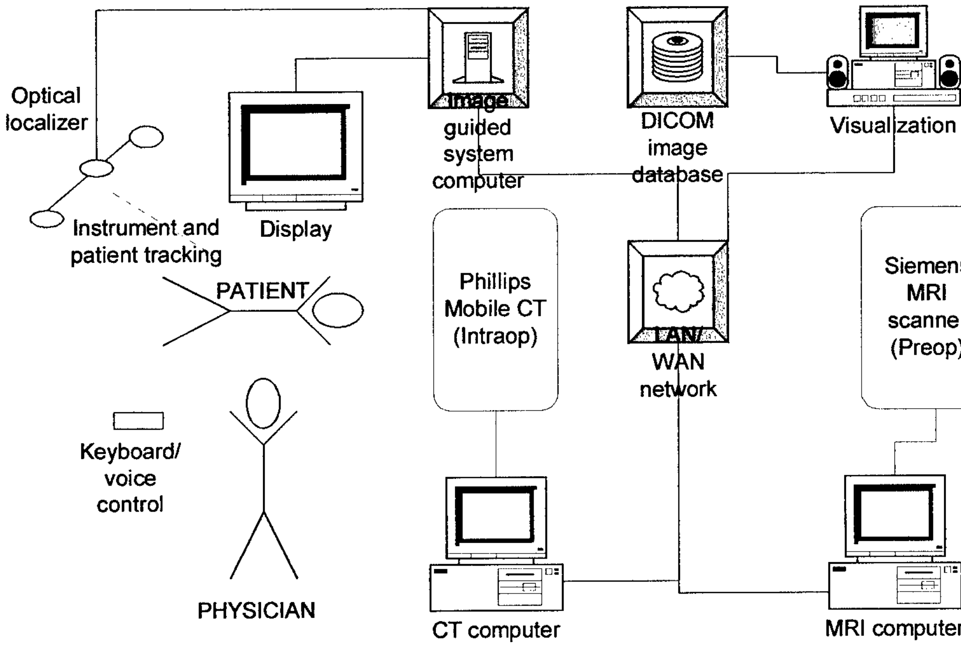

Figure 1: Project Overview

The I-SPINE software currently includes the following capabilities :

- DICOM receiver to accept images from mobile CT, fluoroscopy, and DSA units at Georgetown and elsewhere
- 2-D viewing of DICOM images (single slices or multiple slices up to 8 by 8)
- Segmentation function based on volume histogram
- Multi-surface 3-D visualization for applications such as vertebroplasty
- Registration of DSA images by manual pixel shifting

The opening screen of the software is shown in Figure 2. When the software is first invoked, the user is presented with a hierarchical list of patients and study dates. The user can then select a study and proceed to manipulate or view the images.

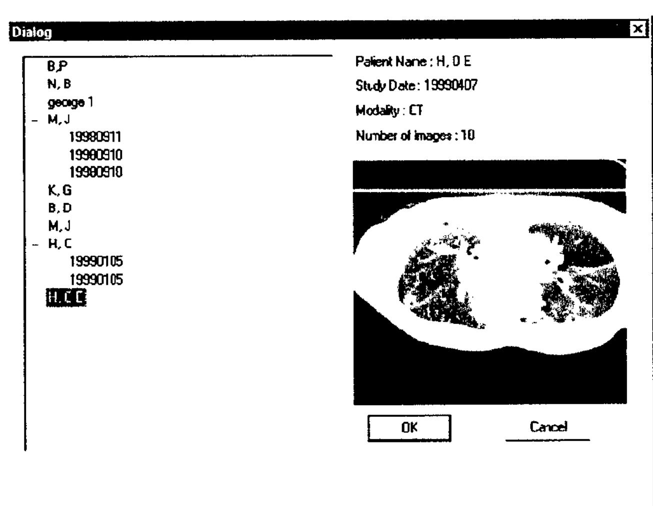

Figure 2: I-SPINE User Interface

4.0 Vertebroplasty Application

As a feasibility study, a 3-D visualization module has been created that can be used to examine the spread of bone cement after vertebroplasty procedures. Percutaneous vertebroplasty is a relatively new interventional technique in which polymethylmethacrylate (PMMA) bone cement is injected into the vertebral body to strengthen the body and stabilize the spine. After the PMMA is injected, a mobile CT is used to acquire a set of CT images. These images are then sent via DICOM over an Ethernet network to the I-SPINE system where the bone cement and vertebral body are segmented based on histogram windowing. The segmented volume is rendered by the multi-surface 3-D visualization algorithm that can visualize the vertebroplasty body and bone cement transparently. The visualization module is also able to compute the percent fill of the vertebral body.

Segmented images from a typical vertebroplasty case and the corresponding histogram are shown in Figure 3. In the following section, the development of the visualization algorithm will be discussed and some sample renderings will be shown.

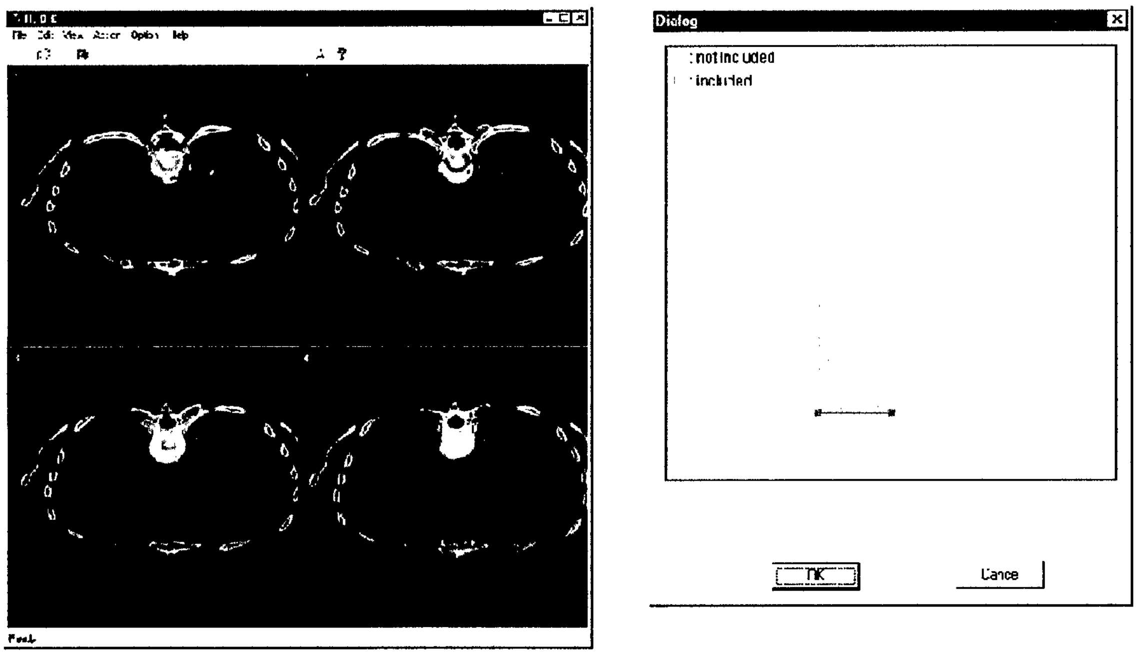

Figure 3: Thresholded Vertebroplasty Images and Histogram

5.0 3-D Visualization

The visualization of 3-D biomedical volume images may be classified into the two categories of surface rendering [1][2] and volume rendering [3][4][5][6]. Surface rendering techniques require the extraction of surfaces that have the same intensity value. The extracted surfaces are then rendered using standard computer graphics hardware. When the number of polygons generated by this technique is small, surface rendering algorithms provide adequate performance for interactive visualization. However, in many cases, the large number of polygons required cannot be easily managed, even on high-end graphics workstations. Disadvantages of surface rendering techniques are that the polygons must be generated again whenever the viewpoint is changed and volume information is not available, which is required if one wants to view the inside of the object.

Volume rendering techniques based on ray-casting algorithms display the volume directly without the need to convert the data to geometric primitives. However, volume rendering requires an enormous amount of computation because 3-D medical images are usually very large. A typical 3-D data set may consist of anywhere from 10 to 100 or more slices and each slice may be as large as ½ megabyte. For example, a CT data set from a spiral scanner typically has a resolution of 512 by 512 pixels and each pixel is stored in two bytes. Thus, a data set with 100 slices requires 50 megabytes of storage

space. With the increasing amount of random access memory (RAM) available in modern personal computers, these large data sets can be read into RAM, but the processing requirements to manipulate them are still very large.

In the I-SPINE software, the vertebroplasty procedure has been selected as a feasibility study. The goal of this study is to evaluate the usefulness of 3-D visualization in understanding how the bone cement spreads in typical cases. This requires that the bone cement and vertebral body be visualized transparently. Therefore, volume rendering algorithms are best suited for this application. However, typical volume rendering algorithms are too computationally expensive for real-time performance. To reduce the computation time, we have been developing an improved efficient ray-casting algorithm based on isosurface ray-casting volume rendering.

The isosurface volume ray-casting algorithm [7] is a recently proposed method for volume rendering, which renders the isosurface structure of volume data and requires less rendering time than traditional volume ray-casting. However, this algorithm cannot render multiple structures of volume data. In this paper, we present a volume rendering method that can render multiple isosurfaces as semi-transparent surfaces. This algorithm overcomes some of the limitations of current isosurface rendering methods and generates high quality images of volume data isosurface structures.

In the next section, the factors that affect the performance of traditional volume ray-casting algorithms are quantitatively analyzed. Performance improvements that we have applied include optimization methods such as minmax map, loose fitting minmax map hierarchy, and memory repositioning which enables interactive rendering of volume data. We also implemented cutting and blending methods of volume data with our system, the results of which show this algorithm has the characteristics of both surface rendering and direct volume rendering.

5.1 Visualization Algorithm

The traditional isosurface ray-casting volume rendering algorithm is an image-space algorithm. The following pseudo code illustrates the typical ray-casting volume rendering algorithm:

```
RAY_RENDERING()
 FOR each ray for the image
   FOR each sample point for the ray
     IF (the sample may contribute to the ray)
       Get shading value for the sample point
       and composite
```

As illustrated above, a typical ray-casting algorithm has two major computation components: traversal and composition. The traversal component includes sampling the voxel value in the volume data through the ray. The traversal component also includes the computation of which sampled values should be included. If the sampled value is selected in the traversal step, the composition component calculates the shading value and accumulates it to the pixel ray value. Following this breakdown, the total rendering time T_{render} is defined by the number of computations and the time for each computation as follows:

$$T_{render} = C_{traversal} \times N_{traversal} + C_{composition} \times N_{composition}$$

where C indicates the cost of each computation and N is the number of computation.

To develop a fast rendering algorithm, the goal is to reduce each term in the above equation. We use a minmax map to reduce $C_{traversal}$ and loose fitting minmax map to reduce $N_{traversal}$. To find the isosurface in the volume, the area including the isosurface value is determined by using a minmax map. A bisection algorithm is used to calculate the exact isosurface. The overall isosurface finding algorithm is:

```
GET_ISO_POINT(tl, tu)
  ASSERT D(tl) <= iso—value;
  ASSERT D(tu) >= iso—value;
  WHILE (|tl - tu| > epsilon){
      t <- (tl + tu) / 2;
      d <- D(t);
```

```
        IF (d > iso—value)      tu <- t;
        ELSE IF (d < iso—value) tl <- t;
        ELSE /* d == iso—value */ EXIT LOOP;
    }
    t_iso = t;
  /* RENDER_ISOSURFACE(t—iso) comes here */
```

This isosurface finding algorithm is used in the multiple isosurface volume rendering algorithm. The pseudo code of the multiple isosurface volume rendering algorithm is:

```
MULTI_ISO_TEST(t)
  d = D(t);
  WHILE (d ?= iso[iso—level + 1]) {
GET_ISO_POINT(t - s, t);
iso_level <- iso_level + 1;
  }
  WHILE (d < iso[iso—level]) {
GET_ISO_POINT(t, t - s);
Iso_level <- iso_level - 1;
}

iso—level <- 0;
MULTI_ISO_RENDER(t_min, t_max)
  FOR t <- t_min TO t_max WITH STEP s
MULTI_ISO_TEST(t);
```

5.2 Visualization Examples

The following figures show some images generated by the algorithm. First, we show some widely used medical image data sets and then show a vertebroplasty image. In Figure 4, some example head CT data sets (UNC head: 256 by 256 by 225 slices) are shown to illustrate the performance of our algorithm. The left image shows one isosurface (skull), while two isosurfaces are shown in the right image (skin and skull).

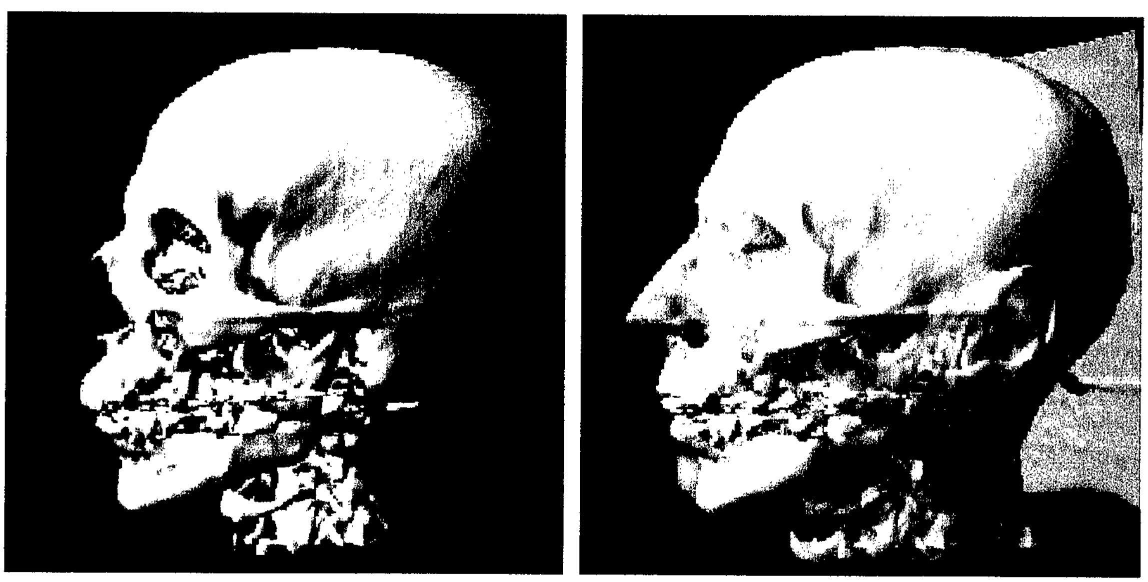

Figure 4: UNC Head Data Sets Rendered Using Improved Algorithm

Example vertebroplasty images rendered using our improved algorithm are shown in Figure 5. On the left side, all the bony anatomy is shown including the vertebral body and ribs. The bone cement is shown in white. On the right side, a close-up view of only the vertebral body is shown. Once again, the bone cement is in white.

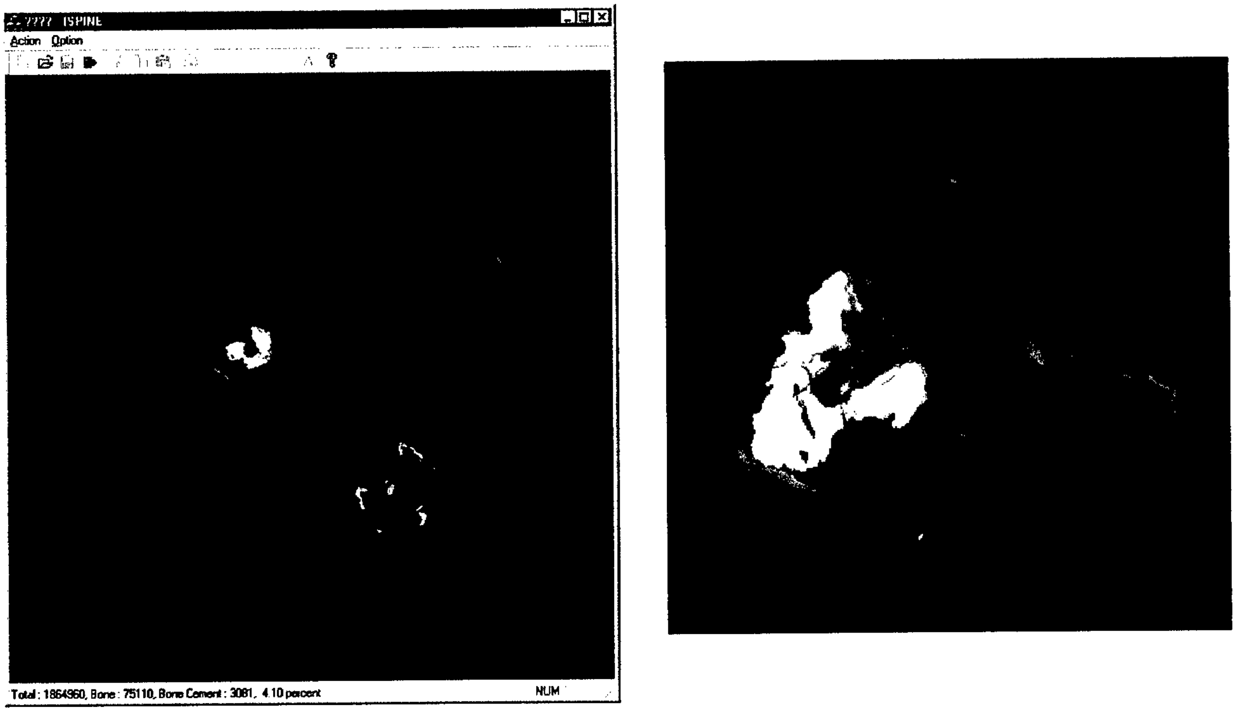

Figure 5: Vertebroplasty Rendered Images

6.0 Summary

This paper presented an overview of our work in image-guided spine procedures, with a focus on 3-D visualization for vertebroplasty. In the next step, we plan to assess the clinical usefulness of 3-D visualization for vertebroplasty by having the interventional neuroradiologist who performs the procedure evaluate a number of sample cases. The next phase of our program will involve the addition of a robotic device for needle spine biopsy procedures. The plan is to integrate a robotic device that could automatically orient a biopsy needle with the intraoperative CT scanner for the purpose of investigating the next generation of computer-assisted spine procedures.

Acknowledgements

This work was funded in part by U.S. Army grants DAMD17-96-2-6004 and DAMD17-99-1-9022. The content of this manuscript does not necessarily reflect the position or policy of the U.S. Government.

References

[1] Herman, G. T., Udupa, J. K. "Display of three-dimensional discrete surfaces." SPIE, 283, 90-97, 1981.

[2] Heffernan, P. B., Robb, R. A. "A new method for shaded surface display of biological and medical images." IEEE Transactions on Medical Imaging, MI-4, 26-38, 1985.

[3] Drebin, R., Carpenter, L., Hanrahan, P. "Volume rendering." SIGGRAPH '88, pp. 65-74, 1988.

[4] Levoy, M. "Display of surfaces from volume data." Computer Graphics Application., 8(3), 29-37, 1988.

[5] Hohne, K. H., Bernstein, R. "Shading 3-D images from CT using grey-level gradients." IEEE Transactions on Medical Imaging, MI-15, 45-47, 1986.

[6] Robb, R. A., Barilot, C. "Interactive display and analysis of 3-D medical images." IEEE Transactions on Medical Imaging, MI-8, 217-226, 1989.

[7] Parker, S., Shirley, P., Livnat, Y., Hansen, C. and Sloan, P. "Interactive ray tracing for isosurface rendering" IEEE Visualization '98 Conference Proceedings, 233-238, 1998.

11.2.2 Choi 1999b: Interactive multi-level isosurface rendering

Reprint begins on the next page and is 8 pages long.

Interactive Multi-Level Isosurface Rendering

Jae Jeong Choi[1,2], Yongjae Lee[3], Yeong Gil Shin[1], Kevin Cleary[2] and Seong Ki Mun[2]

1. Department of Computer Science, Seoul National University, Seoul, Korea
2. ISIS Center, Radiology Department, Georgetown University Medical Center, Washington, DC, USA
3. Triton Tech, Inc, Seoul, Korea

Abstract

We present an interactive multi-level isosurface rendering algorithm. The algorithm extends previous isosurface rendering techniques to represent multiple isosurfaces transparently. To achieve an interactive rendering rate, several optimization techniques are employed. In order to prune out unnecessary pixels and voxels, standard graphics hardware is used. This algorithm also employs LF-minmax map hierarchy, minmax map and memory repositioning for fast searching of isosurfaces. The experimental results show that the new algorithm generates a sharp and high-quality image interactively.

1. Introduction

While volume rendering is now widely used in many applications, it is still difficult to generate a good quality image interactively. In surface rendering [8, 9, 16], a set of geometry primitives are extracted from the volume and rendered by graphics hardware. Even if surface rendering is faster than direct volume rendering, surface rendering has some problems. First, surface rendering is not suitable for operations like cutting because the volume information is lost during the surface extraction process. Second, modifying an isosurface of interest is time consuming because the polygons to be rendered must be extracted again. Third, the rendered image is not smooth when the image is enlarged due to the nature of polygon rendering [7].

Ray casting [3, 4, 5, 6, 11] is the most frequently used algorithm in direct volume rendering [2, 3, 4, 5, 6, 11, 14, 15]. Ray casting generates rays from a viewpoint through each screen pixel into volume space. Voxels are sampled along the ray, and the density value at a sample point is obtained by trilinear interpolation from eight voxels surrounding the sample point. The sampled voxels are accumulated to determine the pixel's intensity. Ray casting is able to generate a high-quality image, but ray casting requires a great deal of computational power and may not resolve thin-layer objects [7].

Isosurface rendering [7, 10, 12] was introduced recently and is similar to ray casting. Isosurface rendering finds the intersection of a ray and an isosurface and calculates a shading value at the intersection point instead of accumulating sampled values along the ray. While ray casting requires many composition operations for each ray, isosurface rendering performs only one composition per ray, which makes the algorithm faster and the rendered image sharper. However, previous isosurface rendering algorithms can render only one isosurface, which makes it impossible to represent multiple objects transparently.

This paper presents an extended isosurface rendering algorithm that is able to render multiple isosurfaces transparently. This algorithm generates a high-quality image from isosurface structures of volume data.

Using standard graphics hardware, isosurface rendering performance can be greatly enhanced. Performance enhancement is achieved by disregarding unnecessary pixels and voxels. The multi-level isosurface rendering algorithm also uses three other optimization techniques to improve rendering performance. These techniques are 1) LF-minmax map hierarchy; 2) minmax map; and 3) memory repositioning.

In the next section, ray casting and isosurface rendering are analyzed to show that isosurface rendering is more efficient. In Section 3, the new multi-level isosurface rendering algorithm is introduced. The performance enhancement techniques using standard graphics hardware, LF-minmax map hierarchy, minmax map and memory repositioning are described in Section 4. In Section 5, example rendering results and computation times are shown. Finally, conclusion and suggestions for future work are given.

2. Rendering Time: Ray Casting Versus Isosurface Rendering

Ray casting and isosurface rendering are both image-order algorithms. These algorithms compute pixel

(a) ray casting

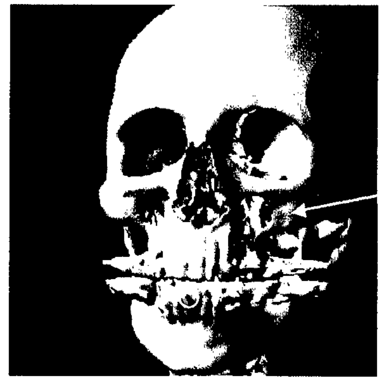

(b) isosurface

Figure 1. Ray casting and isosurface rendered images from the UNC "bighead" data set. Note that the right image is shaper than the left image. In particular, note the "bump" below the mouth (circle) and the region to the right of the nose (arrow).

intensity by traversing the ray generated from a viewpoint through a pixel.

These algorithms consist of two operations: traversal and composition. A traversal operation includes a test as to whether a sampled voxel contributes to the pixel. This test will be called the "skipping test". A composition operation calculates a shading value at the sample point and accumulates it to the ray's intensity value. The total rendering time T_{render} is defined as follows in Equation 1:

$$\begin{aligned} T_{render} &= T_{trav} + T_{comp} \\ &= C_{trav} \times N_{trav} + C_{comp} \times N_{comp} \qquad (1) \\ &= C_{trav} \times (N_{skip} + N_{comp}) + C_{comp} \times N_{comp} \end{aligned}$$

where

T_{trav} : total traversal time
T_{comp} : total composition time
C_{trav} : cost for one traversal operation
C_{comp} : cost for one composition operation
N_{trav} : number of traversal operations
N_{comp} : number of composition operations
N_{skip} : number of traversal operations that pass the skipping test

Equation 1 shows how sampled voxels that pass the skipping test affect the total rendering time. To estimate the percentage of composition operations in ray casting and isosurface rendering, the rendering time was measured and the number of traversal and composition operations was counted in a sample data set. For this experiment, the "bighead" volume data set (256x256x 225) provided by the University of North Carolina was used to generate a 400 by 400 image with each algorithm as shown in Figure 1.

Table 1 shows the results of the computation counts and rendering time. The fourth row in Table 1, "Traversal only", is the algorithm modified so as to not perform composition operations in isosurface rendering. The algorithm was modified to measure the number of traversal operations and traversal time. The composition operations are only 1.9% of the number of operations in ray casting and 0.4% in isosurface rendering. From Table 1, the contribution of the composition operations to the total rendering time is computed as follows:

$$C_{trav} = \frac{2984}{22503213} = 0.0001326 \quad (m\text{sec})$$

$$P_{comp,ray} = \frac{7716 - C_{trav} \times N_{trav,ray}}{7716} = 58.9\%$$

$$P_{comp,iso} = \frac{3860 - C_{trav} \times N_{trav,iso}}{3860} = 20\%$$

where

$P_{comp,ray}$: percentage of composition in ray casting
$P_{comp,iso}$: percentage of composition in isosurface rendering
$N_{trav,ray}$: number of traversal operations in ray casting
$N_{trav,iso}$: number of traversal operations in isosurface rendering

Table 1. The experimental results of the algorithms. (Minmax map is used.)

Method	N_{trav}	N_{comp}	N_{comp}/N_{trav}	Rendering time (msec)
Ray casting	23893237	463839	0.019	7716
Isosurface	23262899	96809	0.004	3860
Traversal only	22503213	0	-	2984

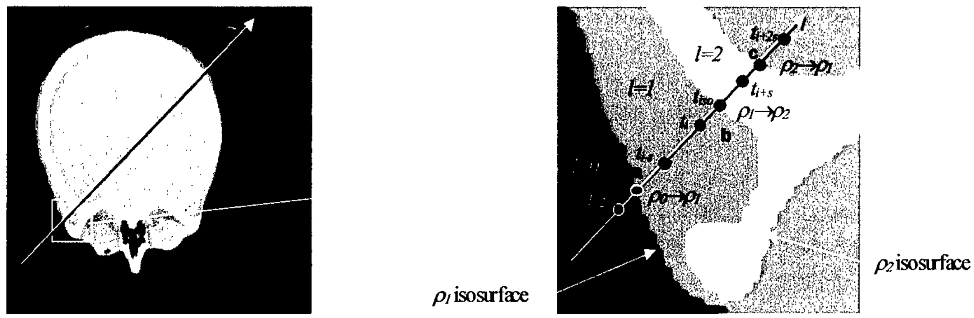

(a) (b)

Figure 2. The multi-level isosurface rendering algorithm

(a) A 2D slice image

(b) The magnified view of the rectangle in (a). The image has two isosurfaces, ρ_1 and ρ_2. l is a level of the ray.

The results show that rendering time is very much affected by traversal time in isosurface rendering. Therefore, in isosurface rendering, reducing the traversal time will greatly contribute to reducing the rendering time. The optimization techniques to reduce the traversal time will be discussed in Section 4 .

3. Multi-Level Isosurface Rendering

In this section, a new multi-level isosurface rendering algorithm is introduced. First, the rendering algorithm for a single isosurface is discussed. It is assumed that each voxel represents the density of material at the point and an isosurface value is represented as a certain density value. The condition that an isosurface lies in the interval $[t_i, t_{i+s}]$ is :

$$D(t_i) \le d_{iso} \le D(t_{i+s}) \quad \text{or}$$
$$D(t_{i+s}) \le d_{iso} \le D(t_i)$$

where

t_i : distance from the viewpoint to the point i
$D(t_i)$: density value at t_i
d_{iso} : isosurface density value
s : sampling distance

When the above condition is satisfied, there exists t_{iso} in $[t_i, t_{i+s}]$, which meets the following condition since the interpolation function is continuous.

$$\text{Condition : } D(t_{iso}) = d_{iso}, t_i \le t_{iso} \le t_{i+s}$$

To find the exact isosurface, analytic methods can be used, as discussed by other researchers [7, 10]. The analytic methods are fast, but there are some trade-offs in image quality and rendering time. In this algorithm, a bisection method is used to find the isosurface because it generates a better image than analytic approach [7].

The multi-level rendering algorithm will now be explained. The example shown in Figure 2 has two isosurfaces, denoted by the density values ρ_1 and ρ_2. A sample ray is also shown, and the initial level of the ray is zero. Voxels are sampled along the ray at equally spaced intervals. When the sampled value becomes greater than ρ_1 (here, at the point t_{i-s}), the algorithm finds the exact isosurface for ρ_1 (point **a**), increases the level of the ray by one and continues to find the next isosurface. At the point t_{i+s}, the sampled value is larger than ρ_2. The algorithm finds the exact isosurface for ρ_2 (point **b**), sets the level of the ray to two, and continues. The opposite case occurs at the point t_{i+2s}, where the sampled value becomes smaller than ρ_2. In this case, the algorithm finds the isosurface for ρ_1 (point **c**), and decreases the level to one.

Now, the example given above will be extended to formalize a multi-level isosurface rendering algorithm. In the case of m isosurfaces, a list of isosurfaces can be defined as follows :

ρ_0 : minimum density value
$\rho_1, \ldots, \rho_m$: sorted list of density values of isosurfaces in increasing order
ρ_{m+1} : maximum density value

Along a ray, for a sampled position of the ray t_i and at a level l, $D(t_i)$ satisfies :

$$\rho_l \le D(t_i) \le \rho_{l+1}$$

At the next position t_{i+s}, the following two conditions are checked to determine whether the interval $[t_i, t_{i+s}]$

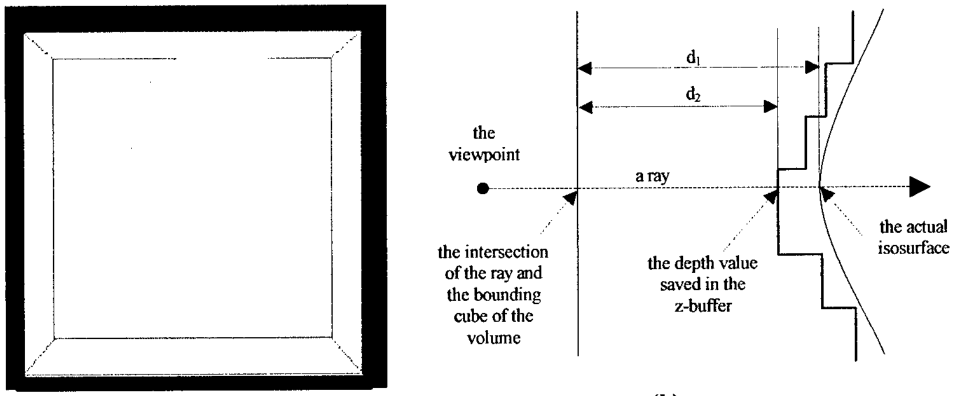

(a) (b)

Figure 3. Enhancement possible with graphics hardware

(a) An example depth image. Unnecessary pixels (white area) can be skipped.
(b) Illustration shows how using a depth value, d_1-d_2 traversal operations can be saved.

includes isosurfaces :

Condition (a): $D(t_{i+s}) \geq \rho_{l+1}$

Condition (b): $D(t_{i+s}) < \rho_l$

When condition (a) is satisfied, the interval includes the ρ_{l+1} isosurface. The rendering algorithm thus calculates a shading value on the ρ_{l+1} isosurface and increases the level l by 1. When condition (b) is satisifed, the interval includes the ρ_l isosurface, so the rendering algorithm calculates a shading value on the isosurface ρ_l and decreases the level l by 1. This process is repeated until the sample position exits the volume or the accumulated opacity exceeds an opacity threshold.

4. Fast Rendering of Isosurfaces

Several optimizations are employed to reduce the traversal time as well as the composition time. To reduce the number of traversal operations, standard graphics hardware and an LF (Loose Fitting) minmax map are employed. To decrease the cost for a traversal operation, a minimax map is used. To decrease the cost for a composition operation, voxels can be repositioned within memory.

4.1 Graphics Hardware

Standard graphics hardware has been mainly applied to surface rendering. In some papers [1, 13, 17], there have been attempts to use graphics hardware in direct volume rendering. However, no one has attempted to use standard graphics hardware in ray casting because of the nature of ray casting.

We use standard graphics hardware in our rendering pipeline to reduce rendering time. The rendering algorithm consists of the following steps:

1. Generate a minmax map of the proper size.
2. Prune out unnecessary blocks in the minmax map using graphics hardware.
3. Perform ray casting using the remained blocks.

A minmax map is used for pruning out the regions of voxels which do not contain surfaces. Also, the minmax map saves traversal time.

When the minmax map of the proper size is determined, bounding cubes of the minmax blocks which contain isosurfaces are put into a display list in OpenGL. After the polygons in the display list are rendered, a depth buffer contains the distance from a viewpoint to the nearest polygon that includes isosurfaces. If the depth value of a pixel is the default value, the algorithm does not have to generate a ray for the pixel. For example, in Figure 3(a), pixels in the white part are unnecessary. In this way, we can prune out unnecessary minmax blocks.

The depth values saved in the depth buffer allow for unnecessary voxels to be skipped. An example is shown in Figure 3(b). In typical rendering algorithms, a ray samples all voxels within the intersection of the ray and the bounding cube of the volume. However, by using the depth value in the z-buffer, only voxels from the depth value of the pixel need to be sampled, which saves the d_1-d_2 traversal operations, as shown in Figure 3(b).

When a fine-grained minmax map is employed with graphics hardware, a more accurate skipping test can be performed using surface polygons of smaller cubes, but performance is degraded. Therefore, to achieve interactive rendering, the appropriate size of the minmax map is chosen according to the capability of the graphics hardware.

4.2 LF(Loose-Fitting) Minmax Map

When voxels are adjacent in the volume, their density values are similar. This property is called "spatial coherence". To exploit this property, some algorithms used a hierarchical data structure such as an octree to traverse the volume efficiently [4]. However, an octree requires a complex operation to advance along the ray. To simply advance along the ray, we propose an LF (Loose-Fitting) minmax map. Another advantage of an LF minmax map is that a minmax map of an arbitrary size can be created, which makes it simple to create a hierarchical data structure suitable for volume data.

In a traditional octree hierarchical structure, the intersection points **a, b, c, d** in Figure 4(a) have to be checked to find the nodes I, II, III that may contribute to the ray. In the LF-minmax map, the nodes are checked with equal spacing as shown by points **a, b, c** in Figure 4(b). In this case, it is possible to miss the part of the line labeled **i** in Figure 4(b) and corresponding to the line between points **b** and **c** in Figure 4(a). This can result in an inaccurate skipping test. To solve this problem, we expand each node in the LF-minmax map to cover a larger area than the original area. The function to compute an intermediate level node is $f(x,y,z) = n_{\lfloor x/m \rfloor \lfloor y/m \rfloor \lfloor z/m \rfloor}$ where the sampling point is (x, y, z) and the size of the intermediate level is $m \times m \times m$. The node $n_{i,j,k}$ saves the minimum and maximum value in the region of $[mi-\beta, mi+m+\beta]$, $[mj-\beta, mj+m+\beta]$, $[mk-\beta, mk+m+\beta]$. Using the larger β value prevents the ray from missing the interval **bc** in Figure 4(a). The shaded part in Figure 4(d) represents the part that can cause a problem when the sampling distance and node size are the same.

The larger the value of β, the less chance the sample will be missed, but the more chance the skipping test will fail. Therefore, the smallest β that does not miss the sample should be chosen. When the node size is 1 and the sampling distance is 1, the best value of β is $\frac{1}{2\sqrt{2}}$ as shown in Figure 4(d).

When an LF-minmax map is used as an intermediate level of the hierarchical structure for the skipping test, the skipping test is performed using the sampling distance of the intermediate level. If the skipping test fails, the level of the LF-minmax map is decreased. Assume that the size of a node is $m \times m \times m$ and the sampling distance is m. If the skipping test fails at the sampling point t, the interval that may include the isosurface is $[t-m, t+m]$. Therefore, the algorithm checks the minmax map in the lower level and resumes at the $t+m$ point.

4.3 Minmax Map

Each skipping test must check as to whether a sample contributes to the ray. The skipping test computes a sample point from eight neighbor voxels. If the minimum and the maximum values for the eight neighborhood voxels are known, the skipping test is simple because only the minimum and maximum values are checked instead of using trilinear interpolation [4, 10].

4.4 Memory Repositioning

Current CPUs employ high-speed cache memory between the main memory and processor to improve performance. In the isosurface rendering as well as ray casting, the voxel data is referenced often. By repositioning the voxel data within the memory, algorithm performance is increased due to the spatial

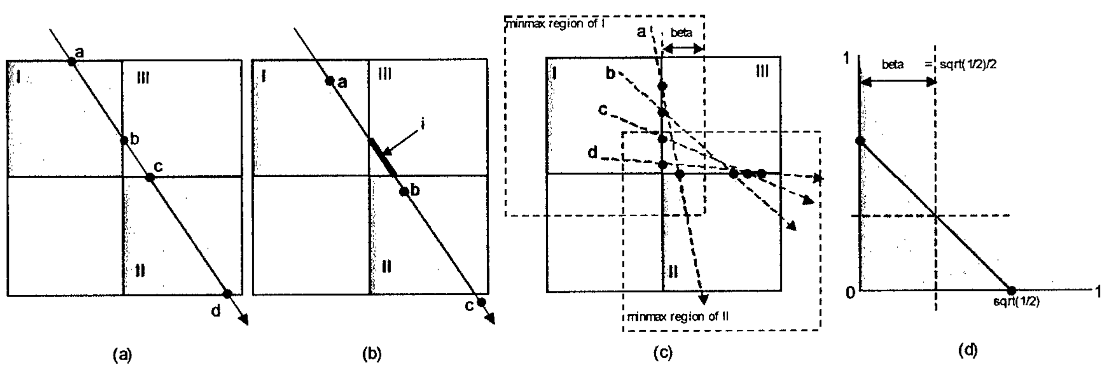

Figure 4. The construction process of LF-minmax map

(a) Node a, b, c, d are checked when using octree, which makes the advance operation complex

(b) Nodes are checked in regular step when using LF-minmax map

(c) The range of minimum and maximum value of each node in the LF-minmax map

(d) The appropriate β value when the size of node is 1x1x1

coherence [10].

5. Results

The isosurface rendering algorithm presented here was applied to a number of sample images as shown in Figure 5. To show the image quality and rendering performance, the first three data sets are well known (Figures 5(a-e)): bighead CT (256x256x225), engine block CT (256x256 x110), and brain MR (128x128x84). Figure 5(f) shows a vertebral body with two isosurfaces. This is from ongoing work at Georgetown University Medical Center, and was developed to visualize the spread of bone cement after a medical procedure. The images are from a mobile CT scanner and the resolution of the data set is 124x132x10. The peanut volume data set (128x128x128) shown in Figures 5(g-h) is acquired from the simulation of an energy field. This data set was developed to test our algorithm in the multi-level case.

The algorithm is also able to represent a cutting plane with blending. Figure 6 shows images that include a cutting plane.

The algorithm was tested on a Silicon Graphics Onyx 10000 (196 Mhz R10000 processor, InfiniteReality Graphics board, 512 MB). To analyze the performance, we implemented graphics hardware acceleration, LF-minmax hierarchy, minmax map and memory repositioning modules on the base multi-level isosurface rendering algorithm. These optimization techniques did not affect the image quality.

Table 2 shows the performance of each optimization techniques in generating the 256 by 256 pixel images shown in Figure 5. With each volume set, three experiments were done: "brute-force", "Minmax+LF+ Memory", and "Minmax+LF+Memory+Graphics Hardware". "Brute-force" is the algorithm that does not use any optimization technique. "Minmax+LF+Memory" uses the three optimization techniques, which are minmax map, LF-minmax hierarchy and memory repositioing without using graphics hardware. "Minmax+LF+Memory+Graphics Hardware" uses all optimization techniques.

The table also shows the improvements in rendering speed for each experiment. The speed improvement varies with the characteristics of the data set. Note that even if all three optimization techniques are used, rendering can still be done 2-4 times faster with standard graphics hardware. The time overhead for rendering polygons is within 30 miliseconds.

6. Conclusion and Future Work

This paper has presented an interactive multi-level isosurface rendering algorithm. Isosurface rendering has advantages of both surface rendering and direct volume rendering. Isosurface rendering can generate a sharp and high-quality image from an isosurface in the volume like surface rendering. Isosurface rendering is also able to represent the inside of the volume data, which is a property of direct volume rendering.

Ray casting and isosurface rendering were analyzed to show that isosurface rendering is more efficient. Based on this analysis, we developed an extended isosurface rendering algorithm to represent multiple isosurfaces transparently. To achieve an interactive rendering rate, several optimization techniques are employed. In order to prune out unnecessary regions of volume, standard graphics hardware is used. This algorithm also employs LF-minmax map hierarchy, minmax map and memory repositioning for fast searching of isosurfaces. The experimental results show that the new algorithm generates a sharp and high-quality

Table 2. The performance of optimization techniques

Data set	# of isosurfaces	Brute-Force (unit : ms)	Minmax + LF + Memory (unit : ms)	Minmax + LF + Memory + Graphics Hardware (unit : ms)	Speedup Factor (Column 3/ Column 5)
Engine	1	7298.4	814.8	288.6	25.29
	2	8366.5	1193.6	672.3	12.44
Brain	1	2563.2	848.1	443.2	5.78
Bighead	1	16345.7	1254.4	386.6	42.28
	2	16817	2093.4	1273.8	13.20
Spine	2	452.5	423	247.9	1.83
Peanut	1	7604.5	979.9	238.4	31.90
	2	7938.5	1112.1	376	21.11
	3	8288.8	1254.5	506.5	16.36
	4	8530.1	1359.8	614.4	13.88
	5	8820.3	1451.3	710.5	12.41

image interactively.

In our experience, the rendering performance of the optimization techniques is affected by the characteristics of volume data. Therefore, in future work, how the structural characteristics of volume data affect the performance of optimization techniques should be studied.

As hardware is being developed rapidly, new rendering techniques that take advantage of hardware are required. This paper discussed how to use standard graphics hardware in isosurface rendering. In the future, other hardware, such as parallel processors, might be used with this algorithm to improve the rendering time.

Acknowledgements

This work was funded in part by U.S. Army grant DAMD17-99-1-9022. The content of this manuscript does not necessarily reflect the position or policy of the U.S. government.

References

1. Cabral, B., Cam, N., Foran, J., "Accelerated Volume Rendering and Tomographic Reconstruction Using Texture Mapping Hardware", *ACM Symposium on Volume Visualization 94* : 91-98, 1992
2. Danskin, J., Hanrahan, P., "Fast algorithms for volume ray tracing", *The 1992 Workshop on Volume Visualization* : 91-98, 1992
3. Glassner, A., "Space Subdivision for Ray-tracing", *IEEE Computer Graphics and Applications*, 4 : 15-22, 1984
4. Levoy, M., "Efficient Ray Tracing of Volume Rendering", *ACM Transactions on Graphics*, 9 : 245-261, 1990
5. Levoy, M., "Volume Rendering : Displays of Surfaces from Volume Data", *IEEE Computer Graphics and Applications*, 8, 29-37 : 1988
6. Levoy, M., "Volume Rendering by Adaptive Refinement", *The Visual Computer*, 6 : 2-7, 1990
7. Lin, C., Ching, Y., "An Efficient Volume-Rendering Algorithm with an Analytic Approach", *The Visual Computer*, 12(10) : 515-526, May 1996
8. Lorensen, W., Cline, H., "Marching Cubes : a high resolution 3D surface construction algorithm", Computer Graphics, 21 : 163-169, 1987
9. Montani, C., Scatenni, R., Scopigno,. R., "A Modified Lookup Table for Implicit Disambiguation of Marching Cubes", The Visual Computer, 10 : 353-355, 1994
10. Parker, S., Shirley, S., Livnat, Y., Hansen, C., Sloan, P., "Interactive Ray Tracing for Isosurface Rendering", *IEEE Visualization 98* : 233-238, 1998
11. Tiede, U., Hohne, K., Bomans, M., Pommert, A., Riemer, M., Wiebecke, G., "Investigation of Medical 3D-Rendering Algorithms", *IEEE Computer Graphics and Applications*, 10, 41-53, 1990
12. Tiede, U., Schiemann, T., Hohne, K., "High Quality Rendering of Attributed Volume Data", *IEEE Visualization 98* : 255-262, 1998
13. Van Gelder, A., Kim, K., "Direct Volume Rendering with Shading via Three-Dimensional Textures", *1996 Volume Rendering Symposium* : 23-30, 1996
14. Westover, L., "Footprint Evaluation for Volume Rendering", *Computer Graphics*, 24, 367-376, 1990
15. Wilhelms J., Van Gelder, A., "A Coherent Projection Approach for Direct Volume Rendering", *Computer Graphics*, 25 : 275-283, 1991
16. Wilhelms J., Van Gelder, A., "Octrees for Faster Isosurfaces Generation Extended Abstract", Computer Graphics, 24 : 367-376
17. Wilson, O., Van Gelder, A., Wilhelms, J., "Direct Volume Rendering via 3D Textures", *Technical Report UCSC-CRL-94-19*, University of California, Santa Cruz, 1994

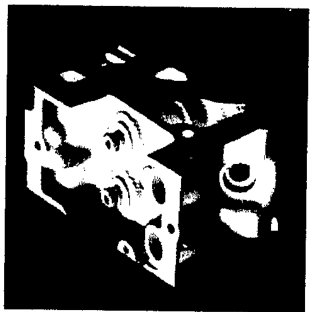

(a) Engine Block – 1 isosurface

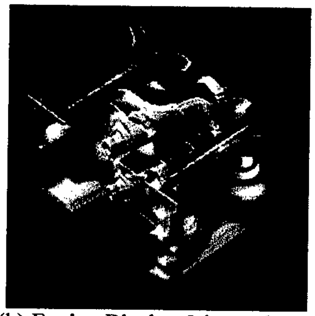

(b) Engine Block – 2 isosurfaces

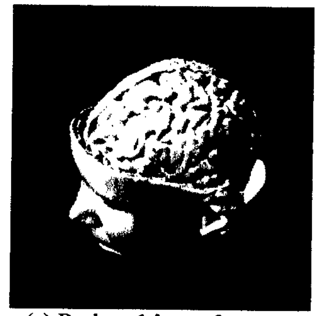

(c) Brain – 1 isosurface

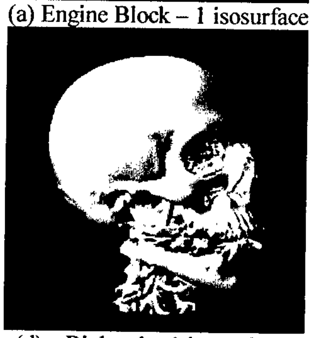

(d) Bighead – 1 isosurface

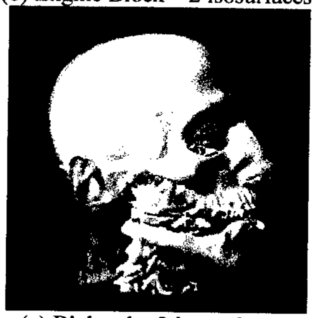

(e) Bighead – 2 isosurfaces

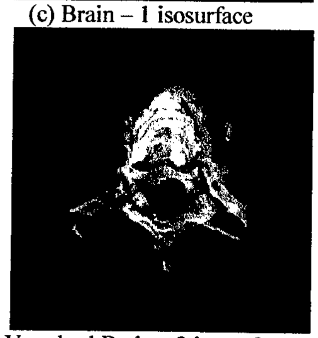

(f) Vertebral Body – 2 isosurfaces

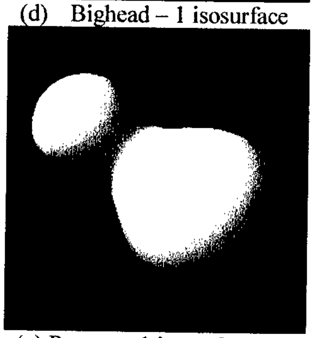

(g) Peanut – 1 isosurface

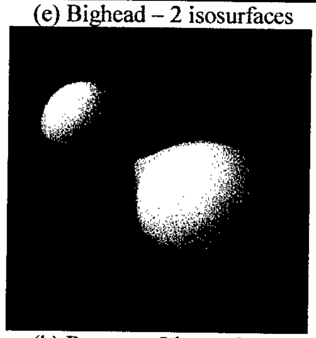

(h) Peanut – 5 isosurfaces

Figure 5. The images generated by the new algorithm

(a) Bighead – 2 isosurfaces

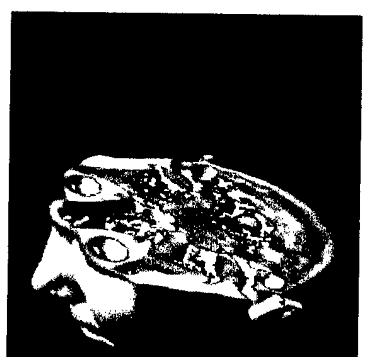

(b) Brain – 1 isosurface

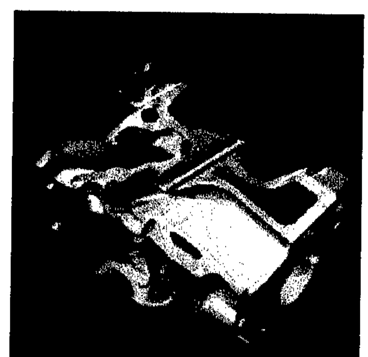

(c) Engine – 2 isosurfaces

Figure 6. The rendered images with cutting and blending

11.2.3 Cleary 1999a: Integrating a mobile CT ... (paper)

Reprint begins on the next page and is 1 page long.

Published in CARS '99, Elsevier Press, page 1053.

Integrating a mobile computed tomographic scanner in hospital operations

Kevin Cleary PhD[a,b], Fraser Henderson MD[c], James Rodgers PhD[d], Vance Watson MD[b], Matthew Freedman MD[a,b]

[a]Imaging Science and Information Systems (ISIS) Center
[b]Department of Radiology
[c]Department of Neurosurgery
[d]Department of Radiation Medicine
Georgetown University Medical Center
2115 Wisconsin Avenue, NW, Suite 603
Washington, DC 20007
Correspondence: cleary@isis.imac.georgetown.edu

A mobile CT scanner enables CT imaging at locations in the hospital where it was previously not available. At Georgetown, we have been using a mobile CT scanner at various locations including the operating room, interventional radiology suite, and radiation medicine treatment area. To successfully integrate the scanner in these locations, several obstacles including radiation safety, maintenance, and printing issues needed to be considered. Radiation safety guidelines were developed to minimize radiation exposure during scanning. Maintenance becomes a larger issue than with fixed CT scanners since the mobile CT is more susceptible to damage as it is moved around the hospital. Printing capabilities need to be provided and direct printing was found to be more reliable than network printing. We will describe our experience to date with these issues, the problems we have encountered, and the solutions we have implemented.

From March until December 1998, the scanner was used for approximately 40 studies, including procedures in the operating room, interventional radiology, radiation medicine, and the pediatric intensive care unit. Hardware and software problems addressed included modifications of patient positioning, separation of the table from the gantry to allow for adequate surgical access, and DICOM image transfer issues. Operational difficulties in integrating the system into the operating room environment have been overcome and the frequency of use of the system is increasing.

For spine tumor procedures in the operating room, intraoperative CT was used with three goals in mind: 1) to identify residual tumor following resection; 2) to ensure adequate filling of the resection cavity with polymethylmethacrylate; and 3) to verify optimum placement of instrumentation for mechanical stabilization. The intraoperative scans provided additional valuable information to the surgeon in all of the cases and altered the procedure in several cases.

This work was supported by the U.S. Army under grants DAMD17-96-2-6004 and DAMD17-99-1-9022. The content of this manuscript does not necessarily reflect the position or policy of the U.S. Government.

11.2.4 Cleary 1999b: Developing a program in image-guided ...

Reprint begins on the next page and is 5 pages long.

Published in CARS '99, Elsevier Press, pages 736-740.

Developing a program in image-guided, minimally invasive spine procedures

Kevin Cleary PhD[a,b], Matthew Freedman MD[a,b], Jianchao Zeng PhD[a,b], Seong K. Mun PhD[a,b], Vance Watson MD[b], Fraser Henderson MD[c]

[a]Imaging Science and Information Systems (ISIS) Center
[b]Department of Radiology
[c]Department of Neurosurgery
Georgetown University Medical Center
2115 Wisconsin Avenue, NW, Suite 603
Washington, DC 20007
Correspondence: cleary@isis.imac.georgetown.edu

Minimally invasive procedures can spare the patient the trauma associated with open surgery, and is expected to lead to improved quality of care. Advances in image-guided techniques are driving the development of minimally invasive procedures. At Georgetow University Medical Center, we are developing a program to provide advanced visualization and image guidance for minimally invasive spine procedures. This new initiative is a comprehensive spine surgical program with three components: patient care, technology research and development, and clinical evaluation. In patient care, physicians from the radiology, neurosurgery, and orthopaedics departments are collaborating. In technology research and development, advances in intraoperative CT, three-dimensional (3D) visualization, instrument tracking, image registration, and mechanical guidance are required. For clinical evaluation, an outcome analysis will be conducted. In this paper, we present our program plan, including the technology developments and the clinical procedures to be investigated.

1 Introduction

Minimally invasive procedures are made possible by improvements in medical imaging technology, which allow the surgeon to view the operative space through small incisions. Image-guided techniques, including the overlay of instruments on the anatomy, have also gained wider use for their increased precision and visualization advantages. Most these techniques have been developed for the brain and limited spine applications such as the placement of pedicle screws. At Georgetown University Medical Center, our focus is on spine procedures that take advantage of this new technology.

A multidisciplinary research team has been forged which includes the following groups:

- Clinical group
- Engineering group
- Outcome analysis

As a first step in developing this program, several technical problems have been identified that must be overcome to advance the state of the art in this field. These problems will be

described in the next section, followed by a description of the planned technical developments. The clinical investigations are then briefly described.

2 Technical Problems

While minimally invasive and image-guided techniques have already been developed in many institutions (for example, see [Jolesz 1996]), there are still some problems that require further study including:

1. Oblique paths cannot be visualized: three-dimensional (3D) visualization and graphical overlay of instruments in 3D will allow oblique paths to a target that crosses several adjacent axial CT slices.
2. Instrument tracking is limited: tracking of surgical instruments and graphical overlay on medical images will allow path planning and path recording. In path planning, there is a need to follow both straight and curved paths to the target. In path recording, there is a need to know where instruments have been to prevent repeated entry into a previously created but no longer desired path.
3. CT and MRI spine images not concurrently available: CT and MRI spine images provide different information about bone and soft tissue structures, both of which are useful in planning and execution of diagnosis and treatment. Because CT and MRI images cannot be obtained concurrent with surgery at a reasonable financial cost, these images need to be registered into a single image that can be made available in the operating room.
4. Instrument placement slow and inaccurate: mechanical instrument guidance will assure accurate placement of instruments from the skin entry point to the target and increase the speed of minimally invasive surgery.
5. Outcome data of conventional and new techniques not available: outcome studies are required to determine the effectiveness of these new procedures.

While some of these problems have been solved in specific domains, there is still a great deal of work to be done. In our program, we will only address some of these issues and plan to leverage the efforts of other researchers wherever possible.

3 Technical Developments

The overall goal of the project proposed here is to develop an integrated system for minimally invasive, image-guided spine work. The overall system that we plan to develop is shown in Figure 1.

This system consists of the following five major components: 1) mobile CT scanner, 2) 3D visualization, 3) Instrument tracking, 4) CT and MRI image registration, and 5) mechanical guidance system (not shown in Figure 1). A key feature is that all images will be DICOM 3.0 compatible. DICOM stands for Digital Imaging and Communications in Medicine, and it allows images to be exchanged between different medical systems.

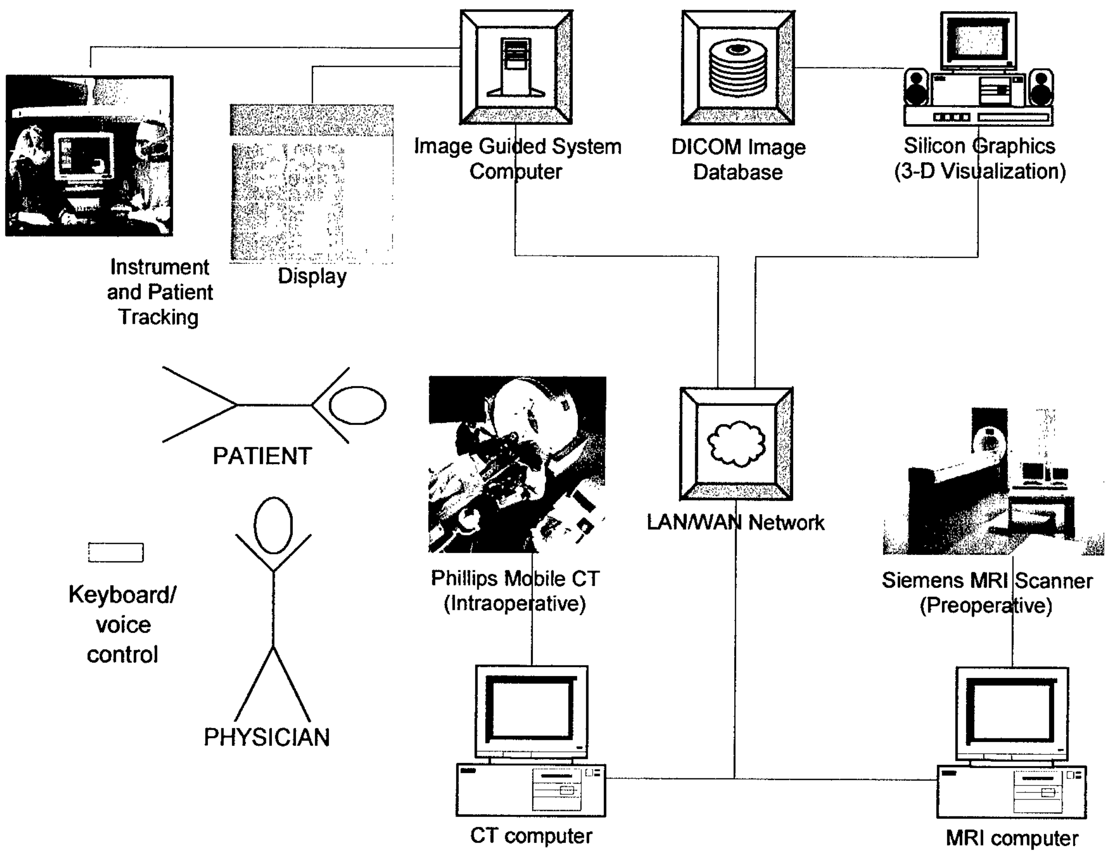

Figure 1. System Block Diagram

3.1 Mobile CT Intraoperative Integration

As an initial step in our research program, we have integrated a mobile CT scanner (Philips Tomoscan) to provide intraoperative images. CT images of the spine provide more information about vertebral anatomy than images obtained with currently available intraoperative modalities such as fluoroscopy or ultrasound. The integration of this scanner into hospital operations is described in a poster session at this conference [Cleary 1999].

3.2 3D Visualization

3D visualization will play a key role in assisting the physician during the operation. Using properly displayed 3D images, the physician will have more information about the abnormality inside the patient's body, and thus can make a more accurate and quicker decision for the treatment. 3D visualization is expected to be particularly helpful in planning and implementing oblique directions for the placement of instruments. It will allow the easier placement of instruments that cross from one axial CT slice to adjacent slices, whether these instruments are needles being placed in vertebra or screws being placed across facet joints for fusion. In spine decompression surgery, it will allow improved understanding of the interconnection and

displacement of bony fragments and should allow improved methods for their removal or displacement. Initially, we plan to develop techniques for the intraoperative 3D display of CT. Later, we plan to develop methods for the 3D display of fused images incorporating pre-operative MRI and intraoperatively obtained CT images.

3.3 Instrument Tracking

In image-guided surgery, medical images and instrument tracking are used to assist a physician in performing procedures. A typical image-guided surgery system consists of a 3D localizer, a medical imaging workstation, and some hand-held instrumentation. While several vendors have introduced commercial products in this area, most of these systems have been developed for either neurosurgical procedures in the brain or pedicle screw positioning in the spine. In our research program, we plan to extend the application of these systems in the spine to procedures such as facet blocks and vertebroplasty.

3.4 CT and MRI Image Registration

Image registration is a key component of the research effort as image registration of CT and MRI images is needed to see both soft tissue and bony landmarks and other structures during surgery.

Different imaging modalities highlight different anatomical features. For the initial clinical investigations, we have selected existing procedures that should require only CT guidance. As minimally invasive techniques for image-guided discectomy and spinal nerve neurolysis are further developed, it becomes necessary to have techniques for simultaneously knowing the location of both bony and soft tissue structures. To achieve this, one will use either an operative CT or an operative MRI machine, depending on what is available and which best shows the anatomy of interest. Full anatomic information will therefore require information from pre-existing images from the other machine.

For this project, the goal is to develop image registration techniques directly related to the planned procedure. The images obtained pre-operatively should correspond as closely as possible to the anatomic orientation we expect at the time of surgery. This is to decrease the complexity of the registration process. Certain operative procedures are best performed with the patient prone and in other procedures the patient is supine. Certain procedures are done with the spine extended and in other procedures the spine is neutral or flexed. If the patient will be in the prone position during surgery, the patient will often be placed on an operative table that avoids compressing the lungs and abdomen to allow greater ease in ventilating the patient. Thus, when the pre-operative CT and MRI images are obtained for future intraoperative guidance, the operative position should be duplicated as much as possible and the positions for the CT and MRI should be as similar as possible.

3.5 Mechanical Guidance System

An inexpensive passive guidance system would be valuable in many image-guided interventional procedures. The system would hold the needle or instrument in the position selected by the physician, would allow the precise position of the needle to be imaged on CT, and would then serve as a directional guide as the instrument is advanced. If it is linked to a computer system, the computer could show the expected path of the instrument, prior to the instrument being advanced. It would become the third hand of the interventionalist, freeing the other hands

for other tasks. Similar systems are being used in areas such as breast biopsy (the ABBI system from U.S. Surgical) and percutaneous renal access procedures [Stoianovici 1997].

4 Clinical investigations

The initial clinical investigations are aimed at documenting the improvements in patient care resulting from image guidance and minimally invasive procedures. To start, we will focus on vertebral body metastatic disease and percutaneous vertebroplasty. In both cases, we will use intraoperative CT to provide 3D image data sets during the procedures. In vertebral body metastatic disease, we have done 13 cases in the operating room and are evaluating the value of intraoperative CT in achieving a more complete tumor resection. Percutaneous vertebroplasty is an interventional procedure in which acrylic bone cement (polymethylmethacrylate: PMMA) is injected into the vertebral body under fluoroscopic guidance. In vertebroplasty, more than 10 cases have been done using intraoperative CT to examine the 3D spread of bone cement after the PMMA is injected. As the other technology components (image registration, etc.) mentioned in this paper are developed, they will be introduced into the clinical investigations.

5 Summary

A program plan to advance the state of the art in image-guided, minimally invasive spine procedures has been presented. The plan includes technology developments and clinical investigations. The goal of the program is to give the physician as much information as possible about the underlying anatomy, so the procedures can be successfully carried out through small incisions with minimal trauma to the patient.

6 Acknowledgements

This program is a joint effort of many individuals and space prohibits thanking them all by name. This work was funded in part by U.S. Army grants DAMD17-96-2-6004 and DAMD17-99-1-9022. The content of this manuscript does not necessarily reflect the position or policy of the U.S. Government.

References

Cleary, K, F Henderson, et al. (1999). Integrating a mobile computed tomographic scanner in hospital operations. CARS '99, Paris, Elsevier.

Jolesz, FA, R Kikinis, et al. (1996). "The Vision of Image-Guided Computerized Surgery: The High-Tech Operating Room." Computer-Integrated Surgery. Ed. Russell H. Taylor, Stephane Lavallee, Grigore C. Burdea, Ralph Mosges. Cambridge, Massachusetts, MIT Press: 717-721.

Stoianovici, D, JA Cadeddu, et al. (1997). An Efficient Needle Injection Technique and Radiological Guidance Method for Percutaneous Procedures. CVRMed-MRCAS, Grenoble, France, Springer-Verlag: 295-298.

11.2.5 Cleary 1999c: Realistic force feedback ...

Reprint begins on the next page and is 10 pages long.

Published in the 1st International Workshop on Haptic Devices in Medical Applications, R. Dillmann, T. Salb, editors, 23 June 1999, Institute for Process Control and Robotics, Karlsruhe University, pages 66-75.

Realistic Force Feedback for a Spine Biopsy Simulator

Kevin Cleary[1], Craig Carignan[2], Laura Traynor[1]

[1]ISIS Center, Radiology Department, Georgetown University Medical Center, 2115 Wisconsin Ave. NW Suite 603, Washington, DC, USA, 20007
cleary@isis.imac.georgetown.edu

[2]Space Systems Laboratory, Aerospace Engineering, University of Maryland at College Park, College Park, MD, USA, 20742
craigc@ssl.umd.edu

Abstract. In some medical simulation applications, realistic force feedback is critical to a believable simulation experience. The availability of commercial force feedback devices has simplified the task of developing these simulators, since the hardware can be purchased off-the-shelf and the software customized for the application. However, the fidelity of the simulation that can be achieved with commercial hardware can be somewhat limited by the actuator drive system and the available sensor hardware. In addition, developing a suitable model for the simulation task that can be implemented in software in real-time is a challenge. This paper will discuss these issues in conjunction with a spine biopsy simulator developed for training purposes at Georgetown University Medical Center.

1 Introduction

There has been a growing interest in surgical simulation over the past few years and many research groups have developed prototype systems. The application areas are varied and include intravenous catheterization [1], nasal endoscopy [2], and spinal needle procedures such as biopsy [3] and nerve blocks [4]. The goal of these systems is to provide a safe training environment for physicians that simulates the actual task as closely as possible. For many of these simulators, realistic force feedback is a critical part of a believable simulation experience.

The paper begins with the system configuration of the spine biopsy simulator developed at Georgetown University Medical Center. Anatomical modeling is discussed next, including a description of modeling for the biopsy simulator. Design and control issues for a commercial haptic device are then presented, followed by a section on advanced controller design. The paper concludes with a summary and discussion of future directions.

Published in the 1st International Workshop on Haptic Devices in Medical Applications, R. Dillmann, T. Salb, editors, 23 June 1999, Institute for Process Control and Robotics, Karlsruhe University, pages 66-75.

2 Georgetown Biopsy Simulator Configuration

The system configuration for the surgical simulator developed at Georgetown University Medical Center is shown in Figure 1. This configuration is typical of many other surgical simulator projects. The figure consists of four blocks: the physician, the visual interface, the patient, and the haptic device. The physician interacts with the simulator by manipulating the position of the haptic devices, which exerts forces back that are similar to the actual patient. The visual interface displays the current CT slice as well as the previous and next CT slices. The position of the needle can also be viewed on the current CT slice. When simulating the procedure as currently practiced, the physician does not get real-time visual feedback. Rather, the physician must press a key on the keyboard each time he wants a new snapshot of the needle position.

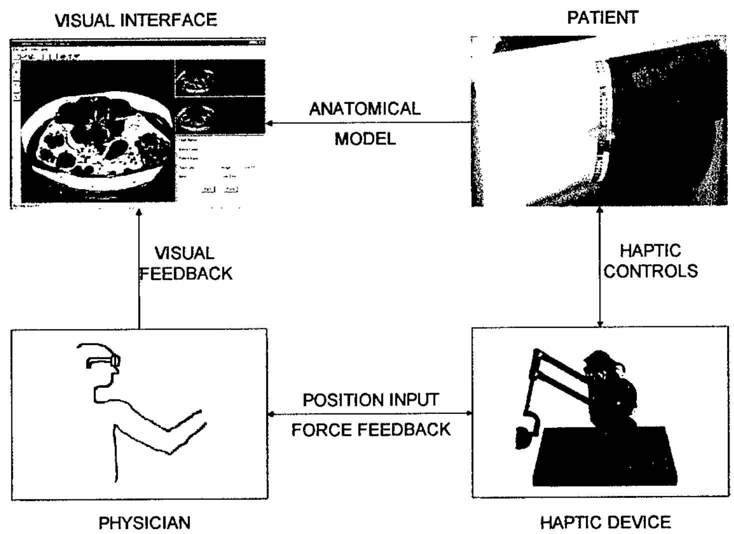

Figure 1: Typical haptic system configuration.

In Figure 1, the patient block includes a dummy torso to add visual realism to the simulation, and a software module to link the anatomical model to the haptic controls. This software module computes the motor torques for the haptic device based on the position input and anatomical model. The motor torques are sent to the haptic device, and any updates to the anatomical model are sent to the visual interface. Note that the haptic and visual computations may be done on different computing platforms, depending on the system architecture.

In a typical implementation, the haptic device must be updated at a fairly high rate (on the order of 1000 Hz) to ensure stability and a responsive interface. On the other hand, the visual interface can be updated at a much lower rate, perhaps as low as 30

Published in the 1st International Workshop on Haptic Devices in Medical Applications, R. Dillmann, T. Salb, editors, 23 June 1999, Institute for Process Control and Robotics, Karlsruhe University, pages 66-75.

Hz. This is because the force information changes much more rapidly and discontinuously than the position information displayed in the visual interface.

3 Anatomical Modeling

Haptic anatomical modeling is concerned with accurate real-time replication of the interaction between a surgical instrument and soft tissue. How realistic the anatomy feels is a difficult parameter to quantify, due to the non-linear nature of soft tissue and the lack of *in vivo* deformation information [5]. Normally, realism is achieved through a trial and error process, in which the physician gives the engineer feedback about the feel of the system. The result is a model that feels like the typical patient [6]. While this method is suitable for simulators intended for training, patient specific models are needed for simulators intended for surgical pre-planning. Attempts have been made to link mechanical tissue properties to cellular interaction through electrical impedance [7] and to Hounsfield units on CT images [8]. However, these techniques are still in their infancy and further research is needed.

As noted by Cotin [5], anatomical models may be divided into three classes: 1) non-deformable models; 2) deformable surface-based models; and 3) deformable volume-based models. The main problem with more sophisticated models is the computational power required since high fidelity force feedback needs a high update rate. Since anatomical structures cannot be defined by simple haptic primitives, most modeling of volumetric datasets results in a large number of polygons that reduce the realism and speed of the haptic rendering [8]. To decrease the complexity of haptic modeling, different force feedback methods have been developed and several are described below.

One such method is the tissue/force profile scheme described by Hiemenz [6]. For the epidural needle insertion procedure, the goal of the work was to create experimentally based realistic force feedback models. Typical forces for penetrating various tissue types in the human back were estimated by measuring the force vs. displacement for various objects (oranges, tomatoes, gelatin, and a canine back). By correlating segmented MRI data to the penetration depth of the needle, the researchers arrived at force profiles for each tissue layer which were stored in look-up tables. The method is extremely fast, but the realism of the simulation was not addressed in this paper.

Surface rendered modeling is another method used to create haptic objects. A mesh model has been used in which the nodes of the mesh are mass points and the lines of the mesh are linear springs [9]. Using basic equations from mechanics, forces on a surgical tool can be calculated based on the deformation of the mesh. The force feedback can be tuned by adjusting the mass and spring. Another method is to render an isosurface of a volumetric dataset as a solid surface [8]. By viewing the volumetric data in this way, an algorithm was developed that calculates the surface normal vector. A smoothing equation is also required, which was judged to result in satisfactory force feedback.

Finite element analysis is a highly accurate but typically computationally expensive method of creating force feedback [10]. To reduce the computation time,

Published in the 1st International Workshop on Haptic Devices in Medical Applications, R. Dillmann, T. Salb, editors, 23 June 1999, Institute for Process Control and Robotics, Karlsruhe University, pages 66-75.

fast finite element algorithms have been developed. Researchers at the University of Washington have developed a preprocessing procedure that reduces the number of equations to be computed, reducing the overall computation time. However, this method requires a large amount of memory, and the size of the model that can be used is thus limited by available memory, rather than processing speed.

Currently, we are investigating several options for creating haptic anatomical models for our spine biopsy simulator. From discussion with physicians who perform needle biopsy procedures, a heuristic model may suffice. Only three different types of forces are critical during the biopsy procedure: 1) an initial needle puncture when the needle passes from fat to muscle; 2) a homogenous force as the needle moves through the muscle; and 3) a hard stop when a bony structure is reached.

This heuristic model may be implemented by dividing the needle position into zones as it is advanced. Three zones of force can be modeled using the position of the needle and mechanics equations. A puncture force can be generated by rapidly ramping up the applied force in the first few millimeters of needle travel. Past this distance, there is a sudden drop off in force. In the muscle zone, the force could be governed by a constitutive law such as a spring-damper-mass model. The feel of hitting bone could be simulated by outputting maximum force. In order to increase the realism of forces in the zones, the parameters controlling the force could be changed during the simulation based on physician evaluation through a simple graphical user interface.

Another possible model for the spine biopsy simulator could be based on the tissues where the needle tip is located during the biopsy process. This could be accomplished by retrieving segmentation information from the CT images used in the simulation. However, some smoothing function might need to be included to guard against discontinuities in the force profile.

In summary, a trade-off needs to be made between the accuracy of the anatomical model and the need for real-time processing. While most current simulators use some type of heuristic or simple anatomical model, improvements in computational power and algorithm development will allow for more realistic models to be incorporated in the future.

4 PHANToM Haptic Design and Control

A key component of the surgical-assist system is the haptic device used to provide force feedback to the surgeon. The haptic can be regarded as a transmission between the human hand and the motors which generate the forces in the simulation. In between these are the surgical tool attached at the interface, the links that make up the haptic, and the transmissions between the link joints and the motor shafts. The motors are driven by the haptic controller which is programmed to replicate the desired tissue density, stiffness, and viscosity of the anatomy as well as interfaces between bones, veins, and soft tissue.

There has been a recent surge of interest in haptics technology fueled largely by the exploding interest in force feedback for virtual reality applications. This has lead to several commercial products including the Personal Haptic Interface Mechanism

Published in the 1st International Workshop on Haptic Devices in Medical Applications, R. Dillmann, T. Salb, editors, 23 June 1999, Institute for Process Control and Robotics, Karlsruhe University, pages 66-75.

(PHANToM™) by SensAble Technologies and The Impulse Engine™ by Immersion, Inc. The PHANToM has been particularly popular among researchers developing haptic displays and serves as the anchor for the spine biopsy testbed at Georgetown University Medical Center.

Shown in Figure 2, the PHANToM is a three degree of motion device consisting of a four-bar parallel linkage attached to a vertical rotational axis. The parallel linkage allows the three motors to be mounted at the base to give an extremely low inertia at the tool tip of around 100 grams. Cables drives are used for torque amplification to reduce the effect of friction usually found in geared mechanisms. A peak force of 10 N can be generated at the tool tip, and a continuous force of 1.5 N can be applied.

Figure 2: PHANToM device and instrumented gimbal.
A biopsy needle has been mounted on the end.

Haptic engineers typically employ three criteria [11] when designing haptic mechanisms: (1) *free space must feel free*, (2) *solid virtual objects must feel stiff*, and (3) *virtual constraints must not be easily saturated*. The first criteria implies that the natural dynamics of the haptic must be virtually imperceptible (< 0.2 N) so as not to interfere with the perception of the environment being simulated. This implies that the haptic must have low mass and low friction. The second criteria says that the haptic must be capable of producing a stiffness convincing enough to believe that contact with an immovable object has taken place. Roughly speaking, this is a minimum of 20 N/cm. Finally, the last criteria implies that the haptic must be capable of producing enough force so that virtual objects feel solid. For fingertip contact, a force of 10 N is rarely exceeded. However, for a grasp situation, the number is probably much higher.

The first criteria can be satisfied either through passive design or by actively removing the effect of the dynamics via the controller. The PHANToM employs the former. The stiffness requirement is satisfied by making the mechanism itself stiff and by using a very high bandwidth controller. The latter requires that the control law be computed at a very fast rate. The force requirement is basically a function of the peak torque outputs of the motors. The higher the force produced at the tool tip, the larger the torques that must be supplied by the motors. For the same force output, the torque requirements can vary substantially for different configurations of the haptic.

Published in the 1st International Workshop on Haptic Devices in Medical Applications, R. Dillmann, T. Salb, editors, 23 June 1999, Institute for Process Control and Robotics, Karlsruhe University, pages 66-75.

A block diagram of the controller supplied with the PHANToM is shown in Figure 3. Encoders mounted on the motor shafts read the angles of the motors and, after decoding, send the angles to a forward kinematics module inside the controller to determine the position of the tool tip. An anatomical model inside the controller uses this position and the desired tissue properties to generated a desired force. The desired force is then mapped using a Jacobian to a set of desired torques to be produced by the motors. This signal is then converted into desired currents to the servo amplifiers for the motors.

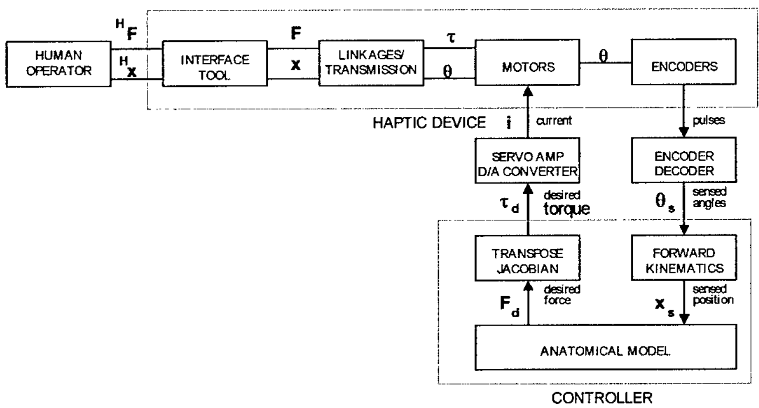

Figure 3: Block diagram of PHANToM controller.

This type of force control is called "open-loop" because there is no force feedback from the device to the controller to regulate the force output of the haptic. The accuracy of the force thus depends largely upon the haptic having negligible dynamics. Any friction or inertia inherent in the device will directly add to the forces felt by the user. In addition, any errors in the geometric modeling or output of the servos will also contribute to inaccuracies perceived by the user.

Haptic devices such as the PHANToM were designed from the outset to have low dynamic properties and thus easily satisfy the first design criteria. However, in many clinical applications, the surgeon exerts far more than 1.5 N of continuous force thus violating the third criteria and rendering low output devices such as the PHANToM inadequate for simulation and training. For example, in lumbar puncture insertion alone, forces typically exceed 10 N of force, and this would be considered a low output procedure [12]. Thus, if haptic devices are to be used for simulating clinical procedures, it seems likely that they will need to produce larger forces than the PHANToM which will increase the mass and nonbackdrivability and require the use of active control for removing the effects of the haptic dynamics.

Published in the 1st International Workshop on Haptic Devices in Medical Applications, R. Dillmann, T. Salb, editors, 23 June 1999, Institute for Process Control and Robotics, Karlsruhe University, pages 66-75.

5 Advanced Controller Design

There are two principle means for reducing the effects of the haptic dynamics: add haptic model feedforward to the control law, or add a force feedback loop to the controller. Model feedforward is not a particularly attractive option as it increases the computational burden of the controller significantly thus reducing the loop rates that can be achieved violating the second design criteria. In addition, modeling phenomenon such as friction is difficult since it is very nonlinear and depends upon various factors such as position and temperature which both vary with time.

The second option which uses force feedback is computationally simpler than adding model feedforward. However, it requires additional hardware to sense the forces and torques at the human interface. This adds cost to the device and adds weight exactly where you don't want it – at the haptic interface! However, the effect of the sensor can be eradicated along with the haptic dynamics through the controller, and the benefits far exceed the penalties involved in their employment. In addition, by incorporating a force/torque sensor, designers can actually measure the forces being applied by the clinician during the simulated procedure.

There are basically two categories of advanced controllers that use force feedback: impedance control with force feedback, and position-based impedance control (or admittance control). The impedance control approach with force feedback is illustrated in Figure 4. It is basically the same as the PHANToM controller in Figure 3 but with a force feedback loop added. The force gain K_F is typically set as high as possible which, in practice, is bounded by the loop rate and the natural frequencies of the device. The errors due to the haptic dynamics are inversely proportional to $1+K_F$. If $K_F=0$, then the controller reverts to the classical open-loop impedance controller used by the PHANToM. An example of a device which uses this approach is the GLAD-IN-ART Arm Exoskeleton which is a portable haptic device worn on the exterior of a human arm ([13] pp. 203).

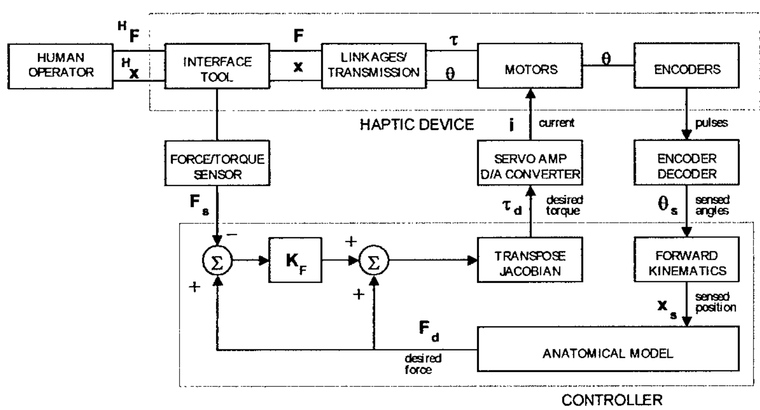

Figure 4: Impedance Controller with Force Feedback.

Published in the 1st International Workshop on Haptic Devices in Medical Applications, R. Dillmann, T. Salb, editors, 23 June 1999, Institute for Process Control and Robotics, Karlsruhe University, pages 66-75.

The position-based impedance controller, shown in Figure 5, has a more complex architecture than the classic impedance control approach. Its multi-loop architecture has significant advantages over the single loop approach in Figure 4. At the outer level, the sensed force is used to generate a desired endpoint position for the haptic device based upon the anatomical model. An inverse kinematics module inside the controller then converts the tool position into a set of desired joint angles for the haptic. A high gain PD controller at each joint is then used to servo the joint angle sensed by the encoders to the desired joint angle coming from the outer loop. While there are no current examples of haptic devices which use this controller, an example of its use in the robotics industry can be found in the AdeptOne Robot by Adept Technologies, Inc. [14].

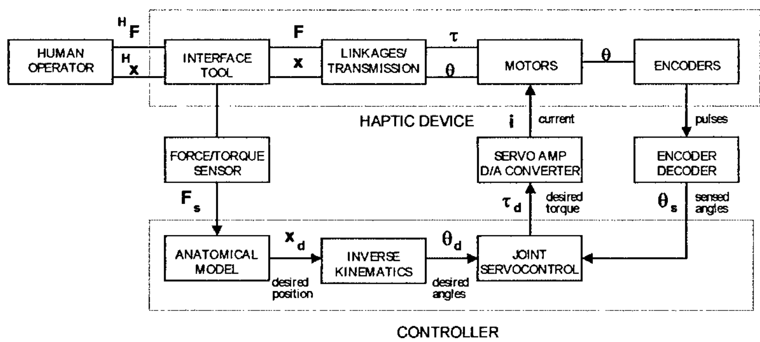

Figure 5: Position-based Impedance Controller.

The chief advantage of the position-based method over the classic impedance controller is that the computation is divided into two levels: the inner joint servo level which is typically performed by motor controller chips at very high speeds (> 500 Hz), and the outer force loop which runs at a much slower rate. The effects of friction, backlash, and torque ripple in the haptic are inversely proportional to these gains which are typically very high because of the fast loop rate. The outer loop, which must perform inverse kinematics, typically runs much slower than the joint servo. However, experimental evidence indicates that the outer loop can run nearly 10 times slower than the inner loop with little sacrifice in performance [14], [15], and [16].

While researchers in the medical arena have yet to foray into high output haptics, it is clear that force feedback controllers will play a vital role in maintaining high fidelity in haptic simulation of surgical procedures. Current research in impedance control provides a gateway to this technology without the contact stability issues so predominant in robotic applications of these controllers. The dual benefit of a force/torque sensor as a measurement device as well as a sensor for force feedback gives increased incentive for their incorporation in future haptic devices.

Published in the 1st International Workshop on Haptic Devices in Medical Applications, R. Dillmann, T. Salb, editors, 23 June 1999, Institute for Process Control and Robotics, Karlsruhe University, pages 66-75.

6 Summary

This paper discussed issues such as anatomical modeling, haptic feedback, and advanced controller design as they apply to developing realistic force feedback for surgical simulation. The spine biopsy simulator testbed developed at Georgetown University Medical Center was also described. In future work, we plan to continue the development and implementation of the anatomical model for this simulator. The visual interface and patient model is also being upgraded through a collaboration with the Korean Advanced Institute of Science and Technology (KAIST). The eventual goal is to train residents using this system and evaluate whether the simulator improves their performance in the clinical arena. This evaluation question is critical to greater acceptance of surgical simulation by the medical community.

Acknowledgements
This work was partially supported by the U.S. Army under grants DAMD17-96-2-6004 and DAMD17-99-1-9022. The content of this manuscript does not necessarily reflect the position or policy of the U.S. Government.

References

1. Ursino, M., *et al. Cathsim: an Intravascular Catheterization Simulation on a PC* in *Medicine Meets Virtual Reality (MMVR 7).* 1999: IOS Press, p. 360-366.
2. Bockholt, U., *et al. Realtime Simulation of Tissue Deformation for the Nasal Endoscopy Simulator (NES)* in *Medicine Meets Virtual Reality (MMVR 7).* 1999: IOS Press, p. 74-75.
3. Cleary, K., C.E. Lathan, and C. Carignan. *Simulator/planner for CT directed needle biopsy of the spine* in *Surgical-Assist Systems.* 1998. San Jose, California: SPIE, p. 218-224.
4. Blezek, D.J., *et al. Simulation of spinal nerve blocks for training anesthesiology residents* in *Surgical-Assist Systems.* 1998. San Jose, California: SPIE, p. 45-51.
5. Cotin, S., *et al. Geometric and Physical Representations for a Simulator of Hepatic Surgery* in *Medicine Meets Virtual Reality 4.* 1996: IOS Press, p. 139-151.
6. Hiemenz, L., D. Stredney, and P. Schmalbrock. *Development of the Force-Feedback Model for an Epidural Needle Insertion Simulator* in *Medicine Meets Virtual Reality (MMVR 6).* 1998: IOS Press, p. 272-277.
7. Avis, N.J., *et al. Anatomical and Physiological Models for Surgical Simulation* in *Medicine Meets Virtual Reality (MMVR 7).* 1999: IOS Press, p. 23-29.
8. Blezek, D.J. and R.A. Robb. *Haptic rendering of isosurfaces directly from medical images* in *Medicine Meets Virtual Reality (MMVR 7).* 1999: IOS Press, p. 67-73.
9. Merril, J.R., *et al. Photorealistic Interactive Three-Dimensional Graphics in Surgical Simulation* in *Interactive Technology and the New Paradigm for Healthcare (MMVR 3).* 1995: IOS Press, p. 244-252.
10. Berkley, J., *et al. Fast Finite Element Method of Surgical Simulation* in *Medicine Meet Virtual Reality (MMVR 7).* 1999: IOS Press, p. 55-61.

Published in the 1st International Workshop on Haptic Devices in Medical Applications, R. Dillmann, T. Salb, editors, 23 June 1999, Institute for Process Control and Robotics, Karlsruhe University, pages 66-75.

11. Massie, T.H. and J.K. Salisbury. *The PHANToM Haptic Interface: A Device For Probing Virtual Objects* in *ASME Winter Annual Meeting, Symposium on Haptic Interfaces for Virtual Environments and Teleoperator Systems*. 1994. Chicago.

12. Popa, D. and S. Singh. *Creating Realistic Force Sensations in a Virtual Environment: Experimental System, Fundamental Issues and Results* in *Proceedings of IEEE International Conference on Robotics & Automation*. 1998: p. 59-64.

13. Burdea, G.C., *Force and Touch Feedback for Virtual Reality*. 1996: Wiley Interscience.

14. Maples, J.A. and J.J. Becker, *Experiments in Force Control of Robotic Manipulators*. Proceedings of IEEE International Conference on Robotics and Automation, 1986: p. 695-702.

15. Pelletier, M. and M. Doyon. *On the Implementation and Performance of Impedance Control on Position Controlled Robots*. in *Proceedings of IEEE International Conference on Robotics and Automation*. 1994: p. 1228-1233.

16. Carignan, C. and D. Akin. *Obtaining Impedance Objectives in Robot Teleoperation*. in *Proceedings of IEEE International Conference on Robotics and Automation*. 1997: p. 3487-3492.

11.2.6 Hum 1999a: Intraoperative CT for complex cranio ...

Reprint begins on the next page and is 15 pages long, followed by 6 pages of figures.

Submitted to Neurosurgery, December 1999

INTRAOPERATIVE COMPUTED TOMOGRAPHY FOR COMPLEX CRANIOCERVICAL SURGERIES AND SPINE TUMOR RESECTIONS

Barbara Hum, MD[1], Frank Feigenbaum, MD[2], Kevin Cleary, PhD[1], Fraser Henderson, MD[2]

Georgetown University Medical Center
[1]Imaging Science and Information Systems (ISIS) Center, Department of Radiology
[2]Department of Neurosurgery

INTRAOPERATIVE COMPUTED TOMOGRAPHY

Fraser C. Henderson, MD
Department of Neurosurgery
Georgetown University Medical Center
PHC 1^{ST} Floor
3800 Reservoir Rd
Washington, DC 20007

(202) 687-4979 Work phone
(202) 687 -3744 Fax

hendersf@gunet.georgetown.edu

ABSTRACT

OBJECTIVE

To improve intraoperative visualization of unexposed anatomy and to verify surgical correction, a mobile computed tomography (CT) scanner has been introduced into the operating room. To date, intraoperative CT scanning has been used predominately for intracranial procedures. We report on the expanded use of intraoperative CT for spinal surgery, as CT provides excellent visualization of osseous pathology. We report on our first 17 cases involving complex craniocervical surgeries and spinal tumor resections.

METHODS

The Tomoscan M CT Scanner is mobile and consists of a translatable gantry, a translatable table, and an operator's workstation. In the operating room, the patient is placed on the CT table and prepped in the usual fashion. The aperture of the gantry is covered with sterile plastic drapes. The gantry is docked to the table for intraoperative CT scanning as needed for navigation and verification during surgery. Each series of scans require approximately 15-20 minutes.

RESULTS

Our initial experience with neurosurgical spine cases shows that the use of intraoperative CT scanning changed the course of the surgery in 6 out of the 17 cases. CT was beneficial in facilitating adequate ventral clival and craniocervical decompressions, assisting in more complete tumor resections, and verifying correct graft and instrument placement before surgical closing. The mobile CT scanner has also been used successfully in the neurointerventional suite, in radiation planning, and in the intensive care unit.

CONCLUSION

Based on our first 17 spinal surgery cases, we conclude that the use of the intraoperative CT for the spine is both feasible and beneficial for select complex spinal procedures from the craniocervical junction to the sacrum.

KEY WORDS

craniocervical surgery, intraoperative computed tomography, spinal tumor resection

INTRODUCTION

The advent of Computed Tomography (CT) in the early 1970's dramatically changed the diagnostic capability of neurosurgeons. An operative suite with a fixed, immobile CT was introduced for intracranial tumor resection by Shalit et al. in 1978 (12,13) and by Lunsford et al. (8) in conjunction with fluoroscopy in 1981. Butler et al. (3) have reported on the use of a mobile CT scanner for "on demand" intraoperative and intensive care unit imaging. To date, intraoperative CT has been used primarily to facilitate resection of intracranial lesions (3,4,8,9,11,12) and to determine intraoperative brainshift during craniotomy. The use of intraoperative CT for spinal lesions has been limited to biopsy and drainage of spinal cord cysts (8). Recently, the mobile CT has also been combined with image-guided navigational systems to provide updated images for instrument tracking (6,7,10).

We present 17 cases that outline our experience with intraoperative CT scanning for complex spinal procedures, in particular, the treatment of craniocervical lesions and spinal cord tumors. We use the mobile CT on selected spinal procedures for several reasons: CT is the preferred imaging modality for visualizing bone, as it best defines subcortical and trabecular bony structures (1), and clearly demonstrates when adequate decompression has been achieved. It provides updated information on bone-based tumor resection and guides more complete tumor removal. CT can also verify graft and instrumentation placement during reconstruction of the spine.

CLINICAL MATERIALS AND METHODS

The Tomoscan M Scanner (Philips Medical Systems, Eindhoven, The Netherlands) is mobile and easily transportable throughout the hospital. The system has three components: the gantry, the CT table, and the operator's workstation (Figures 1 and 2). The gantry weighs 460 kg and measures 1 meter deep, 2 meters wide, and 2 meters high. The aperture of the gantry is 60 cm with a maximal field of view of 46 cm. The gantry and the CT table can translate 35 cm and 150 cm, respectively. The images have a resolution of 512

X 512 pixels, and can be transferred to other systems using the digital imaging and communications in medicine (DICOM) standard. Protocols for cervical, thoracic, and lumbar spine exist with slice thickness options of 2, 3, 5, and 10 mm. The system has a tube voltage of 130 Kv, and uses a relatively low tube current between 10 and 50 mA, thereby minimizing dose exposure.

The CT scanner is warmed up in the operating room before the patient arrives. Pre-sterilized, self-adhesive plastic drapes are applied to the gantry aperture. The patient can be positioned supine, lateral, or prone on the table. For most patients, there is sufficient table movement to scan from the head to the sacrum. The mobile CT can accommodate a patient in a halo-vest with titanium components for cases involving posterocervical or craniocervical surgery. The surgical site is prepared in the usual fashion, ensuring that the table can move unfettered by tubing and drapes into the gantry. An initial CT scanogram (scout view) is obtained to accurately localize the desired surgical level. Intraoperatively, the gantry is moved away from the table as needed to allow complete access to the patient. The gantry and workstation can, if necessary, be transported to another site, such as the interventional suite, the intensive care unit (ICU), or another operating room (OR), then transported back and re-docked to the table for scanning as needed. After scanning, the sides of the operative field are re-draped to maintain sterility. The preparation and CT scanning time averages 15-20 minutes per series.

RADIATION SAFETY

Measurement of scattered radiation levels using phantoms demonstrated minimal radiation 12 feet from the center of the gantry. Radiation safety personnel at our institution determined that either lead protection should be worn or that personnel should remain at least 12 feet from the center of the gantry during scanning. Typically, the operator's workstation is placed outside a 12-foot perimeter from the gantry, and non-essential staff leave the room during scanning. A diagram of the operating room layout is shown in Figure 3 and intraoperative use of the CT during spinal surgery is shown in Figure 4.

RESULTS

Since May of 1998, the mobile CT has been used in over 70 procedures at our institution, including the 17 complex spinal procedures reported here. These consist of 7 transoral decompressions and 10 tumor resections —2 extrapharyngeal, 5 thoracic, and 3 lumbosacral. CT provided information that altered the course of the surgery in 6 of the 17 spinal cases listed in Table 1. CT demonstrated incomplete tumor resections in patients 2 and 16. CT demonstrated residual odontoid bone spicules after initial transoral odontoidectomy was undertaken in patients 9, 12, and 13, and thus prompted us to return to the surgical site to perform a more complete ventral decompression of the brainstem. CT provided intraoperative confirmation of correct placement of a bone graft and anterior plate within and over the remaining anterior C1 ring and the residual body of C2 in patient 9. In addition, CT showed, just prior to closure, that a hook had slipped and rotated off the transverse process in patient 7, allowing for correction of the instrumentation intraoperatively, and averting an unanticipated return to the OR. There were no clinically detectable complications from the intraoperative use of CT.

CASE REPORTS

This section illustrates four complex cases that demonstrate the value of mobile CT in the operating room.

Case 1: Patient 12

A 43-year old woman with severe, deforming rheumatoid arthritis and a history of prior cervical fusion and stabilization presented with spastic quadriparesis, numbness, vertigo, dysphagia, and sleep apnea. CT and MRI images of the craniocervical junction revealed basilar invagination with brainstem compression. A preoperative scout film obtained with the mobile CT in the OR demonstrated previous occipitocervical stabilization (Figure 5). After transoral odontoid resection, intraoperative CT imaging revealed continued

compression of the brainstem by a fractured spicule of the odontoid, which had been obscured from direct visualization by pannus. After further resection, a second intraoperative CT revealed a very small residual bone spicule compressing the neuraxis (Figure 6). The spicule was removed and a third CT demonstrated complete decompression (Figure 7). Postoperatively, the patient enjoyed return of strength and resolution of her brainstem symptoms.

Case 2: Patient 2

A 41-year old woman with breast cancer (T1N0M0) presented with occipital neuralgia. MRI and CT studies revealed a solitary lytic lesion on the C2 vertebra such that the cancellous portion of the vertebral body and odontoid process had undergone near total replacement (Figure 8). Through a left extrapharyngeal approach, the tumor was resected, leaving the uninvolved cortical shell of C2 and its ligamentous attachments intact. The surgical cavity was filled with Omnipaque contrast and an intraoperative CT performed. The CT revealed residual tumor in the left lateral mass of C2, which could not be visualized directly by the surgeon (Figure 9). Excision of the tumor was completed and the resection cavity was filled with polymethylmethacrylate (PMMA). A later intraoperative CT demonstrated adequate filling of the vertebra (Figure 10). Postoperatively, the patient's occipital neuralgia resolved.

Eight months after cervical surgery, the patient developed lower back pain. MRI revealed a metastasis to the lumbar spine. The patient underwent percutaneous vertebroplasty in the neurointerventional suite using the mobile CT to monitor PMMA filling within the vertebral body and to evaluate for possible extravasation. Postoperatively, the patient's back pain resolved. Sixteen months after her cervical spine surgery, she remains active and asymptomatic from disease in the cervical and lumbar spine. X-rays of the cervical spine show no abnormality of alignment or loss of range of motion. There is no evidence of tumor recurrence at C2.

Case 3: Patient 9

A 42-year old man with Klippel-Feil syndrome presented with sleep apnea, vertigo, weakness, and myelopathic symptoms. MRI revealed basilar invagination with ventral brainstem compression, segmentation failure of the atlas (occipital assimilation of the atlas), atlantoaxial subluxation, block fusion of C2- C3, and a cervical syrinx. The patient underwent a transoral odontoidectomy and anterior C1-C2 fusion. Intraoperatively, CT imaging demonstrated inadequate ventral body resection and persisting compression. After further resection, intraoperative imaging confirmed adequate brainstem decompression (Figure 11) and anterior plate positioning (Figure 12). Postoperatively, the patient experienced resolution of vertigo and sleep apnea, and improvement in hand strength and shoulder sensation.

Case 4: Patient 7

A 52-year old woman who had undergone a T8 giant cell tumor resection one-year prior, developed pain radiating from the midback to the left subcostal region and anterior left thigh. On examination, left leg weakness and a left T8 sensory level were found. MRI revealed recurrent tumor in the vertebral body, pedicles, and laminae of T7-T8 on the left and in the epidural space with spinal cord compression. A posterolateral approach with gross total tumor resection was performed. Intraoperative CT revealed that the goal of tumor resection had been met. Instrumentation and fusion from T5 to T10 was completed. A second intraoperative CT revealed that the transverse process hook at T5 had rotated and slipped off the transverse process (Figure 13). The instrumentation was repositioned correctly prior to surgical closure. Postoperatively, the patient enjoyed resolution of her pain and improvement in leg strength. One year later, the instrumentation is sound, and she has no pain, neurological deficit, nor tumor recurrence.

DISCUSSION

In this series of patients, intraoperative CT changed the course of the surgery in 6 of the 17 cases presented. In the case of Patient 2 with a C2 metastases, intraoperative CT identified residual tumor and allowed for

further resection of the residual tumor. A second CT revealed inadequate vertebroplasty, allowing us to perform a more complete vertebroplasty. The patient has had no tumor recurrence or any cervical instability in the 16 months since surgery. In the cases of patients 9 and 12, intraoperative CT demonstrated incomplete decompression of the brainstem, allowing us the opportunity to complete the decompression and achieve the desirable results. In the same patients, intraoperative CT demonstrated adequacy of the anterior fusion and plating at the craniocervical level. In the case of patient 7, intraoperative CT demonstrated that a transverse process hook at the upper end of the construct, which could not be well visualized directly, had rotated out of position. The slipped hook was easily corrected intraoperatively, obviating an unanticipated return to the operating room.

The Tomoscan M mobile CT is advantageous for selected craniocervical and spine tumor surgeries. Intraoperative CT is capable of scanning the entire neuraxis, providing initial scout views. This is particularly useful for cervicothoracic and thoracic vertebrae, where plain film x-rays are notoriously inadequate. Intraoperative CT orients the surgeon to complex anatomy and enables visualization of subsurface structures. CT verifies that the surgical goals are being accomplished, in addition to ensuring correct instrument positioning such that adjustments can be made prior to wound closure. Through this immediate feedback, intraoperative CT improves surgical results and decreases morbidity.

There are numerous disadvantages to the use of mobile CT. These include reduced flexibility in patient positioning, increased OR room time, the need for additional trained staff, and the risk of ionizing radiation exposure. Patient positioning on the CT table is limited to the supine, prone, or lateral positions. A prone position in the adult can only be accomplished with the patient restrained in a halo vest. This limits the ability to reduce deformity intraoperatively or to change head position when needed. As a result, we have not attempted posterolateral or anterolateral procedures to the skull base or neck. For example, a transcondylar suboccipital approach to the skull base requires neck flexion, lateral rotation, and lateral bending. Intraoperative CT would proscribe such complex positioning of the cervical spine. Furthermore, the CT table is not capable of rotation, bending, and tilting. The need for a sliding CT table prevents placement of any fixtures to the table, such as the Mayfield head holder, a raised (aeroplane) armrest, or a

table mounted retractor system. Similarly, a Wilson frame cannot be used. Some of these limitations in positioning of the patient will be overcome as special CT table adaptations become available. Difficulties with equipment malfunction have also occurred, including communication errors between the gantry and the workstation, and overheating of the x-ray tube. However, these difficulties have been rare and have not caused significant delays in the surgery. Another problem is surgeon comfort: the CT table is wider than the standard operating table and requires the surgeon to stoop over the patient more than usual. Initial concerns of radiation exposure were easily handled: the radiation level is minimal outside of the twelve-foot perimeter drawn from the center of the gantry. The risk of radiation exposure with intraoperative CT to the patient and staff is proportional to that of diagnostic CT imaging (3). In the cases presented here, no incidents related to radiation safety were experienced. In general, apart from the limitations of positioning of the patient and the need to practice radiation safety measures, the real and potential drawbacks of the intraoperative CT are minor and surmountable.

The mobile CT scanner is compatible with other emerging technologies. It may be used with image-guided navigational systems, and may be advantageous for screw-fixation procedures, particularly those involving neoplasms, fractures, deformities, and repeat surgeries where the normal anatomical landmarks are obscured (5). There is potential use in 3-D volumetric visualization and registration with preoperative MR or intraoperative endoscopy to provide additional guidance to the surgeon. Intraoperative CT and navigational systems may also potentially interface with the surgical microscope for heads up display.

Mobile CT compares well with other imaging modalities used intraoperatively, including magnetic resonance imaging (MRI) and ultrasound (US). A dedicated intraoperative MRI is currently in use for brain and spine surgeries (2) and offers superior soft tissue visualization compared to CT, without emitting ionizing radiation. The mobile, intraoperative CT is superior for visualizing osseous pathology. It has a lower cost, current instrument compatibility, good patient accessibility, and mobility "on demand" throughout the hospital. The intraoperative roles of both of these imaging modalities will be further determined as the technology matures and is more widely available.

How many spine patients need intraoperative CT? Clearly, the above procedures are routinely performed without CT. Indeed, intraoperative imaging may be unnecessary and time consuming for routine spine procedures. However, we recommend the use of intraoperative CT for selected complex spinal procedures, where visualization is poor or intraoperative guidance to certain anatomical structures is helpful, and where verification of tumor resection or neuraxial decompression is paramount. In our experience, intraoperative CT has been helpful for ventral clival and craniocervical decompressions, for difficult tumor resections, and for intricate instrumentation and fusion procedures. Intraoperative CT appears to translate directly to better patient care in terms of decreased morbidity and improved surgical outcome. Further patient outcome studies are needed.

CONCLUSION

Other investigators have already established the feasibility of using intraoperative CT for intracranial pathology. Based on our first 17 cases, we conclude that intraoperative CT is practical and beneficial for select complex spinal procedures from the craniocervical junction to the sacrum.

ACKNOWLEDGEMENTS

Thanks are due to many individuals who contributed to making intraoperative CT possible. Special thanks to anesthesiologist Dong Tran, MD; neurosurgery nurse specialist Maureen McCarthy, RN; scrub technologist Christine Treiber; and CT technologist David Lindisch.

This work was funded in part by U.S. Army grants DAMD17-96-2-6004 and DAMD17-99-1-9022. The content of this manuscript does not necessarily reflect the position or policy of the U.S. Government.

REFERENCE LIST

1. Algra PR: Diagnostic imaging of vertebral metastases, in Algra PR, Valk J, Heimans JJ (ed): *Diagnosis and Therapy of Spinal Tumors*, Springer-Verlag, New York, 1998, pp 67-86.
2. Black PM, Moriarty T, Alexander E 3rd, Steig P, Woodard EJ, Gleason PL, Martin CH, Kinkinis R, Schwartz RB, Jolesz FA: Development and implementation of intraoperative magnetic resonance imaging and its neurosurgical applications. Neurosurgery 41:831-42, 1997.
3. Butler WE, Piaggia CM, Constantinou C, Niklason L, Gonzalez RG, Cosgrove GR, Zervas NT: A mobile computed tomographic scanner with intraoperative and intensive care unit applications. Neurosurgery 42:1304-1311, 1998.
4. Darabi K, Reisch R, Muller-Forell W, Grunert P, Perneczky A: Intraoperative computed tomography in neurosurgery, in Lemke HU, Vannier MW, Inamura K, Farman A (ed): *Computed Assisted Radiology and Surgery*, Elsevier Science, New York, pp 605-608.
5. Foley KT, Smith MM: Image-guided spine surgery. Neurosurg Clin N Am 7:171-186, 1996.
6. Grunert P, Muller-Forell W, Darabi K, Risch R, Busert C, Hopf N, Perneczky A: Basic principles and clinical applications of neuronavigation and intraoperative computed tomography. Comput Aided Surg 3:166-173, 1998.
7. Koos WT, Roessler K and Matula C: Image-guided neurosurgery with intra-operative CT. Medicamundi 42:26-32, 1998.
8. Lunsford LD, Parrish R, Albright L: Intraoperative imaging with a therapeutic computed tomographic scanner. Neurosurgery 15:559-561, 1984.
9. Lunsford LD, Kondziolka D, Bissonete DJ: Intraoperative imaging of the brain. Stereotact Funct Neurosurg 66:58-64, 1996.
10. Matula C, Rossler K, Reddy M, Schindler E, Koos WT: Intraoperative computed tomography guided neuronavigation: concepts, efficiency, and workflow. Comput Aided Surg 3: 174-182, 1998.
11. Okudera H, Kobayashi S, Kyoshima K, Gibo H, Takamae T and Sugita K: Development of the operating computerized tomographic scanner system for neurosurgery. Acta Neurochir (Wien) 111: 61-63, 1991.

REFERENCE LIST (continued)

12. Shalit MN, Israeli Y, Matz S, Cohen ML: Intra-operative computerized axial tomography. Surg Neurol 11: 382-384, 1979.
13. Shalit MN, Israeli Y, Matz S, Cohen ML: Experience with intraoperative CT scanning in brain tumors. Surg Neurol 17:376-382, 1982.

FIGURE LEGEND

FIGURE 1: Mobile CT gantry and table

FIGURE 2: Operator's workstation

FIGURE 3: Equipment layout of operating room

FIGURE 4: Intraoperative use of CT during spine surgery

FIGURE 5: Scout film showing occipitocervical stabilization, C3-4 anterior spine plate from previous surgery, placement of instrumentation for transoral exposure, and patient stabilized in a halo vest

FIGURE 6: Intraoperative CT scan for transoral odontoidectomy showing resection cavity (small arrow) and spicule of bone remaining in tectorial membrane (large arrow)

FIGURE 7: Complete resection and decompression of the neuraxis

FIGURE 8: Preoperative CT showing lytic lesion of C2

FIGURE 9: Intraoperative CT with Omnipaque contrast shows residual tumor in left lateral mass after initial resection (arrow).

FIGURE 10: Residual tumor removed and the cavity filled with PMMA

FIGURE 11: Intraoperative CT scan of transoral odontoidectomy, note the assimilation of C1 to the occiput (long arrow) and the 15-mm resection of C1 ring and odontoid (double arrow)

FIGURE 12: Tricortical autologous iliac crest bone graft (long arrow) and titanium miniplate fixed with 3 titanium screws (short arrow)

FIGURE 13: Intraoperative CT of slipped transverse process hook on right T5, note artifact from instrumentation does not interfere with interpretation of CT scan

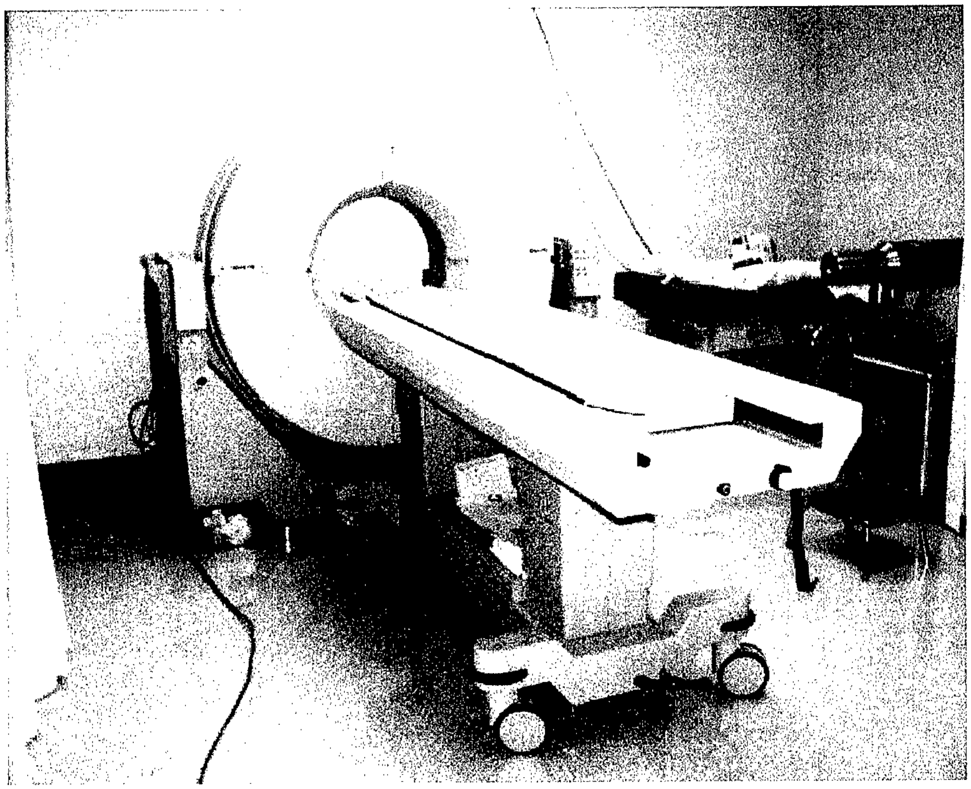

Figure 1: Mobile CT gantry and table

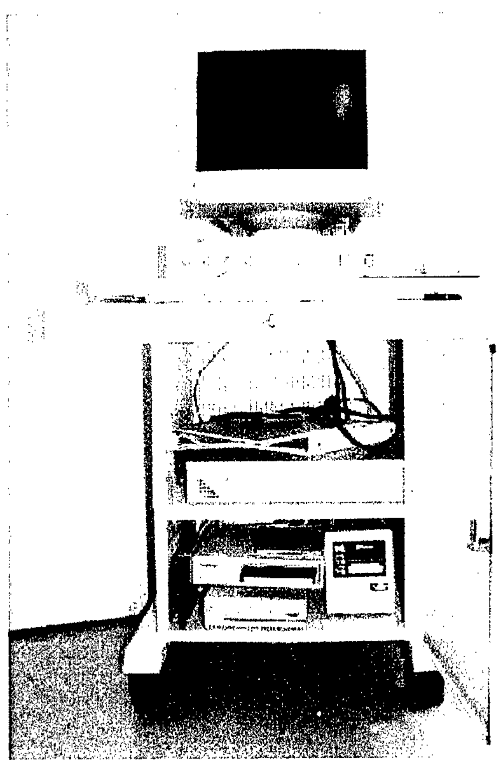

Figure 2: Operator's workstation

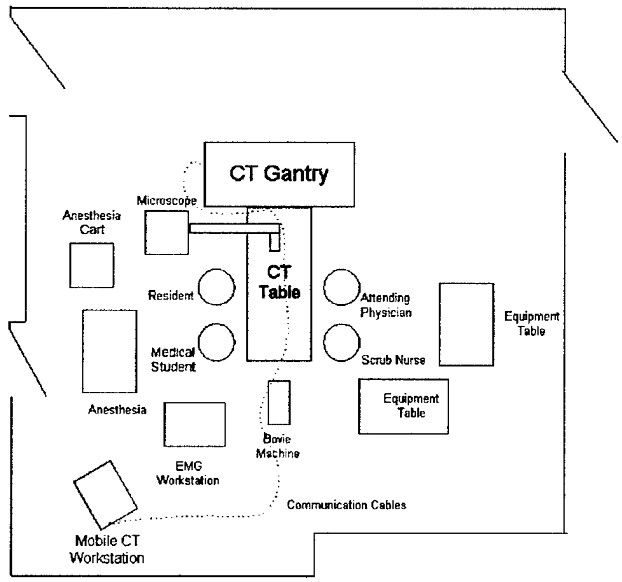

Figure 3: Equipment layout of operating room

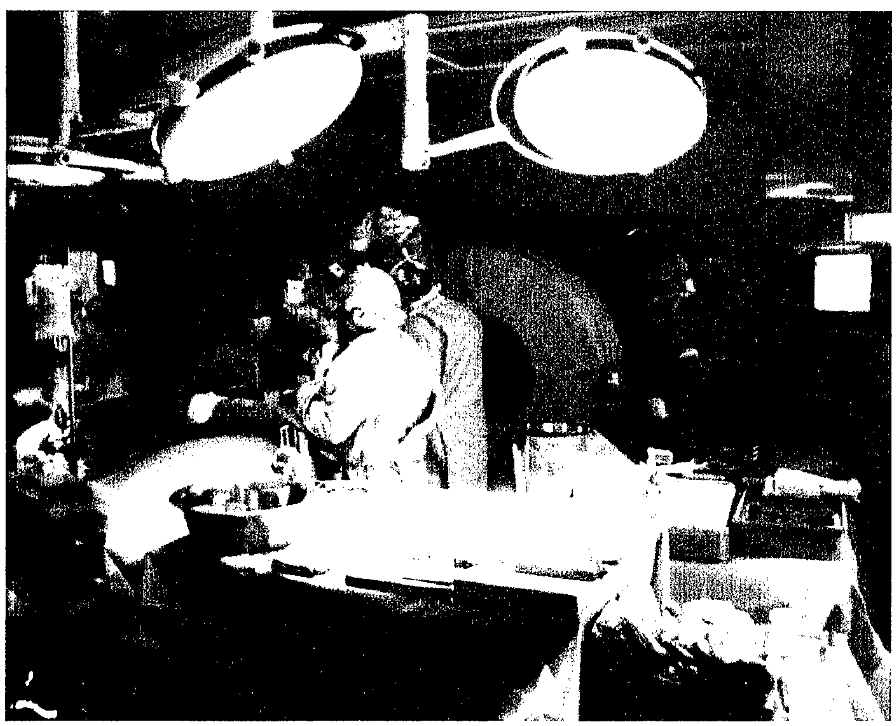

Figure 4: Intraoperative use of CT during spine surgery

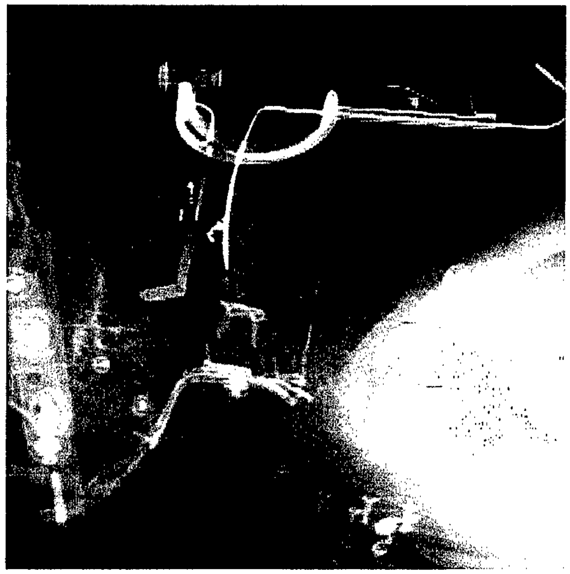

Figure 5: Scout Film showing occipito-cervical stabilization, C3-4 anterior spine plate from previous surgery, placement of instrumentation for transoral exposure, and patient placement in halo vest.

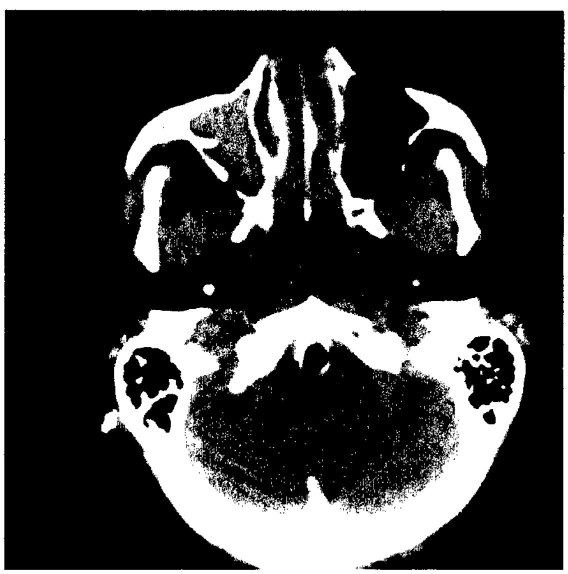

Figure 6: Intraoperative CT scan for transoral odontoidectomy showing resection cavity (small arrow) and spicule of bone remaining in tectorial membrane (large arrow).

Figure 7: Complete resection and decompression of the neuraxis.

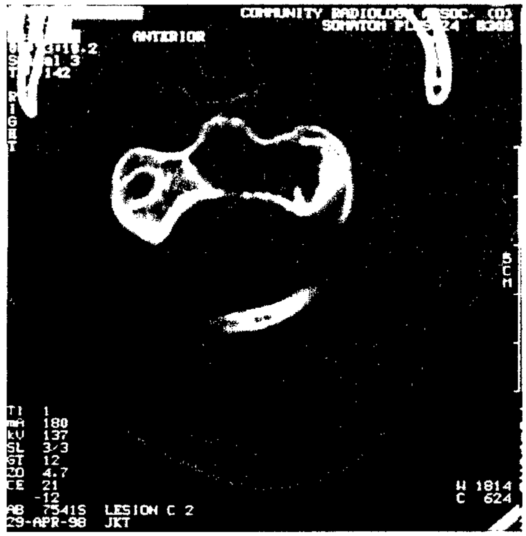

Figure 8: Preoperative CT showing lytic lesion of C2.

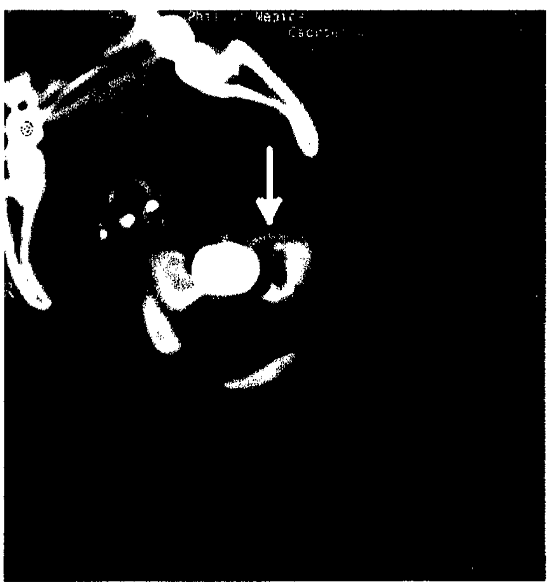

Figure 9: Intraoperative CT with Omnipaque contrast shows residual tumor in left lateral mass after initial resection (arrow).

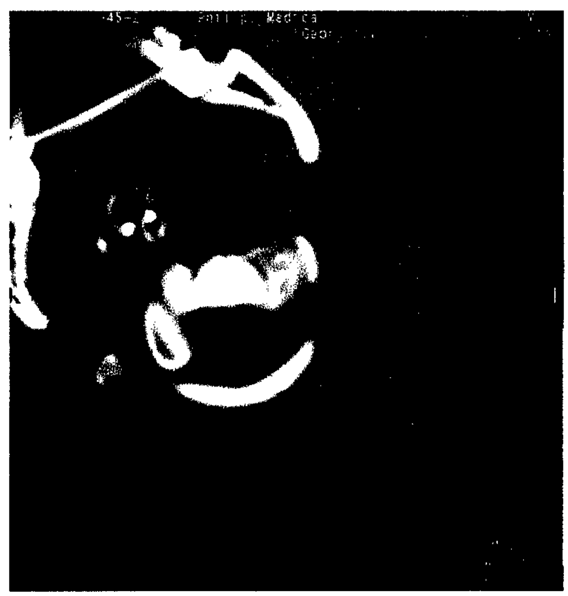

Figure 10: Residual tumor removed and the cavity is filled with PMMA.

Figure 11: Intraoperative CT scan of transoral odontoidectomy. Note the assimilation of C1 to the occiput (long arrow) ; 15mm resection of C1 ring and odontoid (double arrow).

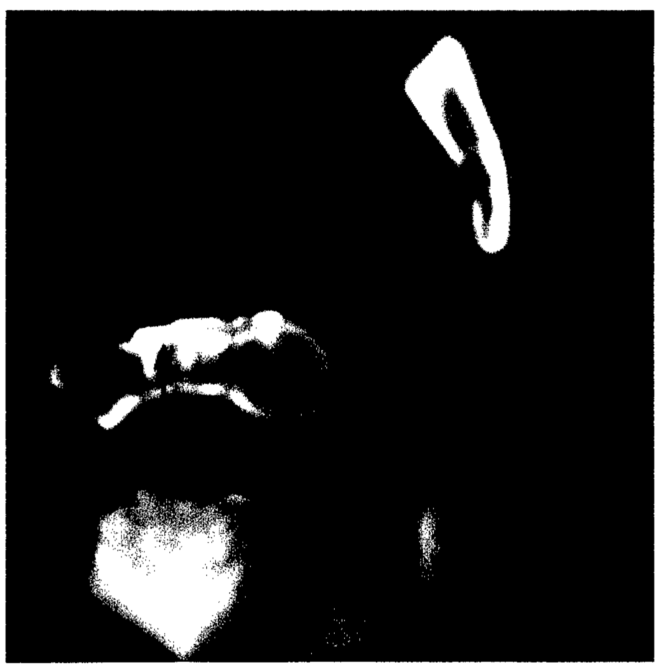

Figure 12: Tricortical autologous iliac crest bone graft (long arrow) and titanium miniplate fixed with 3 titanium screws (short arrow)

Figure 13: Intraoperative CT of slipped transverse process hook on right T5 (note artifact from instrumentation does not interfere with interpretation of CT scan)

11.2.7 Traynor 2000: Software development for registration ...

Reprint begins on the next page and is 6 pages long.

To be published in the proceedings of the 8th Annual Medicine Meets Virtual Reality Conference, January 27-30.2000, Newport Beach, California.

Software Development for Registration of Digital Subtraction Angiography (DSA) Images in Uterine Fibroid Embolization

Laura Traynor, Elliot Levy, Jae Jeong Choi, Kevin Cleary, Jianchao Zeng, and David Lindisch

ISIS Center
Radiology Department
Georgetown University Medical Center
2115 Wisconsin Avenue, Suite 603
Washington, DC, 20007
URL http://www.isis.georgetown.edu

ABSTRACT

The ISIS Center at Georgetown University Medical Center has developed a comprehensive program for image-guided procedures in the spine. As part of this program, ISIS has developed a software application known as I-SPINE (ISIS's Spine Procedure Imaging Navigation Engine). I-SPINE is a Windows NT application, which is based on the Analyze/AVM™ libraries. The software architecture follows the Microsoft Foundation Classes (MFC) single document, multiple view paradigm. This has allowed the developers to add new visualization modules to I-SPINE that aid physicians in procedures outside the spine. One such procedure I-SPINE has been expanded for is uterine fibroid embolization. The idea is that by registering and subtracting post-embolization angiographic images from pre-treatment images the resulting image can be used to quantify the embolization effect on the fibroid circulation and predict the treatment response. The I-SPINE digital subtraction angiography (DSA) module allows the interventional radiologist to open a series of pre and post- embolization DSA images that shows the vascular structures of the uterus and the fibroid or fibroids. From these images, the radiologist selects an appropriate image from each series. The selected images are then hand registered using pixel shifting. Once the images are registered, the pixels are subtracted resulting in an image that shows the embolized arteries that were supplying the fibroids.

1 Introduction

Uterine artery embolization is becoming increasingly popular as an alternative to hysterectomy for the treatment of symptomatic uterine fibroids. The procedure is described by Goodwin [1]. While initial results suggest that the treatment is highly effective, the angiographic imaging assessment of the treatment is limited to the recognition of flow stasis within the target arteries. Treatment efficacy is determined by subjective improvement in symptoms and findings on magnetic resonance imaging studies of the uterus. Treatment variables include the size of the embolization particles, the volume of particles injected, the actual number of arteries or circulatory volume embolized and occluded, and the degree of shrinkage of the fibroid tumors following embolization. If a relationship can be found among these variables, then the embolization treatment can be

further refined, new embolic materials could be more accurately evaluated, and treatment failures could be better assessed. As a first step in quantifying the embolization, we have developed a software package for registration of pre and post-embolization images. This software allows the user to align the pre and post-embolization images by pixel shifting and obtain a quantitative estimation of the amount of embolization.

This paper is organized as follows. First, the image modalities used are described, along with some background on the uterine fibroid embolization procedure. This is followed by a description of the software and an example case study. The communications network is also described, and the paper concludes with a summary and plans for future work.

2 The Uterine Fibroid Embolization Procedure

At Georgetown University Medical Center, uterine fibroid embolization is performed in one of two angiography suites. One of the suites includes a Siemens NeuroStar (Figure 1) biplane fluoroscopic system with DSA capabilities with 1024 x 1024 resolution. The other suite includes a General Electric L-U arm (Figure 2) single plane fluoroscopy unit coupled with an Infimed GOLD 1 DSA unit with 1024 x 1024 resolution.

The pelvic anatomy is shown in Figure 3. Patients receive pre-operative sedation according to the conscious sedation policy at Georgetown. Bilateral femoral access is achieved via the Seldinger technique [2]. Five French inner diameter arterial sheaths are then placed for free access, and 5 French outer diameter preshaped catheters are inserted through the sheaths. Using this technique, the contralateral uterine arteries are then catheterized [3]. After catheterization of both uterine arteries, a pre-embolization DSA is performed to determine the vascular anatomy of the uterus and fibroids. The embolization is accomplished using polyvinyl alcohol (PVA) and is performed under strict fluoroscopic visualization to ensure that the proper vessels are embolized. After the injection of the PVA, a post-embolization DSA is performed to determine the appropriate conclusion of the procedure. At the conclusion of the procedure, the catheters and vascular sheaths are removed and hemostasis is achieved via manual compression.

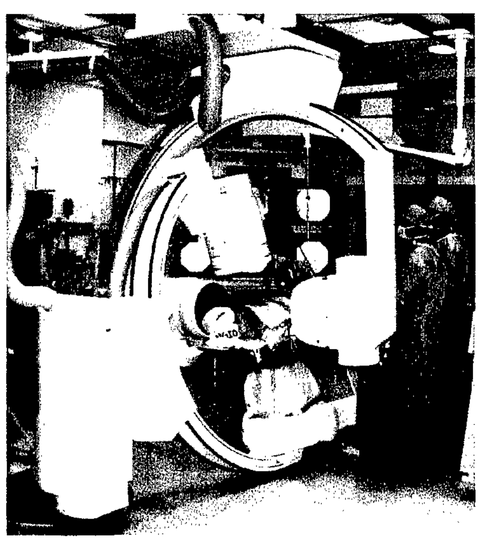

Figure 1: Siemens NeuroStar Polytron Biplane Fluoroscopy

Figure 2: G.E. L-U ARM Single Plane Fluoroscopy

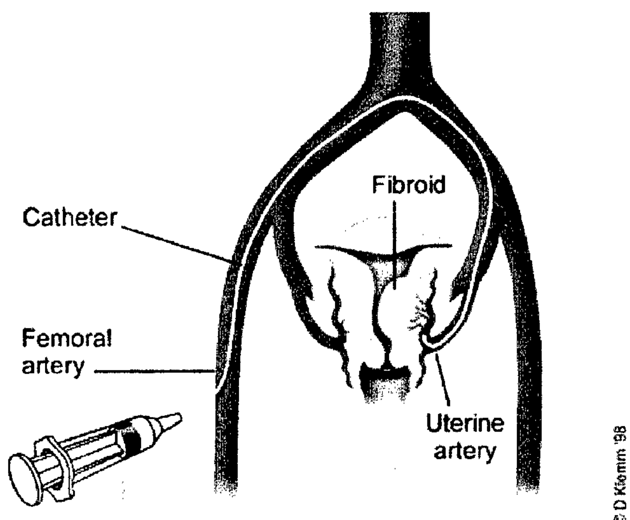

Figure 3: Pelvic Anatomy
(Courtesy of James Spies, MD, Georgetown University)

3 Software Development and Case Study

At the request of the interventional radiologist, ISIS Center software engineers developed a software module for uterine fibroid embolization registration that will be described in this section. This software module is one part of a larger software package called I-SPINE, for ISIS's Spine Procedure Imaging Navigation Engine. I-SPINE was originally developed for 3D visualization of the vertebral bodies and the amount of filling of polymethylmethacrlyate (PMMA) after vertebroplasty [4].

The I-Spine software allows the interventional radiologist to load a series of pre and post-embolization digital subtraction angiography (DSA) images of the uterine circulation (Figure 4). The radiologist selects one pre and one post-procedure image, which are then hand registered (aligned) using pixel shifting (Figure 5). Subtraction of the post-

embolization image from the pre-embolization image is then done, resulting in a single image that reveals the embolized arteries (Figure 6). Efforts are continuing to quantify the embolized uterine circulation using a pixel count from the registered, subtracted images.

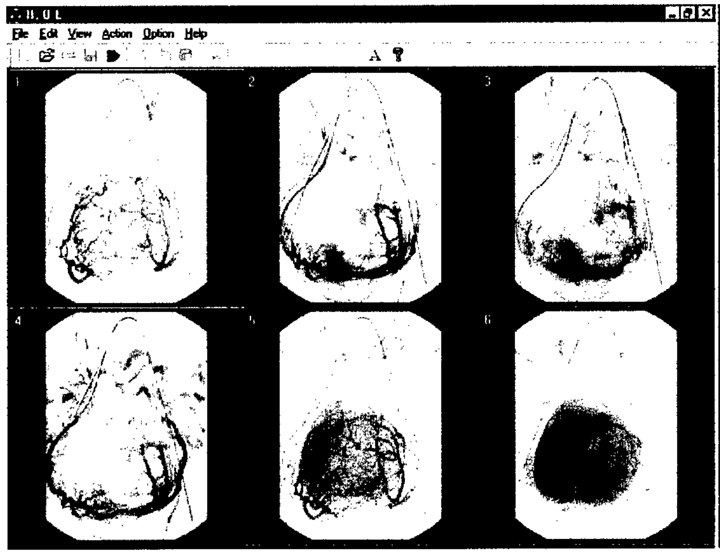

Figure 4: DSA Uterine Circulation Pre and Post-Embolization Images

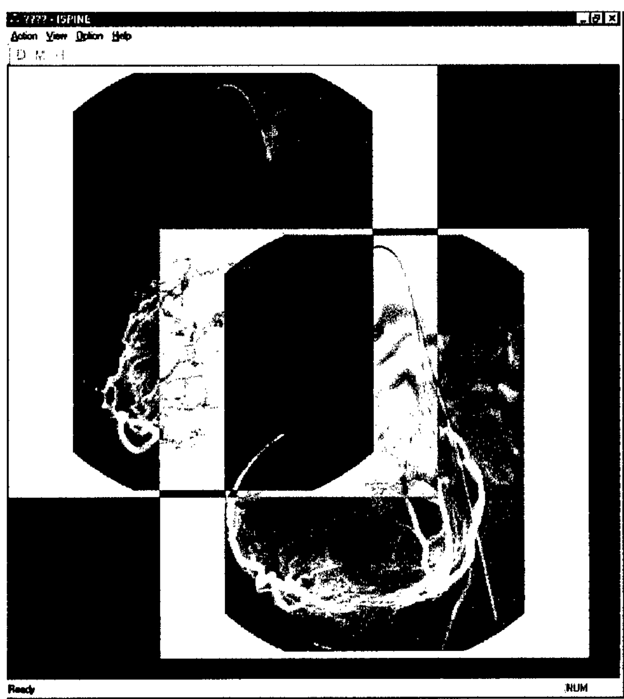

Figure 5. Registering Images by Pixel Shifting

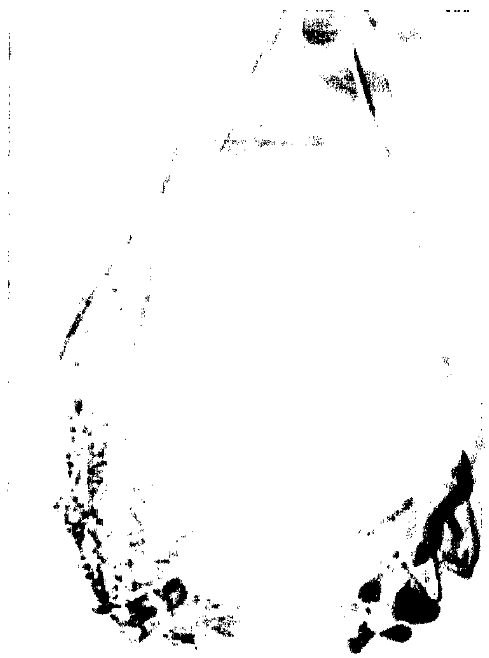

Figure 6. Resulting Image After Registration

4 Communication Network

The I-SPINE software is typically used as follows. After the embolization is completed, the images are transferred using the Digital Imaging and Communications in Medicine (DICOM) format via the hospital intranet (Figure 7) to a NT workstation running the I-SPINE software. The images are stored using the commercial radiology workstation software PiView, which is used as a research database for manipulating medical images. The I-SPINE software can then read the PiView database to access the images for the DSA registration process.

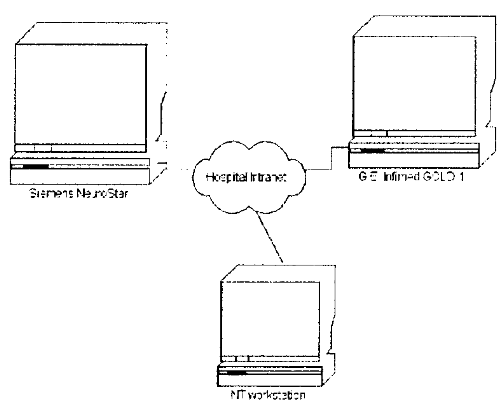

Figure 7: Hospital Data Communications Network

5 Summary and Future Plans

As described in this paper, a software application has been developed for registration of pre and post-embolization images for uterine fibroid embolization. This software is a first step towards a more quantitative evaluation of this new minimally invasive procedure. The next step is to evaluate 10 or more completed procedures to better determine the feasibility of this technique.

The two-dimensional image subtraction technique presented here represents the initial effort to angiographically quantify the vascular volume or circulatory capacity of leiomyomata. The technique will be applied to three- dimensional angiographic studies (rotational angiography) in the future with the goal of more accurately establishing a true vascular "volume" as determined by measuring the voxels representing the occluded vessels.

Uterine fibroid embolization is only one of many potential interventional radiology applications for the I-SPINE software. Potential future applications include other vascular ablative therapies for arterio-venous malformations (AVM's); spinal, peripheral, and visceral tumors; and embolization drug delivery systems.

Acknowledgements
This work was supported by the U.S. Army under grants DAMD17-96-2-6004 and DAMD17-99-1-9022. The content of this poster does not necessarily reflect the position or policy of the U.S. Government.

References

1. Goodwin, S., *et al., Preliminary experience with uterine artery embolization for uterine fibroids.* J Vasc Interv Radiol, 1997. 8(4): p. 517-26.
2. Seldinger, S., *Catheter replacement of the needle in percutaneous arteriography.* Acta Radiology, 1953. 39: p. 368.
3. Levy, E.B., *et al. Two catheter technique for embolization in the treatment of symptomatic uterine leiomyomata.* Abstract presented at SMIT/CIMIT conference, Sep. 1999. Boston, Massachusetts.
4. Choi, J.J., *et al. I-SPINE: A Software Package for Advances in Image-guided and Minimally Invasive Spine Procedures.* In *3D Visualization for Data Exploration and Decision Making*. 1999. Washington, DC: SPIE in press.

11.3 Posters

Copies of the five posters produced are reproduced in this section.

11.3.1 Cleary 1999a: Integrating a mobile CT ... (poster)

Poster is reproduced on the next page.

Integrating A Mobile Computed Tomographic Scanner In Hospital Operations

Kevin Cleary PhD[a,b] Fraser Henderson MD[c] James Rodgers PhD[d] Vance Watson MD[b] Matthew Freedman MD[a,b]
David Lindisch RT[a,b] Laura Traynor BE[a,b] Jianchao Zeng PhD[a,b] Seong K. Mun PhD[a,b]

Introduction

A mobile CT scanner enables CT imaging at locations in the hospital where it was previously not available. At Georgetown, we have been using a mobile CT scanner at various locations including the operating room, interventional radiology suite, and radiation medicine treatment area. To successfully integrate the scanner in these locations, several obstacles including radiation safety, maintenance, and printing issues needed to be considered. Radiation safety guidelines were developed to minimize radiation exposure during scanning. Maintenance becomes a larger issue than with fixed CT scanners since the mobile CT is more susceptible to damage as it is moved around the hospital.

From March until December 1998, the scanner was used for approximately 40 studies, including procedures in the operating room, interventional radiology, radiation medicine, and the pediatric intensive care unit. Hardware and software problems addressed included modifications of patient positioning, separation of the table from the gantry to allow for adequate surgical access, and DICOM image transfer issues. Operational difficulties in integrating the system into the operating room environment have been overcome and the frequency of use of the system is increasing.

Mobile CT

The Philips Tomoscan M is a mobile CT scanner that can be transported anywhere there is sufficient space in the hospital. The system has three components as shown in Figures 1 and 2: a gantry with a 60 cm aperture, a radiolucent table, and an operator's console.

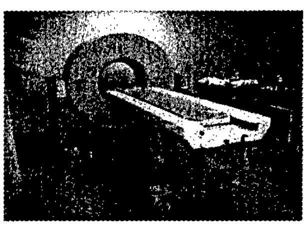

Figure 1. Mobile CT gantry and table.

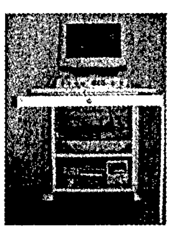

Figure 2. Mobile CT workstation.

All the components are on wheels, use standard electrical power, and fit in an elevator for easy transportability. The system can be used for scanning with or without the table as the gantry itself translates up to 350 mm and can be tilted as well.

Radiation Safety

Radiation safety has been addressed in conjunction with the Radiation Safety Office. Radiation levels have been measured during typical procedures, and the Radiation Safety Office requires that all personnel remain at least 12 feet from the

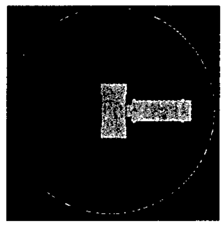

Figure 3. Radiation safety diagram (12 foot circle)

center of the gantry during scanning (Figure 3). This requirement is met in the operating room by positioning the operator's console at least 12 feet from the gantry and ensuring all other personnel are at least 12 feet away during scanning.

Clinical Applications

Tumor Resection

For spine tumor procedures in the operating room

Figure 4. Patient positioning in the operating room.

Figure 5. Viewing the results in the operating room.

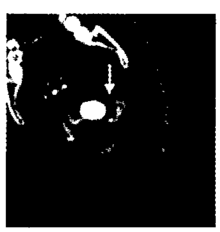

Figure 6. Imaging with Omnipaque reveals residual tumor (arrow) after first resection.

Figure 7. Tumor removed and cavity filled with polymethlymethacrylate.

(Figures 4-7), intraoperative CT is used with three goals in mind: 1) to identify residual tumor following resection; 2) to ensure adequate filling of the resection cavity with polymethylmethacrylate; and 3) to verify optimum placement of instrumentation for mechanical stabilization. To date, approxmimately 15 cases have been done in the operating room. The intraoperative scans provided additional valuable information to the surgeon in all of the cases and altered the procedure in several cases.

Vertebroplasty

In the interventional suite, the mobile CT is used in conjunction with bi-plane fluoroscopy for various interventions including vertebroplasty. Percutaneous vertebroplasty is a relatively new interventional technique in which polymethylmethacrylate (PMMA) bone cement is injected into the vertebral body to strengthen the body and stabilize the spine. While the cannulas are placed and the cement is injected under fluoroscopic guidance, CT is useful in identifying epidural and epineural extravastion of PMMA during the procedure (Figures 8 and 9).

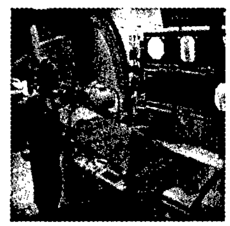

Figure 8. Vertebroplasty in the interventional suite.

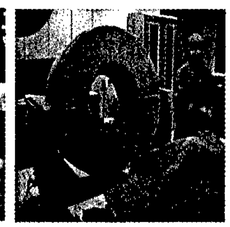

Figure 9. Mobile CT gantry in the interventional suite.

As an adjunct to the clinical work, a software package has been developed under Windows NT that can receive DICOM images from various modalities including CT, MRI, and fluoroscopy. This software is a base for our technology innovations including work in image visualization and registration. As a feasibility study, a 3D visualization module has been created that can be used to examine the spread of bone cement after vertebroplasty procedures. After the PMMA is injected, the mobile CT is used to acquire a set of CT images. These images can then be sent via a DICOM network interface to the software package where the bone cement and vertebral body are segmented based on histogram windowing (Figure 10). The resulting images are rendered in 3D for viewing by the physician (Figure 11).

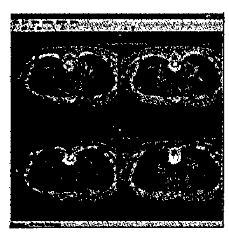

Figure 10. Axial slices showing spread of bone cement.

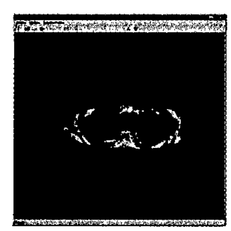

Figure 11. Rendered and segmented image in 3D.

Acknowledgements

This work was supported by the U.S. Army under grants DAMD17-96-2-6004 and DAMD17-99-1-9022. The content of this poster does not necessarily reflect the position or policy of the U.S. Government.

[a]Imaging Science and Information Systems (ISIS) Center [b]Department of Radiology
[c]Department of Neurosurgery [d]Department of Radiation Medicine

Georgetown University Medical Center, 2115 Wisconsin Avenue, NW, Suite 603, Washington, DC 20007

Correspondence: Kevin Cleary
Email: cleary@isis.imac.georgetown.edu
Phone: (202) 687-8253 Fax: (202) 784-3479
Web Site: www.isis.georgetown.edu

11.3.2 Cleary 1999d: I-SPINE: a software package …

Poster is reproduced on the next page.

I-SPINE: A Software Package for Advances in Image-Guided and Minimally Invasive Spine Procedures

Kevin Cleary, PhD[a] Matthew Freedman, MD[a] David Lindisch, RT[a]
Jae Jeong Choi, MS[a] Elliot Levy, MD[a] Jianchao Zeng, PhD[a]
Kevin Gary, PhD[b] Vance Watson, MD[a]

[a]Imaging Science and Information Systems (ISIS) Center, 2115 Wisconsin Avenue, Suite 603, Radiology Department, Georgetown University Medical Center, Washington, DC 20007
[b]Computer Science Department, Catholic University of America, Washington, DC

Introduction

While image guidance is now routinely used in the brain in the form of frameless stereotaxy, it is beginning to be more widely used in other clinical areas such as the spine. At Georgetown University Medical Center, we are developing a program to provide advanced visualization and image guidance for minimally invasive spine procedures. This is a collaboration between an engineering-based research group and physicians from the radiology, neurosurgery, and orthopaedics departments. A major component of this work is the ISIS Center Spine Procedures Imaging and Navigation Engine (I-SPINE), which is a software package under development as the base platform for technical advances.

Software Description

The I-SPINE software currently includes the following capabilities:

- DICOM receiver to accept images from mobile CT, fluoroscopy, and DSA units
- 2D viewing capability (single slices or multiple slices up to 8 by 8)
- Segmentation function based on histogram thresholding
- 3D visualization
- Registration of DSA images by manual pixel shifting

The software runs under Windows NT on a desktop PC (Figure 1). The imaging and visualization software library Analyze, from Mayo Clinic, is used to provide much of the base functionality. This package was purchased off-the-shelf to jump-start the development process.

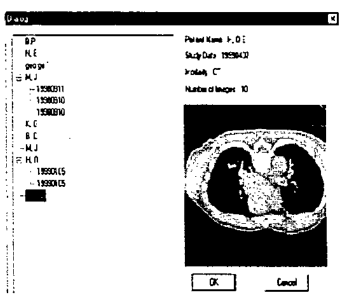

Figure 1. I-SPINE User Interface

Clinical Applications

Vertebroplasty

As a feasibility study, a 3D visualization module has been created that can be used to examine the spread of bone cement after vertebroplasty procedures. A mobile CT scanner is used to acquire a set of images. These images can then be sent to the I-SPINE software via a DICOM network interface where the bone cement and vertebral body are segmented based on histogram windowing (Figure 2). The resulting images are rendered in 3D for viewing by the physician (Figure 3).

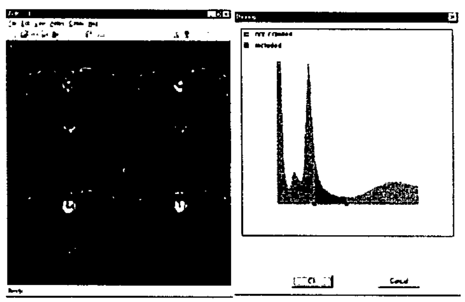

Figure 2. Thresholding of Vertebroplasty Images

Figure 3. 3D Visualization of Bone Cement

Uterine Fibroid Embolization

Uterine fibroid embolization is performed for relief of symptoms related to uterine myomata. Angiographic imaging guidance is used during the embolization to ensure successful vessel catheterization and embolization. We are investigating the feasibility of registering and subtracting postembolization arteriographic images from pretreatment images to determine if the resulting images can be used to quantify the degree of devascularization of the myoma and predict the treatment response (myoma infarction or regression).

The I-Spine software allows the interventional radiologist to load a series of pre- and postembolization digital subtraction angiography (DSA) images of the uterine circulation (Figure 4). The radiologist selects one pre- and postprocedure image which are then hand registered (aligned) using pixel shifting (Figure 5). Subtraction of the postembolization image from the preembolization image is then done, resulting in a single image that reveals the embolized arteries (Figure 6). Efforts are continuing to quantify the embolized uterine circulation using a pixel count from the registered, subtracted images.

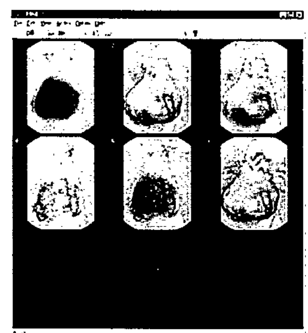

Figure 4. DSA Uterine Circulation Images

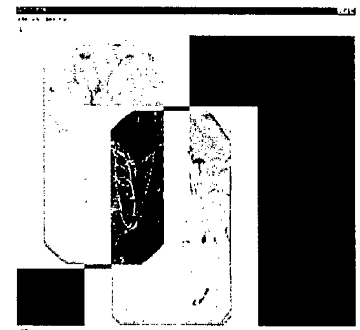

Figure 5. Registering Images by Pixel Shifting

Figure 6: Resulting Image After Registration

Acknowledgements

This work was supported by the U.S. Army under grants DAMD17-96-2-6004 and DAMD17-99-1-9022. The content of this poster does not necessarily reflect the position or policy of the U.S. Government.

Correspondence: Kevin Cleary
Email: cleary@isis.imac.georgetown.edu
Phone: (202) 687-8253
Fax: (202) 784-3479
Website: www.isis.georgetown.edu

11.3.3 Hum 1999b: Intraoperative CT for spinal procedures

Poster is reproduced on the next page.

Intraoperative Computed Tomography for Spinal Procedures

Barbara Hum, MD[1]
Kevin Cleary, PhD[1]
Vance Watson, MD[2]
Frank Feigenbaum, MD[3]
Fraser Henderson, MD[3]

Georgetown University Medical Center, Washington, DC
[1] Imaging Science and Information Systems (ISIS) Center, Department of Radiology
[2] Interventional Neuroradiology, Department of Radiology
[3] Department of Neurosurgery

INTRODUCTION

A mobile CT scanner has been developed and used intraoperatively, predominately for intracranial procedures. We report on the expanded use of the mobile CT for spine procedures in both the operating room and the neurointerventional suite. The purpose of intraoperative imaging is to improve surgical technique by improving the orientation to unexposed spinal anatomy and thus, reducing the surgical risk to the patient. In addition, CT imaging provides intraoperative visualization of spinal pathology for navigation and verification of surgical correction.

The Tomoscan M mobile CT (Philips Medical Systems) has been used at Georgetown University Medical Center for spinal tumor resections, cranio-cervical decompressions, and percutaneous vertebroplasty procedures. The CT is an excellent imaging modality for visualizing bone pathology. In neuorosurgical cases, it has been beneficial in confirming adequate bony decompressions, evaluating the degree of tumor resection, and verification of instrument placement before surgical closing. For interventional percutaneous vertebroplasty procedures, axial CT scans in conjunction with fluoroscopy, help guide the transpedicular placement of the trocar into the vertebral body and allow for immediate evaluation of the polymethylmethacrylate (PMMA) filling for possible extravasation.

METHODS

The Tomoscan M mobile CT scanner is easily transportable within the hospital and consists of three components: a gantry, a CT table, and an operator's workstation (Figures 1 and 2). The aperture of the gantry diameter is 60 cm with a maximal field of view of 46 cm. Both the gantry and CT table can translate, 35 cm and 150 cm respectively.

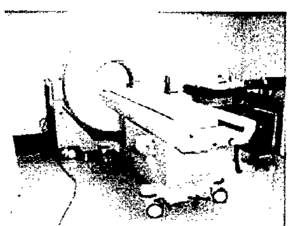

Figure 1: Mobile CT Gantry and Table

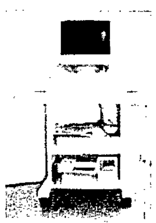

Figure 2: Operator's Workstation

In the operating room, the patient is placed on the CT table. Sterile plastic drapes are applied to the opening of the gantry aperture. An initial scanogram is taken to locate the desired vertebral level of the spine. During the procedure, the gantry can be moved away from the table to allow complete access to the patient. The gantry is re-docked for scanning as needed for intraoperative visualization. The preparation and CT scanning time averages 15-20 minutes per series. The Radiation Safety Office determined that personnel must either wear lead protection or remain at least 12 feet from the center of the gantry during scanning. The operator's workstation is placed outside a 12-foot perimeter. A photograph of the CT scanner in use in the operating room is shown in Figure 3. A diagram of the operating room layout is shown in Figure 4.

Figure 3: Mobile CT in Operating Room

The mobile CT has been used in the spine for over 60 procedures at our institution. In the operating room, 17 complex spinal procedures were performed including: 7 transoral decompressions and 10 spinal tumor resections—2 extrapharyngeal, 5 thoracic, and 3 lumbosacral. In the neuro-interventional suite, more than 20 percutaneous vertebroplasty procedures have been done. Other uses of the mobile CT scanner include intracranial tumor resections, radiation treatment planning, and use in the ICU.

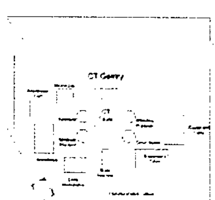

Figure 4: Operating Room Layout

RESULTS

Neurosurgery

In 6 of the 17 spinal neurosurgical cases at Georgetown University Medical Center, the CT provided information that altered the course of the surgery, including: 2 cases of more complete tumor resections, 3 cases of more complete ventral decompression of the brainstem, and one case of a correction of a slipped/rotated transverse process hook. There were no clinically detectable complications from the added use of CT.

Case Study #1

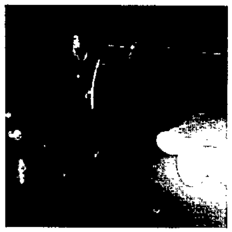

A 42-year-old woman with severe, deforming rheumatoid presented with spastic quadriparesis and numbness. Pre-op MR images of the cranio-cervical junction revealed basilar invagination with brainstem compression. The patient underwent a transoral odontoidectomy (Figures 5, 6, and 7).

Figure 5: Intraoperative Scanogram
The initial scanogram showing occipito-cervical stabilization and C3-4 anterior spine plate from prior surgery, placement of instrumentation for transoral exposure, and patient placement in halo vest.

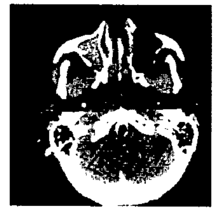

Figure 6: Initial Intraoperative CT
After initial resection, intraoperative axial CT scan revealed continued compression of the brainstem by a fractured portion of the odontiod (long arrow) obscured from direct visualization by pannus and resection cavity (short arrow).

Figure 7: Final Intraoperative CT
After further resection, intraoperative CT scan verified complete odontoid resection. Post-operatively, the patient had return of strength and resolution of her brainstem symptoms.

Case Study #2

An athletic, 41-year-old woman with breast cancer (T1N0M0) presented with occipital neuralgia. Preoperative CT image (Figure 8) revealed a lytic lesion of C2 such that the cancellous portion of the vertebral body and odontoid process had undergone near total replacement. Using a left extrapharyngeal approach, the tumor was resected through a vertebrotomy leaving the uninvolved cortical shell of C2 and its ligamentous attachments intact. Intraoperative CT with Omnipaque contrast filling of the surgical cavity (Figure 9), revealed residual tumor in the left lateral mass of C2 which could not be visualized directly. An additional intraoperative CT verified complete tumor resection and adequate PMMA filling of the resection cavity. Postoperatively, the patient's occiptial neuralgia resolved. The patient later developed another metastasis to the lumbar spine and was treated with percutaneous vertebroplasty in the neurointerventional suite. 16 months post-op, the patient remains active and asymptomatic of disease in the cervical and lumbar spine.

Figure 8: Preoperative CT
Lytic lesion of C2 vertebrae.

Figure 9: Intraoperative CT
After initial resection, residual CT tumor (arrow).

Advantages and Disadvantages of Mobile CT in Spine Surgery

Advantages:

- confirmation of vertebral level with scanogram
- good visualization of bony pathology
- more specific surgical approach
- intraoperative imaging as surgery progresses
- verification of surgical correction of pathology before surgical closing
- mobility of CT scanner

Disadvantages:

- increase in OR time and cost
- need for additional trained staff
- risk of ionizing radiation exposure
- limited patient positioning

Interventional Neuroradiology

Percutaneous vertebroplasty is a relatively new procedure in which PMMA is injected into the vertebral body using a transpedicularly placed trocar. The objective is to maintain the structural integrity of the vertebral body and to bring pain relief to patients with spinal lytic lesions and osteoporotic vertebral body compression fractures. The mobile CT is used in conjunction with fluoroscopy to help guide the trocar placement and to evaluate for possible PMMA extravastation. Figure 10 shows axial CT scans from a thoracic percutaneous vertebroplasty case, using software developed by our research group. Figure 11 shows a 3D reconstruction of PMMA within the vertebral body.

Figure 10: Thoracic CT Scans

Figure 11: 3D Visualization

FUTURE WORK

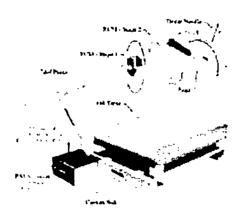

Figure 12: Needle Driver Robot'

Future plans include the development of robotically-assisted, minimally invasive spinal needle procedures, in collaboration with Johns Hopkins University'. The aim is to assist the neuro-interventionalist in placing and advancing needles and associated instruments in and around the spine by using a mechanical needle holder and driver (Figure 12). The long-term goal is to develop a robotic system that can work cooperatively with the physician to improve instrument placement accuracy in spinal procedures.

Footnote: 'Urology Robotics Laboratory and the Computer Integrated Surgical Systems & Technology Engineering Research Center at Johns Hopkins

CONCLUSION

At Georgetown, the mobile CT has been used successfully in the operating room, the interventional suite, radiation medicine, and the ICU. The CT may not be necessary for simple surgical procedures but we believe that it will be an indispensable imaging modality for select complex procedures to improve patient outcomes. In the OR and the interventional suite of the future, it is one of several imaging modalities that should be available "on demand" for intraoperative use.

ACKNOWLEDGEMENTS

This work was supported by the U.S. Army under grants DAMD17-96-2-6004 and DAMD17-99-1-9022. The content of this poster does not necessarily reflect the position or policy of the U.S. Government.

Correspondence: Kevin Cleary, PhD; Barbara Hum, MD
Email: cleary@isis.imac.georgetown.edu; humb@isis.imac.georgetown.edu
Phone: (202) 687-8253
Fax: (202) 687-3479
Website: www.isis.georgetown.edu

Produced by the Department of Educational Media, Georgetown University Medical Center

11.3.4 Watson 1999: Mobile CT assessment of needle ...

Poster is reproduced on the next page.

Mobile CT Assessment of Needle Placement and Distribution of Polymethylmethacrylate (PMMA) during Percutanous Vertebroplasty

Vance Watson[1], MD Patrick Oliverio[2], MD
Kevin Cleary[3], PhD Dave Lindisch[3], RT
Georgetown University Medical Center Washington, DC
[1] Interventional Neuroradiology, Department of Radiology
[2] Neuroradiology, Department of Radiology
[3] Imaging Science and Information Systems (ISIS) Center, Department of Radiology

Introduction

Percutaneous vertebroplasty is a relatively new interventional technique in which polymethylmethacrylate (PMMA) bone cement is injected into the vertebral body to strengthen the body and stabilize the spine. Indications for percutaneous vertebroplasty include painful osteoporotic and pathologic fractures. At Georgetown University Medical Center, the procedure is done in an interventional suite that accomodates bi-plane fluoroscopy, angiography, and a mobile CT scanner.

Vertebroplasty Procedure

Technique

Percutaneous vertebroplasty is a technique wherein polymethylmethacrylate (PMMA) bone cement is injected directly into a vertebral body under fluoroscopic and/or CT guidance. This non-surgical procedure has two desirable results:

1. The structural integrity of the vertebra is buttressed by the bone cement. This is thought to halt the progress of collapse by replacing nonosseous elements of cancellous bone within the vertebral body with a biologically inert substance that has a high degree of compressive strength [Cotten 1996; Jensen 1997; Deramond 1998; Mathis 1998a; Mathis 1998b; Depriester 1999].
2. Pain relief often occurs. This relief is usually within 24 hours [Cotten 1996; Jensen 1997; Deramond 1998; Depriester 1999]. The mechanism of pain relief is not well understood. Possibilities include mechanical strengthening of the vertebral, thermal or chemical injury to pain fibers, or a placebo effect. One interesting observation is that the degree of vertebral filling with methylmethacrylate does not seem to correlate with the degree of pain relief [Cotten 1996].

History and Indications

Percutaneous vertebroplasty was first developed in France in 1984, by P. Galibert and H. Deramond [Galibert 1987]. The conditions that have been reported in the literature as responding to treatment include vertebral hemangiomas, malignant tumors of the spine, and osteoporotic compression fractures [Jensen 1997; Cotten 1998; Deramond 1998; Depriester 1999].

Procedure as Refined and Performed at Georgetown

Percutaneous vertebroplasty (PV) is usually performed with either conscious sedation or with Monitored Anesthesia Care (IV propofol and fentanyl). Local anesthesia is always used. Sterile technique is strictly observed to reduce the risk of infection Prophylactic antibiotics may be administered at the beginning of the procedure and continued for one day following the procedure.

A photograph of a typical case in the neurointerventional suite is shown in Figure 1. The procedure is done under bi-plane fluoroscopy (Siemens Neurostar TOP). The injection of PMMA (bone cement) is shown in Figure 2. The mobile CT scanner (Philips Medical Systems: Figure 3) is used as-needed for several purposes: 1) prior to vertebroplasty to define defects in cortical bone and needle placement; 2) during the procedure to evaluate indeterminant PMMA extravasation and to check needle placement; and 3) post-procedure to verify the amount of filling within the vertebral body. The equipment placement and room layout is shown in Figure 4.

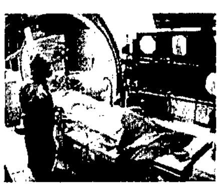

Figure 1. Bi-plane Fluoroscopy

Figure 2. Injection of PMMA

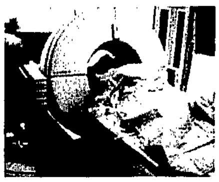

Figure 3. Post-Injection: Mobile CT Gantry

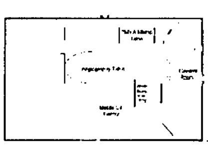

Figure 4. Neuro-interventional Suite

Steps in the Procedure

The procedure is carried out as follows [Deramond 1998]

Step 1: The Vertebral Puncture

The trajectory is identified under fluoroscopy and CT, the skin marked, and 1/4 inch incisions made with a scalpel. A transpedicular puncture of the vertebral body is performed at the level of interest. The needle is set in the vertebral lesion in the lateral part of the vertebral body. Contralateral access is usually employed to ensure filling of the whole vertebral body.

Step 2: The Spinal Biopsy

A biopsy usually precedes the cement injection. A cutting needle or fine aspiration needle is inserted through the vertebroplasty needle.

Step 3: The Vertebral Venography

Vertebral venography evaluates for epidural leakage, displays perivertebral venous drainage, and assures that the needle is not directly in the basivertebral venous plexus (which would place the patient at risk for PMMA pulmonary emboli).

Step 4: The Injection of PMMA

In a sterile mixing bowl, 20 cc of PMMA powder is combined with 7.5 cc of sterile barium sulfate and 1.2 grams of Tobramycin sulfate. The barium sulfate acts as a radiopaque agent for fluoroscopy visualization. MMA liquid (5 ml) is added to the mixture while it is stirred for approximately 30 seconds or until a homogeneous mixture is formed. After standing for 1 minute, the cement has the consistency of paste and is loaded into 10 ml Luer-Lok syringes. The cement is subsequently transferred into 1 ml Luer-Lok syringes.

The cement is then injected through the needle, and the injection is controlled under strict lateral fluoroscopy. The injection is immediately stopped whenever the cement reaches the posterior vertebral wall or fills paravertebral veins to prevent spinal canal or neural foraminal extravasation or pulmonary embolism.

After the procedure the patient is monitored in a stepdown unit of Neuro Intensive Care for 24 hours for bedrest and to assess for possibile complications. Follow-up in clinic begins in 1-2 weeks.

Tabulation of Cases

Percutaneous vertebroplasty procedures have been done at our hospital since 1997 and over 150 procedures have been completed. The mobile CT scanner was introduced in May of 1998 , and has been used in over 25 cases. The mobile CT cases were reviewed by two neuroradiologists, and a tabulation of the results was created. Neuroradiologist 1 is the most experienced and did the procedures, and neuroradiologist 2 is trained in vertebroplasty and blinded to the patients. The data collection was done by the radiology technologist, who had knowledge of both the patient and the procedure.

The neuroradiologists reviewed both fluoroscopic and CT images on a personal computer-based viewing workstation The images were sent from the mobile CT and fluoroscopy systems over a network using the DICOM standard. The information tabulated during the viewing of the images included: level or levels done, percent compression, and whether extravasation was better seen under fluoroscopy or CT (for epidural, epineural, paravertebral, disc, and venous regions).

From this tabulation, the following trends were observed. While extravasation is easily seen in the CT images, it is not always apparent in the fluoroscopic images. More specifically, extravasation into the epidural and epineural regions is easily visualized by CT. Venous and disc extravasation of PMMA is typically readily detected under fluoroscopy.

Case Study 1

A 54 year-old female with lung cancer metastatic to the liver and brain and a known compression fracture at T11 sustained a fall resulting in increased back pain. An MR scan revealed a new L1 compression fracture with destructive features. Under fluoroscopic and CT control, 10 gauge needles were introduced through bilateral parasagittal incisions in a perpendicular fashion into the L1 vertebral body 7 cc of PMMA were injected on the right side and 8 cc on the left side with slight ventral epidural extravasation in the region of the retropulsed fracture fragment. Note that while the epidural extravasation is difficult to see on bi-plane fluoroscopy (Figures 5 and 6), it is well-defined on CT (Figure 7).

Figure 5. AP Fluoroscopy

Figure 6. Lateral Fluoroscopy
Epidural Extravasation (arrow)

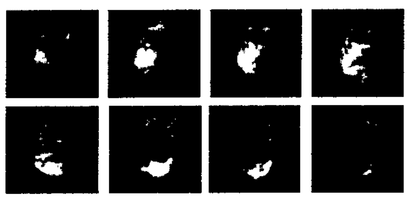

Figure 7. Post-Procedure CT Series
Ventral epidural extravasation of PMMA.

Case Study 2

A 61 year-old female presented with multiple myeloma and multiple vertebral compression fractures. The L4 vertebral body was nearly completely replaced with tumor; it was collapsed and painful. Under fluoroscopic and CT guidance, a 10 gauge needle was placed into the vertebral body via a right transpedicular approach. 3 cc of PMMA was then injected. This resulted in apparently good reinforcement by fluoroscopy (Figure 8), but some epidural extravasation was detected on the post-procedure CT (Figure 9). No neurologic complication resulted.

In a follow-up visit, mobile CT was employed for needle guidance and to gain access to the left hemivertebra because the left pedicle was known to be already destroyed by tumor. Once the needle was placed, bi-plane fluoroscopy was used to monitor injection of PMMA (Figure 10). A mobile CT scan was obtained post-injection (Figure 11).

Figure 8. Procedure 1 (Right Side) AP & Lateral Fluoroscopy
Epidural extravasation is not seen

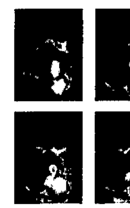

Figure 9. Procedure 1 (Right Side) Post-Procedure CT
Note epidural extravasation of PMMA

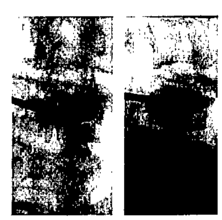

Figure 10. Procedure 2 (Left Side) AP & Lateral Fluroscopy

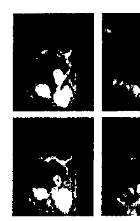

Figure 11. Procedure 2 (Left Side) Post-Procedure CT
Note distribution of PMMA

Conclusion

Mobile CT has added value in vertebroplasty, particularly in identifying extravasation and guiding procedures where vertebral cortex destruction is present.

Acknowledgements

This work was supported by the U.S. Army under grants DAMD17-96-2-6004 and DAMD17-99-1-9022. The content of this poster does not necessarily reflect the position or policy of the U.S. Government.

Correspondence: Kevin Cleary, PhD; Dave Lindisch, RT
Email: cleary@isis.imac.georgetown.edu; lindisch@isis.imac.georgetown.edu
Phone: (202) 687-8253; Fax: (202) 687-3479
Website: www.isis.georgetown.edu

References

Cotten, A., N. Boutry, B. Cortet, et al. (1998). "Percutaneous vertebroplasty: state of the art." Radiographics 18(2): 311-20.

Cotten, A., F. Dewatre, B. Cortet, et al. (1996). "Percutaneous Vertebroplasty for Osteolytic Metastases and Myeloma: Effects of the Percentage of Lesion Filling and the Leakage of Methyl Methacrylate at Clinical Follow-up." Radiology 200: 525-530

Depriester, C., H. Deramond, P. Toussaint, et al (1999). Percutaneous Vertebroplasty: Indications, Technique, and Complications. Interventional Neuroradiology, Strategies and Practical Techniques. J. Connors and J. Wojak. Philadelphia, PA, W.B. Saunders Company: 346-357.

Deramond, H., C. Depriester, P. Galibert, et al. (1998). "Percutaneous Vertebroplasty with Polymethlymethacrylate: Techniques, Indications, Results." Radiological Clinics of North America 36(3): 533-546

Galibert, P., H. Deramond, P. Rosat, et al. (1987). "Preliminary note on the treatment of vertebral angioma by percutaneous acrylic vertebroplasty (in French)." Neurochirurgie 33(2): 166-8.

Jensen, M. E., A. J. Evans, J. M. Mathis, et al. (1997). "Percutaneous polymethylmethacrylate vertebroplasty in the treatment of osteoporotic vertebral body compression fractures: technical aspects." Am J Neuroradiol 18(10): 1897-1904.

Mathis, J., D. Fenton, R. Scribner, et al. (1998a). Biomechanical Comparison Of New Treatments For Vertebral Body Compression Fracture. North American Spine Society Proceedings, San Francisco, CA, pp. 220-221.

Mathis, J., M. Maroney, D. Fenton, et al. (1998b). Evaluation Of Bone Cements For Use In Percutaneous Vertebroplasty. North American Spine Society Proceedings, San Francisco, CA, pp. 210-211.

11.3.5 Zeng 1999: A three-dimensional training system ...

Poster is reproduced on the next page.

A Three-dimensional Training System for Spine Needle Biopsy

Jianchao Zeng, Kevin Gary*, Elliot Levy, Jaeyoun Yi**, Jong-Beom Ra**, Laura Traynor, Kevin Cleary, Jin-Kook Kim**, Keun-Ho Kim**, Seong K. Mun

Department of Radiology
Georgetown University Medical Center
* Department of Computer Science, Catholic University of America
** Korea Advanced Institute of Science and Technology

1. Introduction

Percutaneous vertebral biopsy is a safe and efficacious method for diagnosing destructive pathology of the vertebral column. Physician training may be hampered by the relatively small number of patients requiring the procedure. We have developed a three-dimensional (3-D) spine biopsy training system using advanced computer visualization technology and a force feedback device for physician performance improvement and pre-planning of complicated cases. The system consists of three components: a PC for 3-D display, a body phantom, and a force feedback-assisted biopsy needle simulation device. The needle is attached to the end-effector of the pressure device which can transmit tactile interaction between the various tissue planes to the user's hand. The position and orientation of the needle are tracked dynamically by the computer throughout the biopsy simulation. A set of thin collimation (1 mm thickness) CT images is first selected in the anatomic region of interest. These images are then reconstructed in 3-D volumes to serve as the preliminary target evaluation images. The user can then select the region of interest (ROI) and the corresponding two-dimensional (2-D) CT images are displayed for detailed evaluation. All selected CT images can be viewed prospectively so that the user can identify the optimal image for the biopsy approach. After the target for the biopsy is selected, the user can then direct the needle to the vertebral target in the phantom while viewing the needle's course in real-time on the selected CT image.

The system offers physicians-in-training an excellent opportunity to acquire fundamental biopsy skills in the absence of clinical material. In addition, clinical faculty will have the opportunity to evaluate the proficiency of physicians-in-training in this biopsy modality prior to actual live patient experience. This system can also be used by experienced physicians to plan complicated cases. It can easily be modified to include more functions to enhance the experience in response to specific needs or guidelines. This computer-assisted instructional simulator should reduce morbidity and mortality associated with learning complex image-guided medical procedures such as vertebral biopsy.

2. System Configuration

In order to develop a simulation system that is low-cost, portable and easy to use, we have developed our spine biopsy simulation system in a Windows NT PC platform.

(1) System Hardware
- Processor: 450 MHz Pentium II
- RAM: 256 MB
- Hard disk: 500 MB
- Monitor resolution: full color 1024x768
- Interface device: PHANToM Haptic Device with tracking ability

(2) System Software
- Operating system: Windows NT 4.0
- Software toolkit: Basic I/O and MFC 4.2
- Compiler: Microsoft Visual C++ V5.0
- Model representation: Volumetric modeling
- Interface: 3-D visualization and GUI menu

System Configuration (Cont.)

The spine system basically has two major parts: a haptic device for force feedback and needle position tracking with a dummy torso, and a GUI display for 3D visualization and user menu. The configuration is shown in Figure 1.

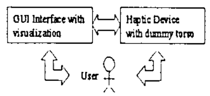

Figure 1 Configuration of the spine biopsy simulation system

Figure 2 shows the setup of the actual spine needle biopsy simulation system. The spine dummy torso is placed on a patient table to serve as a physical object for the user to perform the biopsy procedures on.

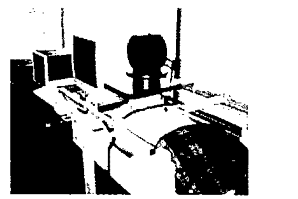

Figure 2 Actual setup of the developed spine biopsy simulation system

3. Technical Development

1. Image Segmentation and 3-D Visualization
In order to visualize individual structures in the CT spine images in 3-D space, segmentation of these structures are necessary. An improved watershed algorithm has been developed for the spine biopsy simulation system, which has incorporated an appropriate seed-extraction process to cope with the narrow gray-level ranges of many structures in the CT spine images and their low contrast characteristics[1]. This algorithm divides a CT spine image into four sub-images by windowing its gray-level histogram, and extracts proper seeds from each sub-image with different methods based on its characteristics. The watershed algorithm is then performed using all the extracted seeds to segment the whole CT spine image. An example of CT spine image segmentation is shown in Figure 3.

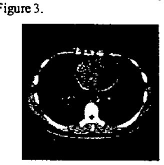

(a) Original CT spine image

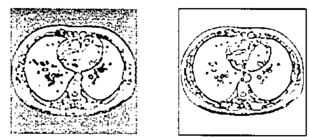

(b) Seed image (c) Segmented image

Figure 3 An example of CT spine image segmentation

A block-based fast volume rendering algorithm has been developed for the 3-D visualization of the CT spine images in the simulation system[2]. This algorithm can handle a large volume data by using images segmentation information as well as 3-D volume information.
It can reduce storage requirements and increase rendering speed since it stores and retrieves data in a block-by-block way instead of using the whole data volume. Figure 4 shows some 3-D rendering examples of the spine.

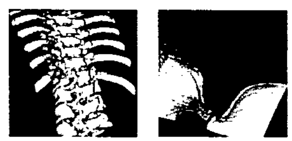

(a) Single object (b) Multiple objects

Figure 4 Examples of 3-D rendering

2. Force Feedback and Physical Interface
The force feedback is applied to the user's hand by the PHANToM haptic device at 1 KHz rate. The magnitude of the force can be calculated by the system based on image pixel values, position of the needle tip or other factors. It can also be set as a constant depending on the needs of the system. In the current version of the system, we have set the force value based on a "Spring Model" or Hooke's Rule. It can be formulated as follows:

$$Force = K * D$$

where K is a coefficient representing the material property of the spring, and its value ranges from 0 to 1, D is the distance of the needle tip from its initial position. Currently, K is set as 0.5.

It is obvious that this force model is not optimal for the application of spine needle biopsy simulation. An improved force model is under development where the force feedback will be based on the properties of the organ tissues where the needle tip is located during he biopsy process. For this purpose, the image segmentation information of the tissues will be utilized and tissue properties will be measured and modeled.

The physical interface includes the mounting of the needle to the PHANToM haptic device, and the setting of a patient table with a spine dummy torso. The haptic device uses a pen stylus as its end-effector for general purpose. In this application, in order to give the physician user maximum degrees of freedom in manipulating the needle, the needle

Technical Development (Cont.)

is mounted vertically with respect to the pen stylus. The user can have a full six degrees of freedom in manipulating the needle while he/she can still completely sense the force that the PHANToM haptic device applies.

A spine dummy torso is fixed to the patient table so that it will not move during the spine biopsy simulation. The PHANToM haptic device is mounted to a support which can be freely moved on a pair of rails along the length direction. By this setting, the haptic device can have access to any part of the spine model. We have also attached a ruler to each of the rails so that any movement of the haptic device on the rails can be accurately measured. By measuring the initial position of the spine body model with respect to the PHANToM haptic device, the spatial relationship between the PHANToM device and the spine body model can always be accurately tracked. Therefore it is possible to accurately track down the needle position at any time during the biopsy simulation. The system setup is shown in Figure 2.

3. Position and Orientation Tracking for the Needle of Spine Biopsy Simulator
In order to link the coordinate system of the biopsy simulator and that of the images, the position and orientation of the needle must be tracked. A new needle has been installed on the original needle (stylus). It is mounted perpendicularly to the original needle, and the offsets of the mounting point with respect to the gimbals and the length of the new needle were measured precisely. To locate the position of the needle in a three-dimensional space, two points on the needle have to be tracked. With x, y, and z coordinates of the two points, the exact position and orientation of the needle are known. The needle tip and the mounting point are chosen for locating the needle.

The origin of the basic coordinate system of the PHANToM is fixed on the rest position of the gimbals. The x, y, z coordinates of the gimbals are tracked by the PHANToM when it is being moved. The three rotational angles of the original needle around x, y, and z axes are sensed by the gimbals. The initial x, y and z coordinates of the new needle tip are known according to the offsets of the mounting point and the length of the needle, and also the initial x, y and z coordinates of the mounting point are known. With these parameters, the new positions of the needle tip and mounting point resulting from motion of the needle can be calculated by doing coordinate transformation. The coordinate transformation consists of two components: translational and rotational transformations. The following equation is used to calculate the x, y and z coordinates of both needle tip and mounting point.

$$newposition = gimbalposition + rotationmatrix * initialposition$$

where the initial position of needle tip $(x_{initneedle}, y_{initneedle}, z_{initneedle})$ = $(113.5075, 7.9375, 81.7563)$ in millimeters, and the initial position of mounting point $(x_{initmount}, y_{initmount}, z_{initmount}) = (0, 7.9375, 81.7563)$ also in millimeters. The gimbalposition $(x_{gimbal}, y_{gimbal}, z_{gimbal})$ is sensed by Phantom. The rotationmatrix is a 3 by 3 matrix and is determined as follows,

$$\begin{aligned} rotationmatrix = \{ & \{cos(t1)*cos(t2), cos(t2)*sin(t0)*sin(t1) - cos(t0)*sin(t2), \\ & cos(t0)*cos(t2)*sin(t1) + sin(t0)*sin(t2)\}, \\ & \{cos(t1)*sin(t2), cos(t0)*cos(t2) + sin(t0)*sin(t1)*sin(t2), \\ & -cos(t2)*sin(t0) + cos(t0)*sin(t1)*sin(t2)\}, \\ & \{-sin(t1), cos(t1)*sin(t0), cos(t0)*cos(t1)\}\} \end{aligned}$$

where t0, t1 and t2 are theta0, theta1 and theta2, respectively, which are returned by get_gimbal_encoders in radians.

The new position of needle tip $(x_{newneedle}, y_{newneedle}, z_{newneedle})$ can be calculated as follows,

$$\begin{aligned} x_{newneedle} &= x_{gimbal} - y_{initneedle}*cos(t0)*sin(t2) + z_{initneedle}*(cos(t2)*sin(t1) + \\ & cos(t1)*sin(t0)*sin(t2)) + x_{initneedle}*(cos(t1)*cos(t2) - sin(t0)*sin(t1)*sin(t2)) \\ y_{newneedle} &= y_{gimbal} + y_{initneedle}*cos(t0)*cos(t2) + x_{initneedle}*(cos(t2)*sin(t0)*sin(t1) + \\ & cos(t1)*sin(t2)) + z_{initneedle}*(-cos(t1)cos(t2)sin(t0) + sin(t1)*sin(t2)) \\ z_{newneedle} &= z_{gimbal} + z_{initneedle}*cos(t0)*cos(t1) + y_{initneedle}*sin(t0) - \\ & x_{initneedle}*cos(t0)*sin(t1) \end{aligned}$$

The above equation can also be used to determine the position of the mounting point $(x_{newmount}, y_{newmount}, z_{newmount})$ by replacing $x_{initneedle}, y_{initneedle}$ and $z_{initneedle}$ by $x_{initmount}, y_{initmount}$ and $z_{initmount}$ respectively. As long as the positions of the two points on the needle are determined, the needle is located in the basic coordinate system of the Phantom.

4. Graphical User Interface
Figure 5 shows a typical example of the GUI of the current version of the spine needle biopsy simulation system.

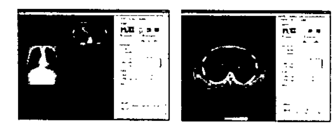

(a) Preview 3-D CT scan (b) A 2-D CT image slice

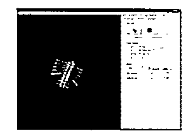

(c) Volumetric rendering of a spine

Figure 5 An example of the system GUI

4. Conclusion

We have developed a prototype 3-D training system for spine needle biopsy using 3-D visualization and haptic force feedback techniques. Some new algorithms have also been developed for the segmentation of CT spine images and the fast rendering of the large data volume of spine. The system aims at providing an alternative platform for physicians-in-training to practice their spine needle biopsy skills before performing on a patient. It can also be used for planning a complicated spine biopsy case. The system is still under development and will be tested by physicians for further improvement.

References

[1] J. Yi et al., Automatic object segmentation scheme for X-ray body images, Proc. SPIE MI, 1999.
[2] S. Kwon et al., A block-based volume rendering scheme for the spine biopsy simulator, Proc. ICIP, 1999

Correspondence: Jianchao Zeng, Ph.D., (202)687-1533, zeng@isis.imac.georgetown.edu

Produced by the Department of Educational Media, Georgetown University Medical Center